

Methods to Enable Open-Loop Synchronization
For Isolated Systems

by

Yaxiang Zhou

A thesis submitted in partial fulfillment of the requirements for the degree of

Master of Science

in

Energy Systems

Department of Electrical and Computer Engineering
University of Alberta

© Yaxiang Zhou, 2016

Abstract

Interconnection of two power systems is a common task. An example is to reconnect an islanded system to the main power grid. Synchronization condition must be satisfied when interconnecting these two systems. Traditionally, feedback-control based methods are used to adjust the generating units of the islanded system to meet the synchronization criteria until satisfied. Implementing such methods can be difficult when multiple generating units need to be adjusted. Moreover, islanded systems might be located in remote areas where infrastructure for feedback loop is not readily available and costly to build.

This thesis proposes a novel method to enable open-loop synchronization of an islanded system to the main grid. The idea is to pre-insert an impedance to reduce the synchronization transients and then bypass it after the initial transients are over. With this method, infrastructure cost and complexity of synchronization can be reduced significantly since the communication links between the breaker and the generators are no longer required. In addition, the extra efforts required for generator adjustments can be avoided. Technical considerations and design method for the selection of pre-insertion impedance size is presented. A simulation study is conducted to evaluate the performance of the method. The results prove that the transient levels can be effectively reduced and open-loop synchronization is indeed achievable. The thyristor based synchronizer to enable open-loop synchronization is also found to be feasible.

Acknowledgement

I would like to express my sincere gratitude to Dr. Wilsun Xu for the continuous support of my M.Sc study and related research, for his patience, motivation, and immense knowledge. His guidance helped me in all the time of research and writing of this thesis. I will always be proud to say I had the privilege of being his student, and I hope to have learned enough to succeed in my future career.

I also thank my parents for supporting me in so many different ways. They have supported my four years in undergraduate studies and my desire to spend another two years in university for graduate studies.

I am pleased to thank everyone working in the PDS-LAB who supported me in the last two years. I would never forget the help I got from Tiago R. Ricciardi and Moosa Moghimi Haji for their extensive knowledge in power system stability. I am grateful to Dr. Jing Yong, provided valuable suggestions and constant support.

Finally and most importantly, I would like to express my gratitude for the encouragement and emotional supports from my wife, Sophie Tian.

Contents

| | |
|---|-----------|
| Chapter 1 Introduction..... | 1 |
| 1.1 The Phenomenon Involved in Connecting Two Systems | 2 |
| 1.2 Different Synchronization Scenarios in Power System | 3 |
| 1.3 Traditional Synchronization Practices and New Challenges | 5 |
| 1.4 Thesis Scope and Outline..... | 7 |
| Chapter 2 Proposed Method for Open-Loop Synchronization Scheme | 10 |
| 2.1 Motivations for New Islanded System Synchronization Strategies | 10 |
| 2.1.1 Synchronous Generator (SG) Based Islanded Systems | 11 |
| 2.1.2 Synchronization Issues Brought by Feedback Control Method. | 13 |
| 2.1.3 Synchronization Concerns and Objectives | 15 |
| 2.1.4 Existing Switching Transient Mitigation Techniques | 16 |
| 2.2 Power Quality Limits for Normal System Operations..... | 18 |
| 2.3 Proposed Synchronization Strategy | 20 |
| 2.4 Design Consideration and Challenges | 24 |
| 2.5 Summary and Conclusion..... | 24 |
| Chapter 3 Design Process of Open-Loop Synchronization Scheme | 26 |
| 3.1 Define Acceptable Level of Transients and Power Oscillations | 27 |
| 3.1.1 Synchronizing Limits Based on IEEE Standard..... | 27 |
| 3.1.2 Define Worst Case Acceptable Surge Level..... | 28 |
| 3.1.3 Acceptable Level of Power Oscillations | 29 |
| 3.2 Minimization of First Switching Surge..... | 30 |
| 3.2.1 Worst Case Transient Levels of Proposed Scheme..... | 30 |
| 3.2.2 Analytical Methods for Obtaining Peak Transients..... | 32 |
| 3.3 Transient Stability Considerations | 36 |

| | | |
|------------------|--|-----------|
| 3.3.1 | <i>Stability Analysis of an Island to System Synchronization</i> | 37 |
| 3.3.2 | <i>Effects of Loading Levels and Impedance Sizes</i> | 42 |
| 3.3.3 | <i>Worst Stability Case of Proposed Scheme</i> | 44 |
| 3.4 | Second Switching Surge Determinations..... | 45 |
| 3.4.1 | <i>Theoretical Analysis of Impedance Bypass Switching</i> | 45 |
| 3.4.2 | <i>Steady State Active and Reactive Power</i> | 47 |
| 3.4.3 | <i>Worst Case Based on PQ Limits</i> | 48 |
| 3.5 | Summary of Design Process | 49 |
| Chapter 4 | Case Study Simulation and Evaluation Results..... | 50 |
| 4.1 | Description of Studied System..... | 50 |
| 4.2 | Design Results of the Proposed Scheme..... | 52 |
| 4.3 | Evaluation of the Proposed Method based on Case Study | 57 |
| 4.4 | Conclusions and Summary | 60 |
| Chapter 5 | Feasibility Investigations of Soft Starter Based Method..... | 61 |
| 5.1 | Synchronization of Two Systems by Soft Starter Method..... | 62 |
| 5.2 | Voltage and Current Waveforms during Soft Start Process | 64 |
| 5.3 | Design Considerations | 66 |
| 5.3.1 | <i>Impacts of synchronizing parameters</i> | 66 |
| 5.3.2 | <i>Constant α Firing Vs Time Voltage Ramp System</i> | 68 |
| 5.3.3 | <i>Other Technical Issues to Consider</i> | 69 |
| 5.4 | Application Example | 70 |
| 5.4.1 | <i>Test System under Study</i> | 71 |
| 5.4.2 | <i>Simulation Results</i> | 73 |
| 5.5 | Summary and Conclusions | 77 |
| Chapter 6 | Conclusion and Future Work..... | 79 |
| 6.1 | Thesis Conclusions and Contributions..... | 79 |
| 6.2 | Suggestions for Future Work | 80 |

| | |
|-------------------------|-----------|
| References | 82 |
| Appendix..... | 87 |

List of Tables

| | |
|--|----|
| Table 1.1: Synchronization Criteria for Synchronous Generators and Distributed Resources | 5 |
| Table 2.1 Interconnection System Response to abnormal voltages..... | 19 |
| Table 2.2: Generators Relay Protections for Off-Nominal Frequency Operations | 20 |
| Table 3.1 Synchronizing Limits Based on IEEE C50.12..... | 27 |
| Table 4.1 Thevenin Equivalent (SUB) Data [10] | 51 |
| Table 4.2 Synchronous Generator Data [10] | 51 |
| Table 4.3 Excitation Control and Governor-Turbine Data [15] | 52 |
| Table 4.4 Synchronizing Conditions for Worst Case Transients..... | 53 |
| Table 4.5 Power flow results for the four possible worst cases..... | 56 |
| Table 5.1 Thyristor Parameters..... | 72 |
| Table 5.2 Case studies on the effects due to voltage magnitude difference ΔV ... | 75 |
| Table A.1 Synchronous Generator Data | 88 |
| Table D.1: Case Investigations into Inductor vs. Resistor Insertion..... | 98 |

List of Figures

| | |
|--|----|
| Figure 1.1 Schematic of the feedback control synchronization method..... | 6 |
| Figure 2.1 Single Line diagram for a single SG based islanded system..... | 12 |
| Figure 2.2 Multiple feedback control loops necessary for islanded system synchronization..... | 14 |
| Figure 2.3 Analogy of synchronizing transients to the generator short circuit transients | 15 |
| Figure 2.4 Methods to reduce switching transients a) Impedance pre-insertion b) Soft starter used for starting motors c) Sequential phase energization proposed for transformer energization | 18 |
| Figure 2.5 The scheme of the proposed method and power quality limits for both sides of the breaker in accordance to utility protocol | 22 |
| Figure 2.6 Procedure for performing the proposed scheme..... | 23 |
| Figure 3.1 Acceptable transient region defined by standard..... | 28 |
| Figure 3.2 Stability limits based on power angle curves for a) steady state operation and b) transient disturbances..... | 29 |
| Figure 3.3 Operating regions of the islanded system and main grid (Bounded by PQ Limits)..... | 31 |
| Figure 3.4 Equivalent circuit representation of closing breaker 1: (a) Circuit before breaker 1 is closed. (b) Circuit after breaker 1 is closed. (c) Equivalent circuits after breaker 1 is closed..... | 32 |
| Figure 3.5 Sample distribution feeder with synchronous-machine DG synchronizes to grid | 35 |
| Figure 3.6 Peak stator current with different impedance pre-insertion values for typical generator parameter values | 36 |
| Figure 3.7 Single Line diagram for unloaded synchronous generator to system synchronization..... | 37 |
| Figure 3.8 P - δ curve representation of the rotor behavior for synchronization.... | 38 |

| | |
|---|----|
| Figure 3.9 Circuits for transient stability analysis: (a) Island to system synchronization single line diagram. (b) Before closing breaker (c) After breaker is closed..... | 40 |
| Figure 3.10 Simplified equivalent circuit of the islanded system after applying Y- Δ transformations | 41 |
| Figure 3.11 Impact of load to islanded system synchronization..... | 43 |
| Figure 3.12 Impact of impedance pre-insertion to islanded system synchronization | 43 |
| Figure 3.13 Worst stability case for islanded system synchronization..... | 44 |
| Figure 3.14 Representing impedance bypass by equivalent voltage source..... | 46 |
| Figure 3.15 Reactive power flows through the impedance insertion..... | 47 |
| Figure 4.1 Single line diagram of case study | 51 |
| Figure 4.2 Time domain simulation to obtain acceptable transient levels for current and torque | 53 |
| Figure 4.3 Worst case transients based on PQ limits..... | 54 |
| Figure 4.4 Peak current versus size of impedance insertion for the worst case.... | 54 |
| Figure 4.5 Feasible impedance range based on first switching transient and transient stability analysis | 55 |
| Figure 4.6 Worst power flow through the impedance based on load flow studies | 56 |
| Figure 4.7 Stator current during synchronization with and without impedance insertion..... | 57 |
| Figure 4.8 Torque transients during synchronization with and without impedance insertion..... | 58 |
| Figure 4.9 Rotor angle behavior with and without impedance insertion..... | 59 |
| Figure 5.1 Proposed Scheme based on soft starter and power quality limits for both sides | 62 |
| Figure 5.2 Islanded system to the main power grid synchronization procedure with thyristors based synchronizer..... | 63 |
| Figure 5.3 Voltage difference across SCRs for a) R-L load impedance applications b) Synchronizing with two voltage sources representation | 65 |

| | |
|--|----|
| Figure 5.4 Voltage and current waveforms at $\alpha=130^\circ$ of the soft starter device (Top), gating pulses applied to SCRs (Bot.) | 65 |
| Figure 5.5 RMS voltage across the SCRs with and without Δf for $\alpha=130^\circ$ | 67 |
| Figure 5.6 Differences in soft synchronizing schemes a) Constant firing angle b) Time voltage ramp system | 68 |
| Figure 5.7 P- δ curve representations of a) constant firing angle b) time voltage ramp system | 68 |
| Figure 5.8 Bypass times for different α between $90^\circ\sim 150^\circ$ | 69 |
| Figure 5.9 System Diagram (Top Level) | 71 |
| Figure 5.10 DG generation module diagram | 72 |
| Figure 5.11 Thyristor based Synchronizer Module | 72 |
| Figure 5.12 Comparisons of Transient machine torque, rotor frequency of SG at angle differences of 5° , 10° , and 20° with and without thyristor based synchronizer ($\alpha=130^\circ$). a) Electric torque of SG, at $\Delta\theta=5^\circ$, b) Frequency of SG, at $\Delta\theta=5^\circ$, c) Electric torque of SG, at $\Delta\theta=10^\circ$, d) Frequency of SG, at $\Delta\theta=10^\circ$, e) Electric torque of SG, at $\Delta\theta=20^\circ$, f) Frequency of SG, at $\Delta\theta=20^\circ$ | 73 |
| Figure 5.13 Impact of Δf on the peak stator current for different voltage levels from 0.9~1.1pu and $\Delta\theta=20^\circ$ | 74 |
| Figure 5.14 Peak current and torque simulation results for cases of $ V_1 > V_2 $ at $\alpha=130^\circ$ | 76 |
| Figure 5.15 Relationship between peak machine torque and product of internal and terminal voltages | 76 |
| Figure 5.16 Peak current and torque simulation results for cases of $ V_1 < V_2 $ at $\alpha_0=130^\circ$, and ramp decrement of $5^\circ/\text{cycle}$ | 77 |
| Figure A.1 Case study of two DG units performing open-loop synchronization with impedance pre-insertion method..... | 87 |
| Figure A.2 Acceptable current and torque transient peaks for a) SG1 and b) SG2 | 88 |
| Figure A.3 Worst case transients based on power quality limits for the two machines | 89 |

| | |
|---|-----|
| Figure A.4 a) Impedance selection based on breaker current. b) Peak stator current based on the designed impedance value. | 90 |
| Figure A.5 Feasible impedance range based on short circuit and stability analysis | 90 |
| Figure A.6 Worst possible power flows through the impedance computed by load flow studies | 91 |
| Figure B.1 Key components for generating the gating pulses to thyristors..... | 92 |
| Figure B.2 Constant/Ramp Firing Scheme building blocks | 93 |
| Figure B.3 Sawtooth outputs (top) and gating pulses (bottom) based on comparisons to the sawtooth outputs at $\alpha=130^\circ$ | 93 |
| Figure C.1 Comparison of short circuit calculation and EMTP simulation at case (2, 3) without impedance insertion | 95 |
| Figure C.2 Gate/valve positions response during islanded system synchronization based on impedance insertion method | 96 |
| Figure C.3 Mechanical power response during islanded system synchronization based on impedance insertion method | 97 |
| Figure C.4 Machine frequencies during islanded system synchronization based on impedance insertion method | 97 |
| Figure D.1 Size of R or X required to limit the first transient | 99 |
| Figure D.2 Rotor angle results for different cases without impedance insertion | 100 |
| Figure D.3 Rotor angle results for the inductor insertion | 100 |
| Figure D.4 Rotor angle results for the resistor insertion..... | 101 |
| Figure D.5 Field voltage results for zero impedance insertion..... | 102 |
| Figure D.6 Field voltage results for inductor insertion..... | 102 |
| Figure D.7 Field voltage results for resistor insertion | 103 |
| Figure D.8 Terminal voltage deviations for zero impedance insertion | 104 |
| Figure D.9 Terminal voltage deviation for inductor insertion..... | 104 |
| Figure D.10 Terminal voltage deviation for resistor insertion | 105 |

Chapter 1

Introduction

In power systems, there exists different scenarios to interconnect two electrical islands: 1) a generator synchronizes to the main power grid 2) an islanded electrical system (such as microgrid) synchronizes to the main power grid 3) one grid synchronizes to another grid, e.g. during system restorations. This process is required to bring the two islanded systems into synchronism with each other.

The connection of the two islanded systems has to be done under certain conditions or according to the synchronizing criteria, which are typically, defined by voltage, phase, and frequency differences across the synchronizing breaker. At the instant the synchronizing breaker closes, the voltage difference across the breaker should be at a minimal value, ideally zero. However, zero voltage difference is difficult to achieve in practice due to the frequency difference and the mechanical delay in closing of most circuit breakers. Therefore, the synchronizing criteria are imposed to ensure a smooth connection.

The process of satisfying these conditions defined by the synchronizing criteria while interconnect two islanded electrical systems is called synchronization. If two islands are synchronized outside the limits specified by the synchronizing criteria, instantaneous high current surge and subsequent power swings may severely damage power system equipment and most importantly, shortening the life span of generators.

Synchronization of islanded systems to the main power grid becomes a common task as more electrical islands are formed. At the turn of the 21st century, islanded systems in the form of microgrids are becoming more common due to their environmental, economic, and reliability benefits. A microgrid includes a variety of distributed energy resource units (including distributed generation (DG) and distributed storage (DS)) and different types of load. Improved reliability and

sustainability are some of the desired characteristics affecting the distribution system provided by the implementations of microgrids [1], [44]. Although current operational practices often prevent islanded operation of microgrids, with fast growth in distributed energy resource units, provisions for operating microgrids in both islanded and grid connected modes are becoming necessary [2]. Traditionally, synchronization of islanded systems is achieved through feedback-control based method to adjust the islanded distributed generators until the synchronization criteria are satisfied. One of the major challenges is that the islanded systems may reside in rural/forestry areas, where the DG units are located far away from the point of interconnection. In such cases, the communication infrastructure for synchronization is not readily available, inadequate, and costly to build. Additional difficulties arise when there are multiple DG units in the island. More specifically, multiple communication links are necessary to allow the tuning of individual DG units, which increases the efforts required to synchronize the islanded system.

This introductory chapter first presents an overview of the synchronization phenomenon. Secondly, synchronization scenarios are discussed in details. Then, the traditional method of synchronization is reviewed, and new challenges are identified for modern islanded system synchronization. Finally, the scope and outline of this thesis is presented.

1.1 The Phenomenon Involved in Connecting Two Systems

The phenomenon of connecting two systems can be illustrated by a close view of the rotor dynamics behavior in the scenario of generator to system connection. Prior to closing the main breaker, the frequency of the induced stator voltage and the angular velocity of magnetic field are governed by the rotor speed. A constant speed is maintained by the balance of mechanical power input and electrical power output of the machine. The rotor is driven by the prime mover connected by a mechanical shaft in between. For an unloaded generator, only a small mechanical power is required for the rotor to reach approximately the

synchronous speed due to the rotational/frictional losses. This mechanical power is adjusted by the governing and turbine system of the machine controls in order to meet the load demand within the islanded system.

Once the generator main breaker is closed, the generator is connected to the power system, so the frequency of the stator voltage is governed by the power system frequency. The rotor and the rotating masses of the mechanical system have to change speed and angular position to become aligned with the power system. If the angular speed and position of the rotor is closely matched with the main power grid at the instant of breaker closing, the transient torque that is developed in order to bring the rotor into synchronism with the grid is considered to be acceptable. Otherwise, the resulting transient torque can go beyond the acceptable limit of the generator, and severe damages can be imposed on the machine's rotor and shaft. Moreover, this transient torque is a function of the transient current. As a result, a high transient current can damage the stator and the transformer windings of the machine. The peak synchronizing current depends heavily on the voltage difference the instant breaker is closed. Similar to a short circuit at the generator terminal, the synchronizing current contains both AC and DC components, where the DC component decays exponentially as a function of time.

1.2 Different Synchronization Scenarios in Power System

Synchronization of power system islands generally involves three scenarios: a generator synchronizes to the main power grid, an electrical islanded system synchronizes to the main power grid, and a power grid synchronizes to another grid (appeared in system restorations).

The basic mechanism behind generator to grid synchronization has already been discussed in the previous section. Connecting generators to the grid allows generating facility owners to sell power to the utility companies. Furthermore, at higher load demands, where there is shortage of electricity power supply, more

generators are needed to be dispatched and synchronized to the grid, in an order specified by utility practice.

Power system islands can operate in parallel to the main power grid, or can operate in islands by providing power to critical loads locally. For effective operation in islanded mode, several different methods have been proposed for controlling the islanded system [3]-[5]. The unique feature of a power system island enables high penetration of DG without having to re-design or re-build the distribution system. Distributed generation units within the islanded system can be categorized as either conventional DG (such as reciprocating engines, and small hydro sources [6] using synchronous generator as an interface medium to grid), or nonconventional DG (including primary energy sources such as wind, micro-turbines, solar PV, and fuel cell, which use power electronic converter as an interface/inversion to grid).

Synchronization of islanded systems to the main power grid is different from that of a single generator scenario. Voltage and frequency of the islanded system, when operating in islanded mode, is determined by multiple distributed generation units (DGs) and loads. After the reconnection process, the individual DG's electric power output and frequency are mainly affected by the power vs. frequency droop control characteristics. Moreover, local DGs prior to synchronization should be providing automatic voltage regulation and reactive power support to the island to ensure reliability and voltage stability of the distribution system. Therefore, a voltage magnitude difference is expected across the synchronizing breaker if the system voltage deviates from the voltage of the islanded synchronizing bus. Although an islanded system is architecturally far more complex than a single generator, but the synchronization phenomenon still remains the same. Consequently, similar synchronization criteria were developed, which is shown in the next section.

Although the last scenario is not discussed in further details in this report, but fast synchronization process is certainly quite desirable to have as part of a system

restoration plan. Under emergency situations, immediate and fast restoration of power can become very beneficial to both the utility and electricity consumers.

1.3 Traditional Synchronization Practices and New Challenges

In the traditional synchronizing practices, voltage across the breaker at the substation location is monitored and sent to the operator at the generation site. The operator then uses these measurements to adjust machine controls (governor and exciter settings) to meet the synchronization criteria [7].

Different synchronization criteria have been shown in Table 1.1, which are specified by IEEE standards. As shown, for similar power ratings, both standards IEEE C50.12 [8] and IEEE 1547 [9] provided similar synchronizing limits, except IEEE 1547 stated a slightly higher frequency difference, $\Delta f = +0.1\text{Hz}$, and a slightly lower voltage magnitude difference of $\Delta V = 3\%$. It is important to realize the main difference between the two standards is the type of the islanded system's DG energy source. IEEE C50.12 and C50.13 are more specific to synchronous generator based power islands, but the IEEE 1547 is established to include both rotating prime movers and power electronic interfaced renewable energy resources.

Table 1.1: Synchronization Criteria for Synchronous Generators and Distributed Resources

| Standards | ΔV (%) | $\Delta \theta$ (Deg.) | Δf (Hz) | Purpose of standard |
|---|----------------|------------------------|-----------------|---|
| IEEE C50.12 & C50.13 [Salient pole and cylindrical rotors] | 0 ~ +5 | $\pm 10^\circ$ | ± 0.067 | Synchronizing criteria established for synchronous generators for hydraulic turbine applications rated $\geq 5\text{MVA}$. |
| IEEE 1547 [Distributed Resources (DR) including both rotating and non-rotating prime movers] | 10 | 20° | 0.3 | Aggregate rating of DR units: 0-500 (kVA) |
| | 5 | 15° | 0.2 | Aggregate rating of DR units: 500-1500 (kVA) |
| | 3 | 10° | 0.1 | Aggregate rating of DR units: 1500-10000 (kVA) |

Automatic synchronization methods based on feedback control strategies have been presented in literature [10], [11]. Recently, an active synchronization strategy that takes into account voltage unbalances and harmonic distortions is presented in [12]. In order to implement such feedback control systems in practice, infrastructure support such as communication links must exist to carry the signals from the breaker location (substation) to the local machines as shown in Figure 1.1.

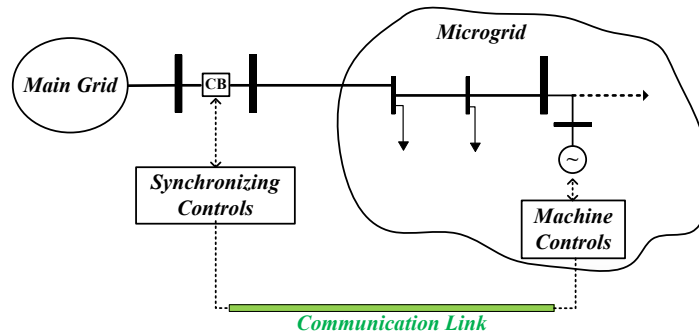


Figure 1.1 Schematic of the feedback control synchronization method

In reality, synchronizing systems exist to perform controls to the machine and close the circuit breaker as close to a zero-degree angle difference as possible. Generators traditionally have been synchronized by manual means, such as observing synchronizing lamp and electromechanical synchroscope by the operator. Based on the visual indicators, the operator, which is usually at the generating site, can determine whether to raise or lower the generator voltage and frequency. Over the years, automatic synchronizers that can perform all functions required to synchronize generators are also in place [13]. This form of synchronizer can send the slip and voltage difference measurements at the breaker as an error signal to the generator control system. The machine control system then adjusts the generators until the synchronizing criteria are met before the reconnection to the main power grid.

Based on the feedback control synchronization scheme, various control strategies are presented in the field of recent islanded system synchronizations. However, new synchronization challenges are essentially caused by the

geographical locations and structure of the islanded system. One of such examples is related to the technical difficulties of controlling a significant number of DG units within the islanded system for the purpose of synchronization. In addition, the fundamental problem associated with fast sensors and complex control structure is low reliability. More specifically, one software error or component failure in the control system is very likely to bring the entire system down [14]. Moreover, in most of the modern research and literature regarding islanded system synchronizations [10], the existence of the communication link, such as the one shown in Figure 1.1, is only assumed rather than truly justified. Therefore, as one of the key highlights of this report, is to clearly identify the issues related to the traditional feedback control scheme as a first step, which will be presented in the next chapter.

1.4 Thesis Scope and Outline

The scope of this thesis is to propose a new synchronization strategy for connecting DG units within a power system island to the utility substation, as opposed to the traditional feedback-control scheme. Most of the past research in the field of generator and islanded system synchronizations focused primarily on the automatic control methods based on feedback-control strategies such as in [10]-[12]. However, the modern structure of an islanded system is dominated by the large number of DG penetrations, which may drive up the synchronizing efforts and costs significantly due to the increase in the total complexity of the islanded system control architecture. Hence, new challenges and concerns should be contemplated in regard to islanded system synchronization. Some of the key questions, which this thesis intends to answer, are as follows.

1. What are the challenges and issues associated with the traditional synchronization scheme by the method of feedback-control? More specifically, is this approach still an effective method towards the concept of islanded system synchronization?

2. What are the real concerns of synchronizing a synchronous generator (SG) based islanded system to the main power grid? Are there any existing solutions that can be utilized to mitigate the synchronizing concerns?

3. How to develop a new scheme towards islanded system synchronizations so that, both the issues brought by feedback controls and concerns of synchronization can be effectively mitigated?

4. How to design the new synchronization scheme? What are the practical and technical issues to consider when designing the new synchronization method? How to ensure the impacts due to synchronization is within an acceptable limit?

5. Under the proposed scheme, is there any other feasible method to mitigate synchronization concerns of an islanded system?

In order to address the above questions and concerns, this thesis proposes an open-loop based synchronization strategy. To allow the implementation of the new scheme, several transient reduction methods are considered, designed, and their supporting technical studies are presented. The following paragraphs briefly summarize the organization of individual chapters of this thesis.

Chapter 2 first gives an overview of the SG based islanded system structure. The dominant energy sources based on this particular interface are identified. By knowing this type of structure, the issues brought by the traditional feedback control method are investigated. Then, the real synchronization concerns are identified, and hence, the system-wide synchronization objectives are clearly stated. Existing transient reduction methods to address the synchronization concerns are briefly explained.

Secondly, a method to enable the open-loop synchronization scheme is proposed. Before the islanded system is connected to the main grid, the operating conditions of the islanded system, similar to the main grid, are within the power quality (PQ) limits established by utility protocol. In order to synchronize the power system island within the PQ limits, the impedance pre-insertion method is

adopted, which is widely used in industry for reducing switching transients. However, there are a series of technical design considerations that need to be further investigated and verified when implementing this method.

Some of the design considerations when implementing the proposed scheme are explored in the details of chapter 3. In order to limit the first switching surge due to the breaker closing, an acceptable transient level must be established as a first step. Then, the design considerations regarding the method of impedance pre-insertion are discussed in the order of the actual synchronization process: 1) switching surge by closing the synchronizing breaker 2) Transient stability impacts on the SG units 3) Second switching surge due to impedance bypass.

Chapter 4 presents the design results to show the feasibility of the proposed scheme. Various analytical and simulation studies have conducted in this chapter to evaluate the effectiveness of this method in synchronization of an islanded system to the main power grid.

Chapter 5 investigates the feasibility of the soft starter method in synchronization. Furthermore, in order to enable open-loop synchronization based on the PQ limits, practical design considerations on the thyristors based synchronizer are discussed and key simulation results are presented.

Finally, the main conclusions of this thesis and future works for this field are summarized in chapter 6.

Chapter 2

Proposed Method for Open-Loop Synchronization Scheme

As discussed earlier, for an islanded system to the main power system synchronization, there are reliability and economic challenges related to the feedback-control synchronization scheme, which forms the motivations behind finding a new synchronization strategy. In response to these issues and challenges, a novel open-loop synchronization scheme is developed and proposed in this chapter.

As the name implies, the method does not require a communication link between the DG units and the breaker location. The proposed method is inspired by the practices of controlling switching transients. The idea here is to pre-insert an impedance to reduce the synchronization transients. With this method, infrastructure cost and complexity of synchronization can be reduced significantly since the communication link between the breaker and the DG unit is no longer required. Therefore, substantial improvements in the economic and reliability aspects by this proposal are expected. In the process which leads the proposed scheme, first, the motivations for a new synchronization strategy for islanded systems are elaborated in section 2.1. The power quality limits for normal system operations are reviewed in section 2.2. The open-loop synchronization scheme is demonstrated in section 2.3 in more detail. The design considerations of this scheme are identified and summarized in sections 2.4 and 2.5, respectively.

2.1 Motivations for New Islanded System Synchronization Strategies

A critical initial step in finding a new feasible and practical solution towards islanded systems synchronization is to understand the structure of the electrical island, and identify the main drawbacks of the traditional synchronization method.

As discussed earlier, the traditional synchronization approach is mainly based on the feedback control scheme, where the control signals to the machine are based on remote sensing of the information communicated from the synchronizing breaker. However, based on the structure of the islanded system, and potential issues introduced by the feedback control scheme, it is worthwhile to reconsider the real concerns of synchronization to clearly understand which, are the true synchronization objectives.

This section is organized as follows. In sub-section 2.1.1, the concept of the synchronous generator (SG) based islanded system is briefly introduced. In addition, the advantages and the importance of synchronous generator in the islanded system are reviewed. In sub-section 2.1.2 recognizes the issues regarding the feedback control scheme, and hence, the real impacts and concerns of synchronization are identified through a review of literature in sub-section 2.1.3. Finally, in sub-section 2.1.4, existing methods to mitigate switching transients are discussed and summarized, which some of these practical techniques are utilized for enabling the proposed open-loop scheme followed in section 2.2.

2.1.1 Synchronous Generator (SG) Based Islanded Systems

Synchronous machine have been widely used in the power system as generators to provide three phase electric power to the grid. Moreover, synchronous machines are also used as synchronous motors (for driving large loads) and synchronous condensers (to provide reactive power compensation and voltage support) [15].

The advantages of synchronous generators partially explain their dominance in the power system today. The term “synchronous” describes the nature of the machine to operate at a constant power system frequency. With proper machine controls, the synchronous machines can ensure a balance of power in supply and demand of the power system. By adjusting the field excitation, which is provided by an external DC source, synchronous generators can simply operate in both

leading and lagging power factor. Therefore, they can be used to generate or absorb reactive power as required by the power system, hence can ensure the power system is operating within its power quality limits. Furthermore, synchronous generators are inertia based, which can maintain in synchronism with the grid due to transient disturbances.

Among the various types of distributed generators proposed for islanded systems, the synchronous generators are actually the most common type [16]. Synchronous generators are widely used as the interface between the energy source and the islanded system in several DG technologies including combined heat and power (CHP) [17]-[18], internal combustion engine, and small hydro. A simplest single SG based electrical island is shown in Figure 2.1. The prime mover is connected to the rotor of the synchronous machine by a mechanical shaft. In islanding mode, both the real and reactive power outputs of the SG must match the local load consumption. Each time the islanded system is supposed to switch by the circuit breaker from islanded to grid-connected operation mode, the SG has to be synchronized with the main grid at the point of common coupling (PCC).

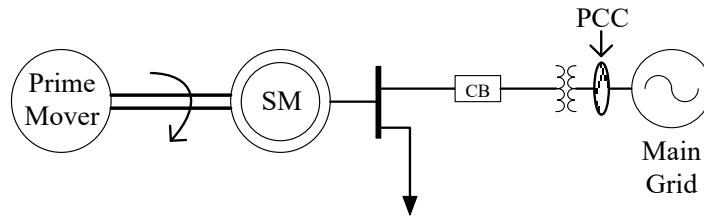


Figure 2.1 Single Line diagram for a single SG based islanded system

Especially in the case of CHP, where it is one of the most promising applications in the new concept of islanded system because, an increase in the number of CHP applications will lead to an increase in the overall energy efficiency of the whole system [14]. Since CHP implies an integrated energy system, which delivers useful heat and electricity from energy sources such as natural gas, it is more likely for this type of DG unit to be located near heat loads. Therefore, DG units can be placed quite scattered geographically.

Moreover, MW-scale islanded systems based on hydro energy supplying small towns in rural areas are becoming a common scenario in Brazil. Put it into perspective, Brazil has more than 500 small hydro plants with total installed capacity over 2.5 GW [19]. Most of these hydro plants have the potential to operate on an island mode. However, one of the most challenging tasks, which prevent the implementation of an intentional islanding, is the difficulties encountered in automatic reconnection to the main grid [10]. These difficulties are analyzed and summarized in the next section, which are the important issues that motivated the intention of this thesis.

2.1.2 Synchronization Issues Brought by Feedback Control Method

This sub-section is presented to clearly identify the issues brought by the feedback control synchronization scheme, especially in the case of an islanded system. As discussed earlier in section 0, background to the feedback control method used in the traditional synchronization methods was introduced. In summary, whether if the synchronization process is implemented manually or automatically, some forms of communication must exist between the DG site and the PCC point, such as by phones, communication links (fiber-optics) [7], etc. This process of synchronization is achieved by feedback control tuning of DG units, such that the synchronization criteria is met through tuning of the DG units before closing the breaker. The following summarizes the key issues introduced by this method of feedback control related to islanded system synchronizations:

1. In order to implement feedback control systems in practice, infrastructure support such as communication links are necessary to carry the signals from the PCC location (substation) to the local DG machines. However, the problem is that the DG units might be located in a rural or forestry area, which is far away geographically from the PCC to the main grid. Therefore, the cost of communication infrastructure can be prohibitively high. One of such example is stated in [10], where rural islanded systems are becoming common in Brazil.

2. Additional difficulties arise when there are multiple DG units in the islanded system shown in Figure 2.2. In this case, multiple communication links are necessary to allow the tuning of individual DG units. Therefore, synchronizing by feedback control can further drive up the cost of infrastructure support and increase synchronization effort. Especially in the case of CHP based DG units. Due to the fact that this type of resource can provide useful heat to consumers, they tend to be located near heat loads as mentioned earlier, so CHP plants can be located quite scattered [14] within the area where multiple communication links are required.

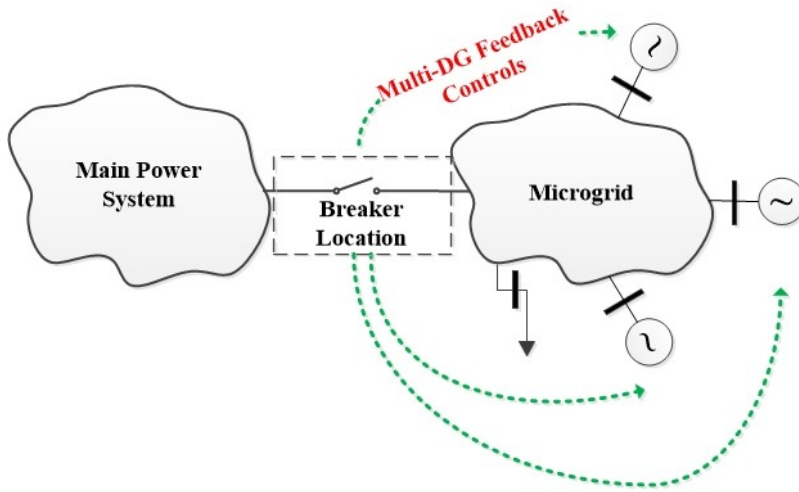


Figure 2.2 Multiple feedback control loops necessary for islanded system synchronization

3. Low reliability is also one of the major concerns associated with islanded system communications and control structure. Low reliability is resulted from two main consequences: system failures and inadequate communication infrastructures. System failures can be resulted from software errors, one of such errors can significantly impact the control system, which may lead to system shutdowns [14]. Inadequate communication infrastructures are referring to communication means such as by phones, which is quite common in rural areas of Brazil [10]. Therefore, not only the synchronizing criteria are difficult to meet by the operators on phones, but also the synchronization process can be delayed in order to reconnect to the main grid.

In response to the above challenges, a novel open-loop synchronization method is proposed in section 2.2 of this chapter. Before the method is introduced in more detail, it is worthwhile to realize the main concerns related to synchronization of two power systems. This is reviewed in more details in the next sub-section.

2.1.3 Synchronization Concerns and Objectives

The main concern relates to synchronization of two power systems or a generator to system is the transients produced when the synchronizing circuit breaker is closed. Excessive transients can lead to large inrush current and transient torque, damaging the generator and other equipment. This is similar to a generator terminal short circuit like closing to a fault shown in Figure 2.3.

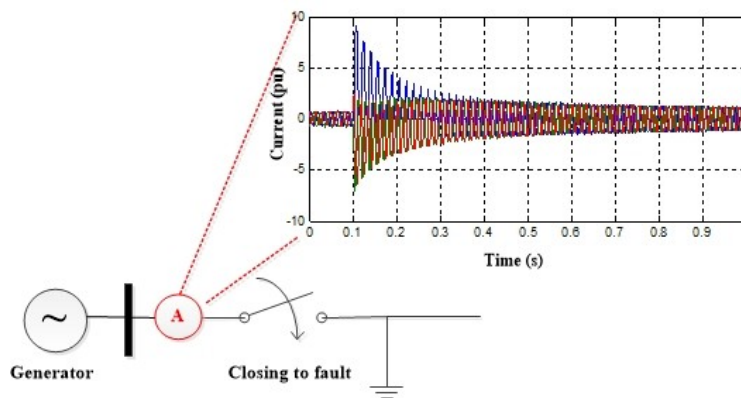


Figure 2.3 Analogy of synchronizing transients to the generator short circuit transients

However, the instantaneous current transients can be more severe than a three-phase fault that the generator or the transformer windings designed to withstand. The consequences to a poor or faulty synchronization of two systems can be summarized as:

1. Damage the windings of generator and transformer caused by high synchronizing current [7], [20]-[21].

2. Damage the shaft and prime mover of the generator because of high mechanical stresses caused by transient torque incurred by synchronization [22]-[23] .

3. Inability to synchronize to the main power system due to generators becomes rotor angle unstable.

Based on the real concerns stated above, the main objectives for synchronizing an islanded system are to reduce switching transients to protect power system equipment and ensure stability of all DG units. The current practice of reducing synchronization transients is to limit the voltage, angle, and frequency difference between the two parties through feedback control of DG units. However, there are other ways to reduce switching transients, which are briefly introduced in the next sub-section.

2.1.4 Existing Switching Transient Mitigation Techniques

Based on the common practices and concerns related to two power systems synchronization, what the synchronization process is really trying to accomplish is a soft, transient-free synchronization of two islands, which leads to normal and stable power system operation after two islands have been connected. The common practice as addressed earlier uses an auto-synchronizer to reduce the voltage difference across the synchronizing breaker by providing feedback control signals back to the generating unit, this way, the switching transient is minimized within the synchronizing criteria.

However, the method of reducing voltage difference is only one of ways to reduce switching transient. Actually, it is one of the most difficult ways to synchronize an islanded system to the main power grid because of the feedback control issues identified in sub-section 2.1.2. There are other existing methods to reduce switching transients [24], which open up the possibilities to simplify the synchronization of an islanded system to the main power grid:

- Impedance pre-insertion (Used Capacitor energization)

- SCR based Soft Starter (Used in Motor starting)
- Point on Wave Switching (Used in Capacitor and transformer energization)
- Sequential phase Energization (Proposed for transformer energization)

Some of the schematic diagrams for these methods have shown in Figure 2.4 below. A good example is the impedance pre-insertion/bypass scheme used to limit capacitor switching transients shown in Figure 2.4 (a). Both pre-insertion inductors and resistors can be used to limit the capacitor switching transients. A relatively new technology is also developed to reduce capacitor switching transients, which is called the point-on-wave switching or synchronous closing technique. In this method, the switches for each phase are timed to close at a zero crossing of the phase voltage for initially uncharged capacitor banks. However, due to its control complexity, the costs of the switches are higher than normal circuit breakers.

The connections of soft starters to the motor are shown in Figure 2.4 (b). One of the main reasons to implement such device for reduced voltage start is to limit the inrush current the motor draws from the main power grid when it is started [25]. This is a concern because the large inrush current may cause voltage sags, which is a power quality concern for voltage sensitive loads. In addition, the reduced voltage applied to the motor can be achieved by simply adjusting the firing angle to the gates of the six silicon controlled rectifiers (SCRs).

In more recent literature, a low cost transient mitigation scheme that connects a single resistor to neutral is proposed for sequential transformer energization [26], which is shown in Figure 2.4 (c). Rather than closing three circuit breakers at the same time, the breaker in each phase is closed sequentially with some time delay in between. This way, an optimal resistor size can be determined based on the minimum inrush currents of all three phases.

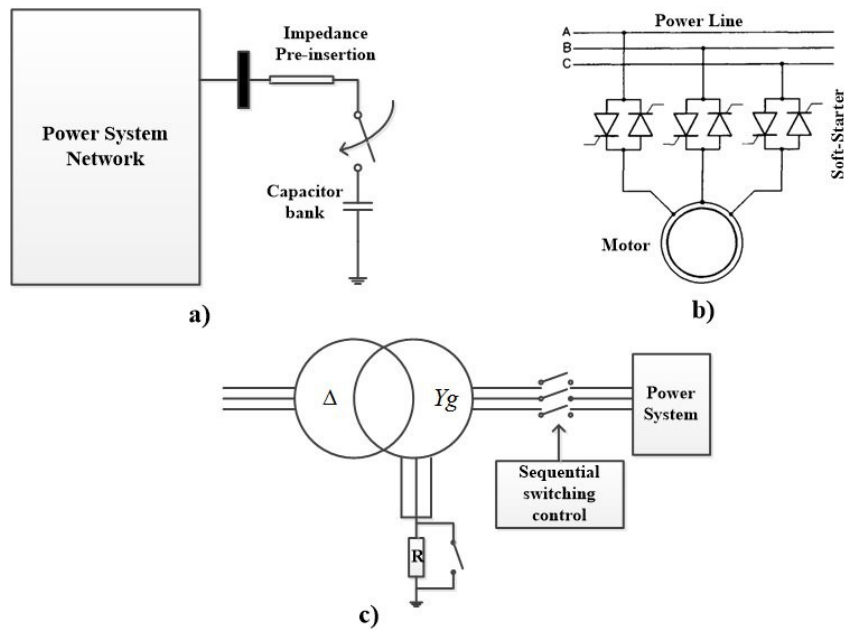


Figure 2.4 Methods to reduce switching transients a) Impedance pre-insertion b) Soft starter used for starting motors c) Sequential phase energization proposed for transformer energization

In view of the excellent performance of the impedance pre-insertion scheme on reducing switching transients, one may wonder if it can be used to simplify the synchronization of an islanded system to the main power system. Therefore, an impedance insertion method has been proposed in section 2.3 to enable open-loop synchronization scheme of an islanded system. Before introducing the open-loop scheme, it is important to realize the typical operating regions for both the islanded system and the main power grid before the reconnection process. This is also referred to as the power quality limits for the both sides to be connected in the section 2.2.

2.2 Power Quality Limits for Normal System Operations

The indices of interest in the context of power quality, from a synchronization perspective, are the voltage and frequency levels on both sides of the breaker before it is closed. It is important to ensure that these indices are within the power quality limits, in order to minimize any adverse effects to cause power equipment malfunctions [27].

According to the technical requirements for connecting generators to the Alberta Interconnected Electric System (AIES) [29], the typical operating voltages at the PCC are expected to vary within $\pm 10\%$ of the nominal voltage level. This variation in voltage magnitude also agrees with the IEEE standard 1547, which stated when the voltage is in the range given in Table 2.1, the DG shall cease to connect to the main power grid within the clearing times as indicated. As shown, the normal voltage operating range or the continuous operating region suggested by IEEE 1547 is from 89% to 110% of the nominal voltage [9]. This requirement of voltage levels can be maintained by means of reactive power compensation, such as by adjusting field excitation levels for synchronous generators or by switching in capacitor banks.

Table 2.1 Interconnection System Response to abnormal voltages

| Voltage Range (% of Nominal Voltage) | Clearing Time (s) |
|---|--------------------------|
| $V < 50$ | 0.16 |
| $50 \leq V < 88$ | 2.00 |
| $110 \leq V < 120$ | 1.00 |
| $V \geq 120$ | 0.16 |

The requirements on the power system voltage levels are one of the seven possible disturbance events defined by the Information Technology Industry Council (ITI) curve [28]. According to the definition steady-state tolerances, the RMS variation between $\pm 10\%$ from the nominal voltage may be present for an indefinite period of time, and are due to the effects of normal loading and system losses.

Similar requirements are also developed by utilities on the frequency range before synchronizing an islanded system to the main power grid. For example, the expected frequency range on the Alberta electric grid under normal system condition is between 59.95Hz and 60.05Hz. For any Generating Facility Owners that intended to interconnect a synchronous generator that may become islanded with a portion of the system loads, must maintain the island frequency within 59.7Hz to 60.2Hz [29] range before the island is able to synchronize to the main power grid. In order to achieve this frequency range, islanded generators must be

equipped with their own speed governors, which the governor droop settings shall be 5%.

Maintaining the system frequency near the nominal value, such as 60Hz of North America power system frequency, is not only due to the reason for efficient flowing of power in the fundamental frequency, but also because of reliability issues related to system-wide disturbances resulted from off-nominal frequency operations. Large frequency deviations from nominal can incur potential system collapses, cascading outages, and difficulties in restoring the system to normal operations [31]. In fact, the two parties to be synchronized under normal operation are operating within a frequency range, which is usually within the continuous operating range, as shown in Table 2.2. In the unlikelihood of a change in the system frequency and steps out of this range, under and over load shedding schemes are in place to accommodate this change in frequency in accordance to the requirements by the Western Electricity Coordinating Council (WECC) [30]. By the WECC requirements, the continuous operating range for frequency setting is from 59.5HZ to 60.5Hz for generators connected the main grid.

Table 2.2: Generators Relay Protections for Off-Nominal Frequency Operations

| Under-frequency Limit | Over-frequency Limit | Minimum Time |
|------------------------------|-----------------------------|-------------------------------------|
| 60.0-59.5 Hz | 60.0-60.5 Hz | N/A (Continuous operating range) |
| 59.4-58.5 Hz | 60.6-61.5 Hz | 3 mins |
| 58.4-57.9 Hz | 61.6-61.7 Hz | 30 s |
| 57.8-57.4 Hz | | 7.5 s |
| 57.3-56.9 Hz | | 45 power cycles |
| 56.8-56.5 Hz | | 7.2 power cycles |
| Less than 56.4 Hz | Greater than 61.7 Hz | Instantaneous trip |

2.3 Proposed Synchronization Strategy

As discussed previously in sub-section 2.1.3, the main concern on synchronizing two power systems is the transients produced when the synchronizing circuit

breaker is closed. Excessive transients can lead to large inrush current and transient torque, damaging generator and other equipment. The current practice of reducing synchronization transients is to limit the voltage, angle, and frequency differences between the two parties through the method of feedback control.

However, there are other ways to mitigate the transient problem as presented earlier in sub-section 2.1.4. A good example is the impedance pre-insertion/bypass scheme used to limit capacitor switching transients. In this scheme, the inserted impedance increases the total circuit impedance and thus reduces the inrush current. The impedance is bypassed after the system has reached the steady-state. In view of the excellent performance of this scheme on reducing switching transients, one may wonder if it can be used to simplify the synchronization of an islanded system to the main power grid.

The theoretical principles of the impedance pre-insertion scheme in reducing synchronizing current transient can be understood by studying the relationship given in Equation (2.1). The peak current transient I_{peak} is proportional to the voltage across the breaker and inverse proportional to the total impedance seen across the breaker,

$$I_{peak} \propto \frac{|\Delta V|}{X_{total}} \propto \frac{|\Delta V|}{X_{insert} + X_d'' + X_{eq}} \quad (2.1)$$

Where ΔV is the voltage across the synchronizing breaker before closing in RMS value, X_{insert} is the impedance (primarily inductive) inserted near the breaker location, X_d'' is the synchronous machine's direct axis sub-transient reactance, and X_{eq} represents the rest of the equivalent system impedance, which may include any transformer leakage reactance, series line impedance (positive sequence), and system impedance.

The power quality limits established by the utility protocol have been discussed previously, in section 2.2. Before synchronization, the island and the system are expected to operate within their respective power quality limits. This means that each party has a known operating region of voltage and frequency at

the synchronization point. The proposed idea is to establish a value of the pre-insertion impedance such that the resulting transient is always within acceptable limit as long as the two parties are operating within their power quality limits at the time of synchronization. Consequently, feedback control is not needed to adjust the operating point of the islanded system, and related feedback control issues can be effectively mitigated.

Figure 2.5 illustrates the proposed open-loop synchronization scheme. The power quality limits have been established in accordance to the requirements of Alberta Interconnected Electric System [29].

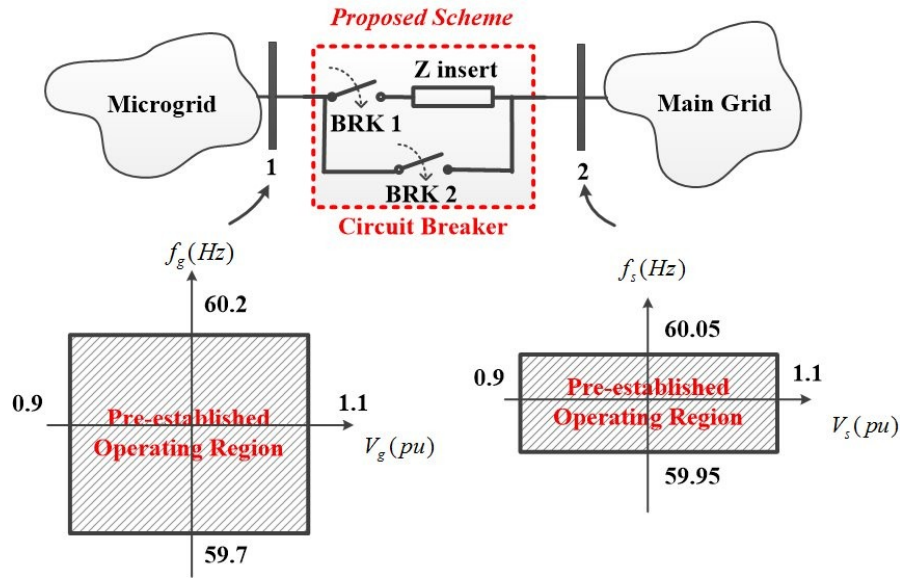


Figure 2.5 The scheme of the proposed method and power quality limits for both sides of the breaker in accordance to utility protocol

The corresponding power quality limits are in close agreements with that proposed by WECC since the province of Alberta is part of the western interconnected grid of North America. The proposed scheme is comprised of two switching states. The first switching is operated by closing the first breaker (BRK1) as shown to insert the impedance to reduce the switching transient. The second breaker (BRK2) is used to bypass the inserted impedance once the system has reached the steady-state operation and the voltage measured across the impedance is within the acceptable voltage level.

In order to demonstrate the procedure of the proposed open-loop synchronization in accordance to the above scheme, the flow chart diagram is shown in Figure 2.6. All the required measurements including voltage, angle and frequency (or slip) are performed at the circuit breaker location. If both parties are not operating within their respective PQ limits, then it implies that the power system do not fulfill the requirements of power quality that was pre-established by the utility protocol, which should be resolved before synchronization can be proceed further.

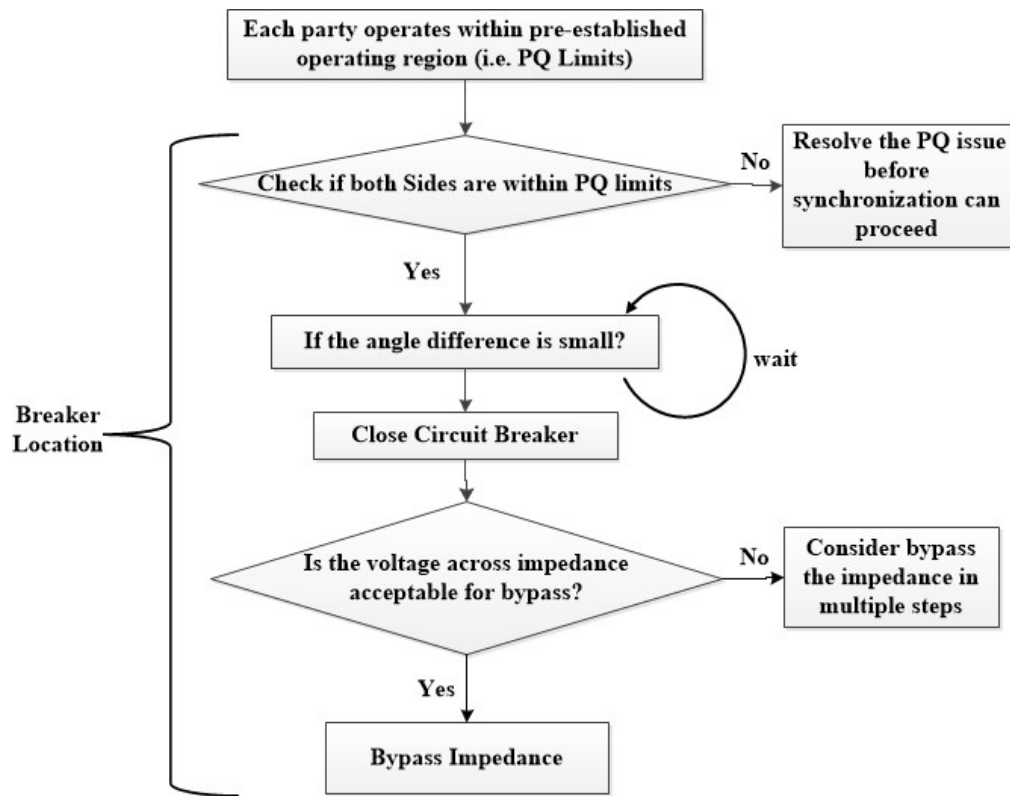


Figure 2.6 Procedure for performing the proposed scheme

2.4 Design Consideration and Challenges

From section 2.3, it is clear theoretically that a larger Z_{insert} will result in more reduction of inrush currents. However, it may increase the transient when the impedance is bypassed. In addition, larger Z_{insert} will weaken the synchronizing power between the islanded system and the main grid so instability may occur. Therefore, the following issues must be addressed for the proposed scheme:

1. What is the acceptable synchronization transient level? Is there a worst case to determine for the acceptable level of transients for stator current and machine torque?
2. What is the minimum impedance value of Z_{insert} which can lead to acceptable level of synchronization transients under the proposed scheme, i.e. open-loop synchronization?
3. What is the maximum value of Z_{insert} that can maintain system stability? Are the DG units remaining in synchronism with the grid after the first impedance switching?
4. Is the value Z_{insert} determined by issue 3 also results in acceptable bypass transients? How to determine the worst case bypass transients given that synchronization takes place under the proposed scheme?

In the chapter 3, the above issues are addressed one by one. A method to design the proposed scheme is developed accordingly. Chapter 4 shall present the design and simulation results on a case study.

2.5 Summary and Conclusion

An open-loop synchronization scheme based on the method of impedance pre-insertion to reduce switching transients has been proposed in this chapter. Some of the key points and highlights to summarize this chapter are:

- ✓ Both the power system islands and main power grid under the normal operating conditions before synchronization are already working in a pre-established utility protocol, which is inside the power quality limits.
- ✓ Based on the power quality limits of the two parties to be synchronized and the method of impedance pre-insertion to reduce switching transients, an open-loop synchronization scheme has been proposed.
- ✓ With the proposed scheme, infrastructure costs and the complexity of islanded system synchronization can be significantly reduced. This is because the communication links as needed by the traditional feedback control scheme are no longer required between the breaker and the islanded DG units.

Chapter 3

Design Process of Open-Loop Synchronization Scheme

In this chapter, the design issues and challenges for the proposed scheme are addressed and explained from both theoretical and analytical perspectives. These perspectives are essential to consider in the process of deriving a design method. In other words, they can help in understanding why such issues occur and also why they are important to the proposed scheme. For example, why does synchronization of two systems produce a high transient if the synchronizing criteria have not met the requirements? Therefore, this chapter investigates each issue in much more detail. Consequently, after the issues have been fully investigated, a method to design the proposed scheme is developed accordingly.

As well, these issues have been presented in individual sections, which follow the order of events happening throughout the open-loop synchronization process. In section 3.1, the maximum acceptable levels of surge (transient) and power oscillation from the perspective a synchronous generator are determined. As mentioned in the proposed scheme in the chapter 2, this method based on impedance pre-insertion is meant to enable open-loop synchronization of the islanded system to the main power grid. Therefore, section 3.2 shall determine the worst case surge resulting from the first switching operation when both parties have synchronized under their own power quality limits. Every time the islanded system has to be synchronized to the main grid, transient stability of the generators is one of the primary concerns. The effects of the proposed scheme on transient stability are evaluated in section 3.3. Similar to the first surge, bypass the impedance produces a second switching surge, which its severity must be within the acceptable level. Therefore, section 3.4 determines the worst case bypass transient. Finally, at the end of this chapter, a design method towards the proposed scheme is presented in section 3.5.

3.1 Define Acceptable Level of Transients and Power Oscillations

Define the acceptable level of surge must take into considerations of the maximum current and power oscillation tolerance levels from the perspective of the generators. Faulty synchronization is probably the most unwanted situation because the intense currents and torques may cause severe damage to the machines and prime movers. Therefore, based on current practice, strict limits have been applied to synchronizing synchronous generators to the system. One of such example is the IEEE standard C50.12 [8] and C50.13 [32] for synchronizing 60Hz synchronous generators/motors for hydraulic turbine applications. The details of synchronizing limits in this standard will be shown in subsection 3.1.1. Based on these limits, a method to determine the maximum acceptable current and torque limits are illustrated in subsection 3.1.2.

3.1.1 Synchronizing Limits Based on IEEE Standard

The synchronizing limits for synchronous generators rated 5MVA and above are shown in Table 3.1. The standard specifies that the generators should be designed to be in service without the need for inspections or repairs if it is synchronized with in the limits below.

These limits are established to ensure an acceptable transient level experienced by the generator in terms of stator current and shaft torque. The consequences due to improper synchronizations, such as synchronizing out of the ranges specified in Table 3.1, are discussed earlier in sub-section 2.1.3. It should be noted that for the most severe faulty synchronizations, such as 180° or 120° out-of-phase synchronizing to a system, the machine might require partial or total rewind of stator, or even replacement of rotor in the worst case [8].

Table 3.1 Synchronizing Limits Based on IEEE C50.12

| | |
|---|----------------------|
| Breaker Closing Angle | $\pm 10^\circ$ |
| Generator side voltage relative to system | 5% Max |
| Frequency difference | $\pm 0.067\text{Hz}$ |

3.1.2 Define Worst Case Acceptable Surge Level

The limits from IEEE standard C50.12 are established to ensure an acceptable transient level experienced by the generator in terms of stator current and shaft torque for synchronous generator to grid synchronizations. In order to find the worst transient, the limits have been transformed into an acceptable region shown in Figure 3.1. The possible worst case transients have been identified to be the four corners of the transformed region. The explanation is as follows.

As the synchronizing condition moves away from the origin, the current transient level will increase due to an increase in the voltage across the breaker. In addition, as the frequency difference (slip) increases as the synchronizing condition moves away from the origin, there will be a large transient torque on the mechanical system to bring the rotating masses to have the same angular velocity as the power grid [7]. As a result, the four corners of the region should be examined through simulations to determine the maximum acceptable current and torque, since they are farthest from the origin. The simulation results for the worst case are presented in the next chapter.

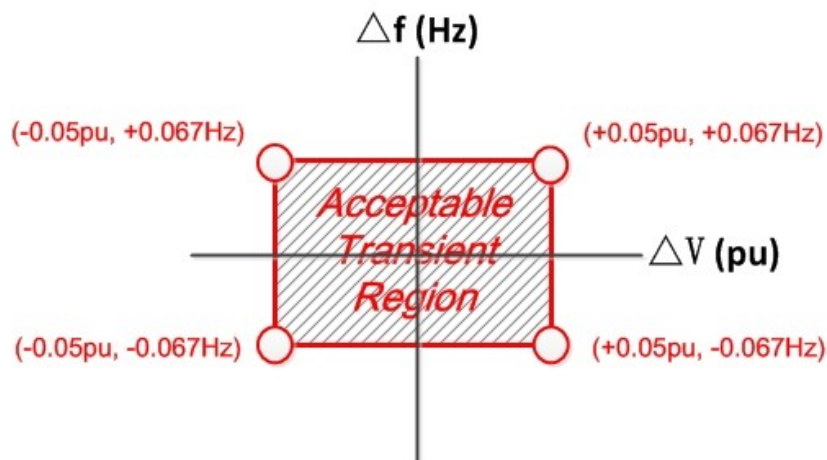


Figure 3.1 Acceptable transient region defined by standard

3.1.3 Acceptable Level of Power Oscillations

So far, a way to find the maximum acceptable current and torque transient levels based on synchronizing limits is presented in this chapter. Once the acceptable levels are determined, the current and torque transients of the islanded system DG units can be analyzed under the open-loop synchronization scheme. Consequently, a minimum size of impedance can be determined.

The maximum power oscillation level is expressed by the maximum rotor angle which usually happens during the first transient swing. A limit is required to ensure that the synchronous generator of the DG unit will successfully be synchronized with the grid and will not become unstable. The industry practice is to consider 45 degrees as the maximum rotor angle for transient stability studies [33] as shown in Figure 3.2 (b). The same value is used in this thesis as the maximum acceptable rotor angle in order to characterize the maximum allowable power oscillation. Maximum rotor angle reached below 45 degrees can ensure the stability of the generators because there are sufficient stability margin between the mechanical power P_m and the maximum power transfer capability limit, P_{max} , which typically occurs around 90 degrees in the power-angle curve, which is the maximum power transfer capability as shown in Figure 3.2 (a).

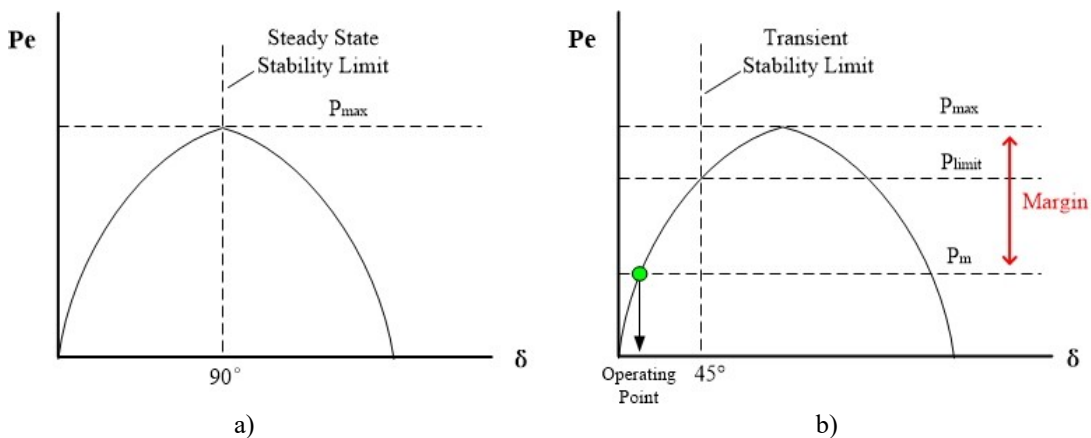


Figure 3.2 Stability limits based on power angle curves for a) steady state operation and b) transient disturbances

3.2 Minimization of First Switching Surge

As mentioned in the proposed scheme in chapter 2, the goal is to select a proper impedance size to enable open-loop synchronization when the two parties are synchronized under their corresponding power quality limits. The power quality limits based on the technical requirements for connecting generators to the Alberta Interconnected Electric System (AIES) has been presented in the proposed scheme shown previously in Figure 2.5. In order to reduce the first surge resulted from the first breaker closing, an appropriate size of impedance shall be chosen carefully so that the peak current and torque transients incurred within the power quality limits are within the acceptable level pre-established in section 3.1.

Similar to the procedure of obtaining the worst case acceptable transients, the regions of power quality limits (PQ Limits) of the islanded system and the main power grid are firstly established in the next sub-section 3.2.1. Moreover, the worst cases based on the PQ Limits are identified. In sub-section 3.2.2, analytical methods and equivalent schematic diagrams are presented in order to have an intuitive view on the phenomenon of synchronizing transients, and the minimum impedance size could essentially be determined by this analytical approach given system data and the open-loop synchronizing criteria. Although every steps of the design process can be accomplished through repetitive EMTP or dynamic simulations, but the analytical methods can provide a convenient way of simplifying the design process and verify the results obtained from simulations.

3.2.1 Worst Case Transient Levels of Proposed Scheme

As mentioned before, the method is meant to enable open-loop synchronization of the islanded system at any normal operating point defined by the power quality limits as shown in Figure 3.3. To make sure that the current and torque transients are both lower than their acceptable limits, all of the operating points of the two systems should be examined. However, it is evident that the

largest voltage and frequency mismatch will result in the largest synchronizing transients. As discussed earlier previously, a large voltage difference across the breaker can incur excessive inrush current transients, which can severely damage the generator and transformer windings. Moreover, a large frequency difference (slip) can primarily increase the transient torque stress on the generator shaft and the connected prime mover due the generator rotor speed tends to match the grid's frequency. The impacts due to slip across the synchronizing breaker is analyzed in further details in section 3.3.

Therefore, there are four combinational cases to consider based on Figure 3.3: *Case (2, 3)*, *Case (4, 1)*, *Case (3, 2)* and *Case (1, 4)*. Where, the first number inside the bracket refers to the operating point within the islanded system, and the second number refers to the main power system operating point.

It is worth to mention that 10 degrees angle difference is used to find the transient limits according to IEEE standard C50.12 [8]. In practice, according to an industrial survey on generator synchronizing report published in IEEE [34], the maximum closing angle can reach up to 20° when synchronization is done manually by an operator. In addition, a slow closing breaker due to mechanical delays can also result in an unexpected large angle closing difference [35]. Therefore, a worst case angle difference of 20° is used throughout the process of impedance design.

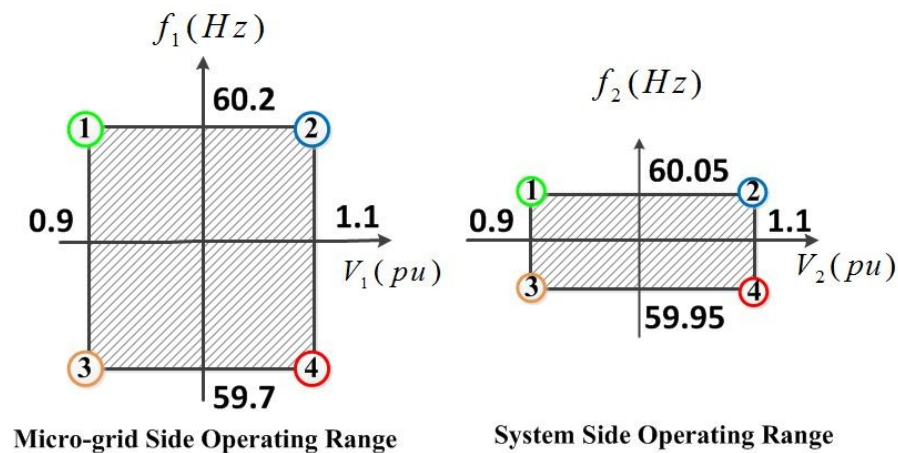


Figure 3.3 Operating regions of the islanded system and main grid (Bounded by PQ Limits)

3.2.2 Analytical Methods for Obtaining Peak Transients

The worst (highest) transient current and torque could be determined by simulating the four aforementioned cases. However, to have a better insight, an analytical expression is derived for the case of having only one synchronous generator based DG unit for the islanded system side.

The power system island is modelled as a synchronous generator with a constant impedance type load connected to its terminal, where the synchronous generator is represented by a fixed voltage behind its sub-transient reactance. This is usually a quite common assumption for short circuit and switching transient studies in power systems [36]. Before the breaker is closed, the current through the impedance is zero. However, the stator current of the synchronous machine consists of a steady state flow of load current as shown in Figure 3.4 (a). At the instant of the first breaker switching, this switch can be represented by two opposing voltage sources in series based on the method of superposition, as shown in Figure 3.4 (b). By applying the superposition theorem, the circuit shown in Figure 3.4 (b) can be split into two equivalent circuits shown in Figure 3.4 (c).

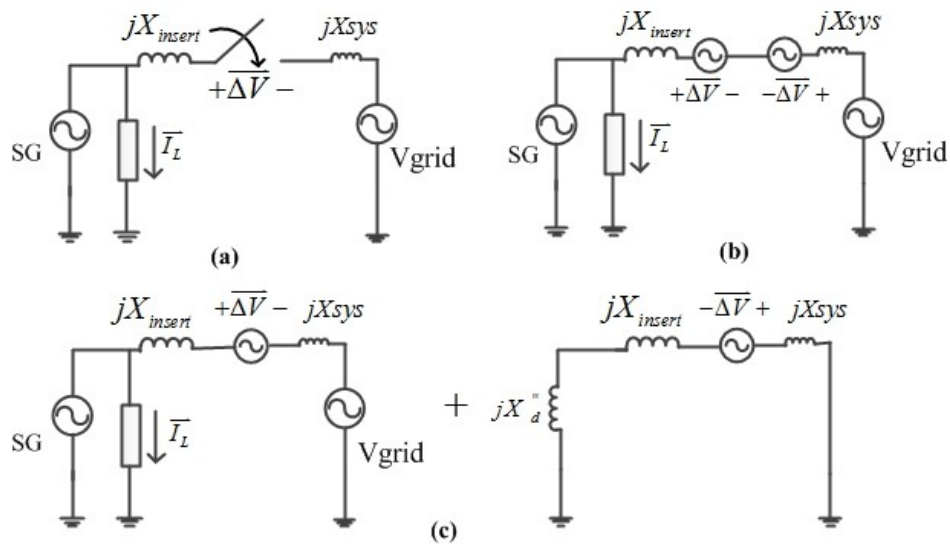


Figure 3.4 Equivalent circuit representation of closing breaker 1: (a) Circuit before breaker 1 is closed. (b) Circuit after breaker 1 is closed. (c) Equivalent circuits after breaker 1 is closed.

The circuit on the left side of Figure 3.4 (c) represents the same circuit before breaker is closed in steady state. Therefore, the current in this circuit represents the steady state component. In the context of synchronization, clearly as shown in Figure 3.4 (c), the steady state current is zero before the breaker closes. However, the transient current that is resulted from the first switching can be realized by the circuit on the right of Figure 3.4 (c). The right side circuit can be used to calculate the transient current from the switching voltage based on the principles of superposition. Note that the magnitude of the voltage is the same as the steady state circuit but in opposite polarity. Assuming Δf is equal to zero before the breaker is closed, the analytical expression for the transient component based on Kirchhoff's voltage law (KVL) for the circuit is,

$$L \frac{di(t)}{dt} + Ri(t) = \sqrt{2} \|\Delta V\| \sin(\omega t + \alpha) \quad (3.1)$$

where, $\|\Delta V\|$ is the magnitude of the RMS voltage at the instant of breaker switching, L and R are the total equivalent inductance and resistance, respectively, seen by the first breaker. ω is the angular frequency and α is the voltage phase difference across the breaker. The solution to the differential equation of (3.1) can be solved by using the techniques of solving ordinary differential equations (ODE) such as the method of Laplace Transformations, and the synchronizing current $i(t)$ can be obtained,

$$i(t) = \frac{\sqrt{2} \|\Delta V\|}{\sqrt{X_{eq}^2 + R^2}} \left[\sin(\omega t + \alpha - \varphi) - \sin(\alpha - \varphi) e^{-Rt/L} \right] \quad (3.2)$$

X_{eq} is the sum of series reactance X_d'' , X_{insert} , and X_{sys} . The total impedance angle φ is given by $\tan^{-1}(X_{eq}/R)$. As shown in equation (3.2), the synchronizing current due to the first switching consists of both AC and DC components. Therefore, the peak current is affected by both of these components, and if $\alpha = \varphi$, the DC component is completely eliminated. However, if $\alpha - \varphi = 90^\circ$, the peak current can reach twice as high as the steady state AC component. The decay of the DC offset in the second term is dependent on the L to R ratio of the total equivalent impedance seen by the breaker including the pre-inserted impedance.

The peak stator current from the perspective of the synchronous generator can be obtained by computing the sum of the pre-synchronizing load current and the synchronizing transient current from equation (3.2).

Based on equation (3.2), introducing the inserted impedance near the breaker location can add to the total series impedance of the line, therefore reduces the peak inrush current by reducing both the AC and DC parts of the total current. This is crucially important because at high angle differences across the breaker, such as 20°, regardless of the DC offset on the peak current, the magnitude of the voltage difference is already exceeding the acceptable level of voltage at 10° based on the IEEE standard C50.12. In other words, the methods of reducing the switching transient must be able to reduce both the AC and DC parts of the peak current, such as the impedance pre-insertion method. For example, the synchronous closing method [24], [37] alone is not sufficient enough to reduce the peak transient because it can only eliminate the DC offset, but the AC component still remains to have potential negative impacts on the life of DG units.

It is worth mentioning that the equations stated above are derived on the basis $\Delta f=0$ because the frequency difference under the power quality limits have negligible effects on the transient peak current. An explanation is realized by considering two voltage sources connected together with different frequencies. If one voltage source is taken as a reference running at angular frequency ω_1 , and the other voltage is running at a slightly higher frequency with an angle difference from the first voltage phasor, the instantaneous voltage difference when the breaker is closed at $t=0$ is given by,

$$|\overline{\Delta V}| = |V_1 e^{j\Delta\omega t} e^{j(\omega_1 t + \Delta\theta)} - V_2 e^{j\omega_1 t}| \quad (3.3)$$

where, $\Delta\omega$ equals to $2\pi(\Delta f)$, represents the angular frequency difference between the two voltage phasors having magnitudes V_1 and V_2 , respectively.

Based on the time window of the sub-transient period, the peak inrush current typically occurs within $t < 2$ cycles from the synchronization instant. Therefore,

the value of $\Delta\omega t$ is very close to zero for small frequency differences, so the impact of Δf on ΔV across the breaker will be negligible.

Based on the above analysis and theoretical equations established for the synchronizing current, one can understand the impacts of the different synchronizing parameters (ΔV , $\Delta\theta$, Δf) and the inserted impedance size $|Z|$ on the peak stator current. In addition, a minimum value of impedance can be chosen either by analytical equations or by EMTP simulation programs to reduce the peak current less or equal to the acceptable level of transients.

In order to illustrate the transient reduction effect due to the Z_{insert} , typical generator data values for both turbo and hydro generators [36] are adopted to compute the maximum stator current using equation (3.2) resulted from connections to the main grid.

The power capacity for the generator is assumed to be 5MVA. The step up transformer has a total leakage reactance equals to 5.5% based on the transformer's power rating. Prior to grid connection, an impedance load is connected to the terminal of the machine consuming full load current from the machine. The sample distribution feeder with synchronous-machine DG is shown below in Figure 3.5. The system side is represented by a Thevenin voltage source behind the short circuit impedance, which is based on the nominal voltage and the short circuit power capacity from the utility substation. The peak transient current comparisons between a turbo and hydro synchronous machines are shown in Figure for different values of impedance pre-insertions.

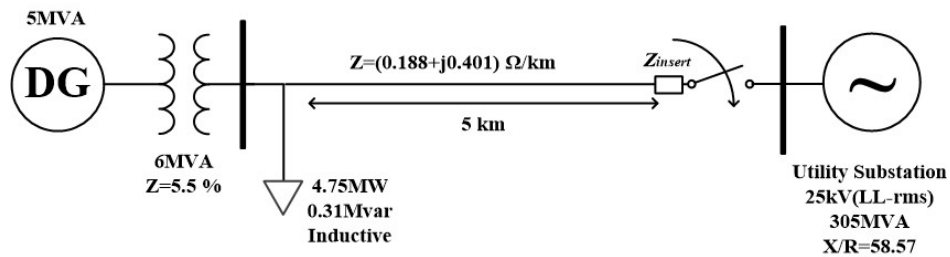


Figure 3.5 Sample distribution feeder with synchronous-machine DG synchronizes to grid

The typical effective reactance values X_d'' for the synchronous DG unit are 0.24 p.u. and 0.12 p.u., for hydro and turbo synchronous machines, respectively. As shown in Figure 3.6, two different acceptable stator current levels are established for the two machine types because of the difference in the X_d'' values. The peak current curves (solid black and blue lines) are obtained by equation (3.2) under the operating condition of case (2, 3) shown in Figure 3.3. Based on the analytical results, it can be seen that the machine's sub-transient reactance can significantly impact the minimum size of the impedance needed to reduce the peak current to an acceptable level.

For this sample distribution system with typical system parameters, the minimum required impedance sizes for turbo and hydro synchronous machines are, 0.206 p.u. (25.75Ω) and 0.319 p.u. (39.87Ω), respectively.

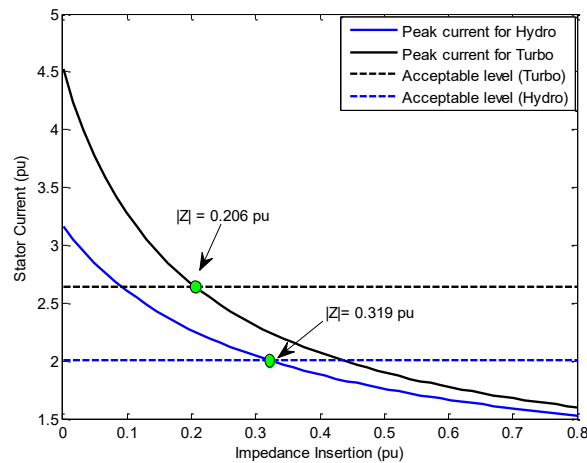


Figure 3.6 Peak stator current with different impedance pre-insertion values for typical generator parameter values

3.3 Transient Stability Considerations

Every time the islanded system has to be synchronized with the main grid, transient stability is one of the main concerns. The effect of inserting the impedance on the transient stability will be evaluated in this section. Then, the worst case which causes the maximum rotor angle will be identified. The ultimate

goal is to ensure that the maximum rotor angle in the worst case does not exceed the transient stability limit of the generator.

The worst cases of switching transients have been identified based on the pre-established power quality limits for both sides of the breaker, which is shown previously in section 3.2. Moreover, analytical derivations have been presented to show the impacts on the peak stator current of DG generator due to different synchronizing parameters and the size of impedance pre-insertion. Most importantly, a minimum size of impedance can be determined based on the worst synchronizing condition from the PQ limits. However, inserting the impedance at the breaker location adds to the total line impedance, therefore reduces the maximum power transfer capability, and hence, decreases the transient stability margin from the DG unit to the main power grid. This may result in the DG unit unable to become synchronized with the main power grid. Therefore, this section investigates the synchronization impacts on the stability of the islanded DG units through rotor angle stability analysis, which is shown in subsection 3.3.1. Effects of loading levels and the size of impedance pre-insertion are explained based on the power-angle relationships in subsection 3.3.2. Lastly, a worst case scenario is chosen based on the pre-established power quality limits.

3.3.1 Stability Analysis of an Island to System Synchronization

First, a simple case including a single unloaded synchronous generator shown in Figure 3.7 is considered for the islanded system. The system is represented as a constant voltage source behind its system short circuit impedance.

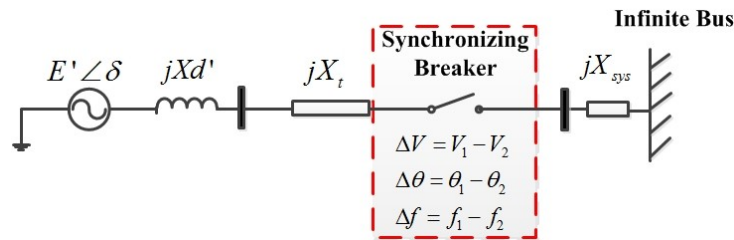


Figure 3.7 Single Line diagram for unloaded synchronous generator to system synchronization

The behavior of rotor angle oscillations can be better visualized by the well-known power-angle curve ($P-\delta$) as shown in Figure 3.8.

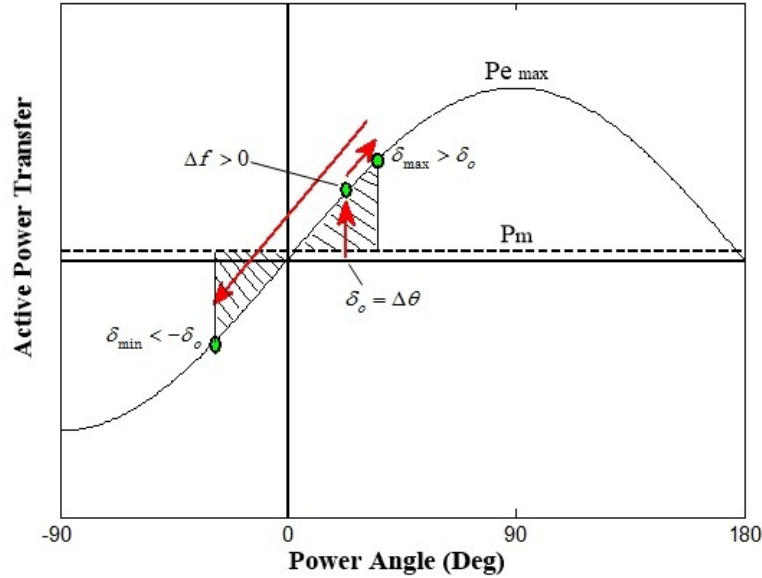


Figure 3.8 $P-\delta$ curve representation of the rotor behavior for synchronization

Immediately after the synchronizing breaker is closed as in Figure 3.7, the sudden torque and power surges are dependent on the instantaneous angle difference δ_o in Figure 3.8 across the open breaker before it is closed. Then, the direction of the rotor swing is dependent upon the relative power system island frequency compared to the main system voltage frequency. If the island's frequency is higher than the grid, the rotor angle advances further due to the need to dissipate the extra kinetic energy stored in the rotor. Therefore, a maximum rotor angle value will be reached, denoted by δ_{max} . At δ_{max} , the speed of the DG units or the frequency of island is equal to that of the system. At this point, the kinetic energy initially stored in the rotor and the rotating masses have been fully dissipated. Afterwards, the rotor dynamics can be explained by the famous transient stability analytical technique, the Equal-Area Criterion [36].

The rotor dynamics can be expressed by the classical definition of the swing equations with damping ignored [15],

$$\begin{cases} \frac{2H}{w_{syn}} \frac{d^2\delta(t)}{dt^2} = P_m - P_e \\ \frac{d\delta(t)}{dt} = \omega(t) - \omega_{syn} \end{cases} \quad (3.4)$$

Where, P_m and P_e are mechanical and electrical power, respectively. H is the machine inertia constant. $\omega(t)$ and ω_{syn} are the generator and system angular frequency, respectively. $\delta(t)$ represents the rotor angle or the power angle as function of time between the machine's internal voltage E' and the system voltage. The electrical power transfer characteristics in terms of power angle δ can be expressed as,

$$P_e = \frac{E'V_s}{X_d' + X_t + X_{sys}} \sin(\delta) \quad (3.5)$$

E' represents the internal voltage behind X_d' direct-axis transient reactance, V_s is the voltage magnitude of the system, and X_t and X_{sys} are the transformer's leakage reactance and system equivalent impedance, respectively.

In order to obtain an expression to find the maximum possible rotor angle, which is the most important parameter in characterizing the transient stability of the generator in the first swing, the following can be derived from the first of equation set (3.4),

$$\frac{H}{w_{syn}} \left[\frac{d\delta}{dt} \right]_{\delta_0}^{\delta_{max}} = \int_{\delta_0}^{\delta_{max}} (P_m - P_e) d\delta \quad (3.6)$$

For the special case of an unloaded generator to system synchronization, since the mechanical power P_m is close to zero, (3.6) can be integrated and expressed in a closed form to obtain the value of δ_{max} in the first swing,

$$\delta_{max} = \cos^{-1} \left(\cos(\delta_0) - \frac{HX_T}{E'V_s w_{syn}} [2\pi(f_1 - f_2)]^2 \right) \quad (3.7)$$

Where, X_T is the total series impedance including the inserted impedance. Given the magnitudes of the generator voltage and system voltage, angle difference prior to closing the breaker, and the frequencies of both sides, the

maximum rotor angle in the first swing can be obtained. The damping effects usually do not provide a significant impact on the result within the first swing.

In the scenario of islanded system synchronizations, the impact of the loading levels must be considered. Equivalent diagrams for stability analysis are shown in Figure 3.9 (a). Before the breaker is closed, the power is mainly consumed by the local load inside the islanded system, as shown in Figure 3.9 (b). After the breaker is closed, the power is exchanged with the main grid, as shown in Figure 3.9 (c).

For power system studies, generators are typically modelled as PV busses and the loads are connected to PQ busses. This means that typically the active and reactive powers at these busses are typically specified. As a result, in Figure 3.9 (b), a power flow solve should be done first to determine the voltages and angles at every busses within the island. Then, the loads can be converted to constant impedance given the solved power flow results.

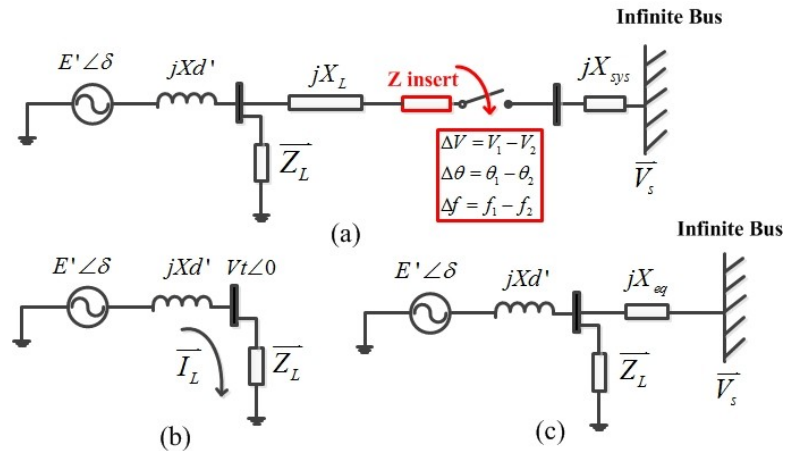


Figure 3.9 Circuits for transient stability analysis: (a) Island to system synchronization single line diagram. (b) Before closing breaker (c) After breaker is closed.

By modeling the loads as constant impedances and applying Y- Δ transformations, the circuit shown in Figure 3.9 (c) is transformed to the circuit shown in Figure 3.10.

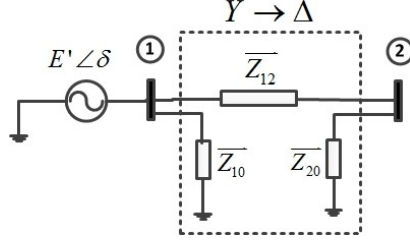


Figure 3.10 Simplified equivalent circuit of the islanded system after applying Y-Δ transformations

From network theory [38], the real power at node 1 of Figure 3.10 is given by $\text{Re}\{E'I^*\}$ or,

$$P_{e_after} = E'^2 Y_{11} \cos(\theta_{11}) + E'V_s Y_{12} \cos(\theta_{12} - \delta) \quad (3.8)$$

Where, $Y_{11} = Y_{10} + Y_{12}$, $Y_{10} = 1/Z_{10}$, and $Y_{12} = -1/Z_{12}$. Z_{12} is the series impedance of the transmission network, including transformers, lines and the inserted impedance. Z_{10} is the equivalent shunt impedance connected to the machine terminal, which includes any local loads. θ_{11} and θ_{12} are the impedance angle corresponding to Y_{11} and Y_{12} , respectively.

Similar to synchronization of single machine to an infinite bus, the theoretical δ_{max} for the first swing when the island in Figure 3.9 (a) synchronizes to system can be obtained by substituting (3.8) into (3.6), which gives a non-linear equation,

$$E'V_s Y_{12} [\sin(\theta_{12} - \delta_{max}) - \sin(\theta_{12} - \delta_o)] + H / W_{syn} [2\pi(f_1 - f_2)]^2 + (P_m - P_c)(\delta_{max} - \delta_o) = 0 \quad (3.9)$$

where, $P_c = E'^2 Y_{11} \cos(\theta_{11})$ represents the power dissipation in the network. The result of δ_{max} can be solved numerically such as the Newton-Raphson method.

This subsection summarizes the analytical derivations in the aspect of islanded system to system synchronizations from a transient stability's point of view. An unloaded generator is first examined at the beginning of the subsection. Then, the effect of the load impedance is considered in the power system islands synchronization scenario. For each scenario, a new power transfer characteristic as a function of the power angle relative to the system is derived. As one can

imagine that for every new generator introduced into the electrical island, a new power transfer equation will have to be derived analytically. Therefore, for a more complicated islanded system where multiple DG units and loads are needed to be analyzed, a systematic approach such as numerical solutions and dynamic simulation software are recommended to investigate the transient stability of the system due to synchronization.

3.3.2 Effects of Loading Levels and Impedance Sizes

Based on the analytical derivations presented for islanded system synchronizations in sub-section 3.3.1, effects of increasing both loading levels and size of impedance pre-insertions are investigated in this subsection to show the impacts on the stability of the generator.

To consider the transient stability in designing the impedance, first the worst case should be identified. Then stability of the system under the worst case should be ensured. The effect of increasing the loading level on the transient stability is shown in Figure 3.11.

As it can be seen, increasing the loading level of the islanded system reduces the stability margin, where the margin is defined as $(P_{max}-P_m)/P_{max}$. The reason is that the initial operating angle of the rotor will be higher as the load is increased. At high loading levels, the mechanical power supplied by the prime mover must also be high to meet the load demand, which is near 1.0 p.u. based on machine rating at peak loading.

For example, the maximum rotor angles in Figure 3.11 are compared for both light and heavy loading cases. The same synchronizing criteria apply to both cases. As shown, heavy loading level results in a high operating power angle before synchronization, therefore, the maximum angle δ_{max1} reached is also the highest.

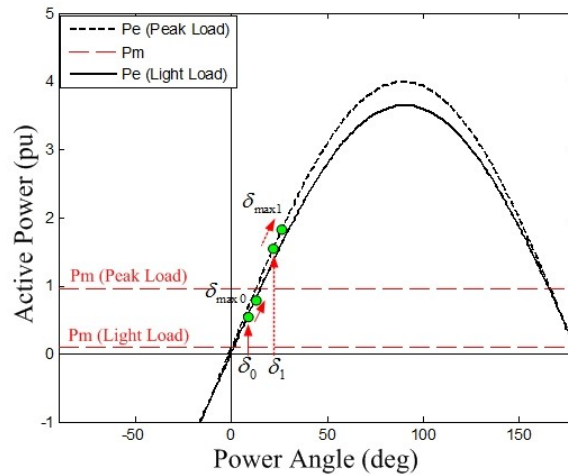


Figure 3.11 Impact of load to islanded system synchronization

The effect of inserted impedance on the transient stability is shown in Figure 3.12. As it was expected, the inserted impedance will reduce P_{max} and consequently reduce the transient stability margin further. As a result, a higher rotor angle δ_{max} is reached. However, it is important to note that this increase in rotor angle is purely dependent on the frequency difference across the breaker. More specifically, if $\Delta f=0$, there will not be an increase in the rotor angle due to the impedance pre-insertion because the effect of increasing the impedance shown in Figure 3.12 only lowers the P_{max} , which may only prolong the time required for the rotor oscillations to reach steady state due to a smaller stability margin.

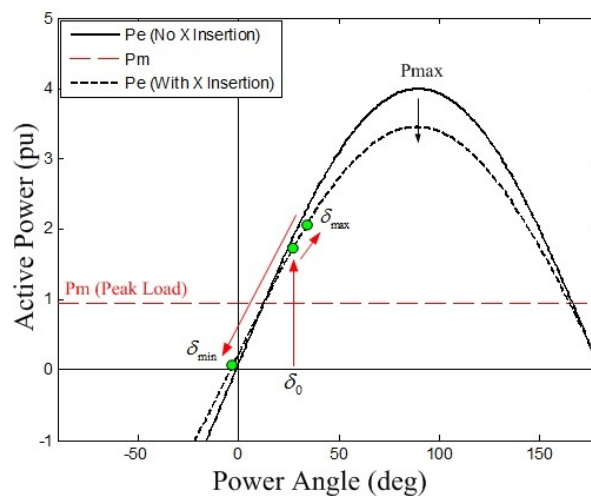


Figure 3.12 Impact of impedance pre-insertion to islanded system synchronization

As it will be seen in the case study in chapter 4, since the frequency difference based on the power quality limits between the two systems is still small, the inserted impedance will only have a small impact on the maximum rotor angle.

3.3.3 Worst Stability Case of Proposed Scheme

In this subsection, the worst transient disturbance due to synchronization under the power quality limits is identified provided the above analysis. As mentioned in subsection 3.3.2, the worst case rotor angle in the first swing should be examined based on the peak loading level and the designed impedance value due to the fact that, both factors result in the minimum stability margin. In addition, the voltage magnitude levels (islanded system and grid sides) should be at the lowest (i.e. 0.9 p.u.) of the power quality limits according to equations (3.5) and (3.8).

Since the worst case angle difference based on earlier assumption is $+20^\circ$ across the synchronizing breaker. In order to result in further rotor angle advancement, the frequency difference should be positive (i.e. higher islanded system frequency than the main grid). As a result, the worst case open-loop synchronization scenario from a transient stability point of view is *case (1, 3)* in red dots shown in Figure 3.13.

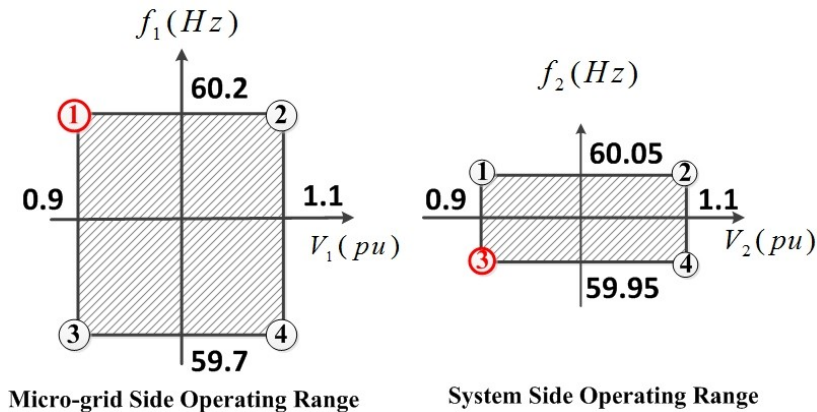


Figure 3.13 Worst stability case for islanded system synchronization

Although not recommended by the synchronizing standard of IEEE, but if the angle difference at the instant of breaker closing is -20° with $\Delta f > 0$, the δ_{max} reached will be the same as the $+20^\circ$ case if the effects of damping is ignored during the first swing. This is evident from equation (3.7) for a single machine to grid sample system. When the islanded system is at its peak loading level, the first swing δ_{max} values for both closing angles of $+20^\circ$ and -20° are simulated to be, 44.7° and 42.9° respectively based on the hydro based islanded system of Figure 3.5. The reason is because the damping effects for the -20° case is larger, so that the rotor takes a longer time to reach δ_{max} and resulted in a smaller value.

3.4 Second Switching Surge Determinations

Similar to the first breaker switching, impedance bypass also produces a transient effect on the system which must be evaluated to ensure an acceptable disturbance level.

First, a way to analyze the bypass transient is presented in subsection 3.4.1. Based on the analysis, the voltage across the impedance needs to be determined in order to evaluate the severity of this second switching surge. Since the bypass is performed after the transient is over and system reached steady state operation, power flow tool can be used to determine the voltage across the inserted impedance. The details of performing the power flow analysis are shown in subsection 3.4.2. Lastly, a method to determine the worst case bypass surge is shown in section 3.4.3.

3.4.1 Theoretical Analysis of Impedance Bypass Switching

Similar to the first breaker switching, impedance bypass also produces a transient effect on the system which must be evaluated to ensure an acceptable disturbance level. According to the principal of superposition, bypass switching can be represented by two opposing voltage sources as shown in Figure 3.14, which is equivalent to a single voltage source in the transient circuit. This circuit

is quite similar to the first impedance switching circuit, but with $\Delta f=0$. Therefore, the analytical equation (3.2), which is used for the first switching, also can be applied to the second switching surge. As shown in the equation previously, the bypass current surge is directly proportional to the voltage across the impedance before bypass. Therefore, if the voltage is less or equal to the acceptable level of voltage according to the IEEE standard, then the peak current surge is also limited to the acceptable level. Therefore, in this section, the voltage across the impedance before bypass is used to characterize the severity of the second switching surge.

The voltage difference across the impedance before the bypass depends on both the impedance value and the amount of current flowing through the impedance. Therefore, power flow studies are used to determine the voltage difference across the impedance before bypass, which is illustrated in more details in subsection 3.4.2.

In practice, the voltage across the impedance can be measured directly. Therefore, if the voltage reading is less than the acceptable voltage level, then the impedance is safe to bypass. Otherwise, the impedance can be bypassed in multiple steps or segments.

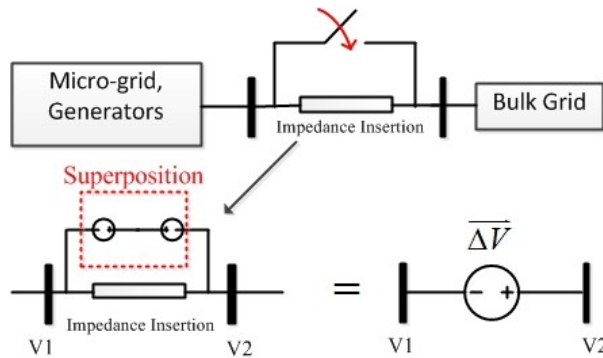


Figure 3.14 Representing impedance bypass by equivalent voltage source

3.4.2 Steady State Active and Reactive Power

Power flow studies are done to determine the worst cases of voltage across the impedance before bypass. As discussed earlier, voltage rather than peak current is used here because the peak current surge is directly proportional to the magnitude of the voltage difference across the impedance before bypass. The steady state active and reactive power flowing through the impedance before the second switching depend on the governor and Automatic Voltage Regulation (AVR) settings of the synchronous generators.

Due to the nature of the open-loop synchronization scheme, the voltage set-point of AVR is not adjusted through any means of control during the process of synchronization. Therefore, the AVR is assumed to be in terminal voltage regulating mode prior to synchronization. As a result, a reactive power flow is expected which can flow in either directions depending on the voltage levels of the synchronous generator and the main grid, as is shown in Figure 3.15.

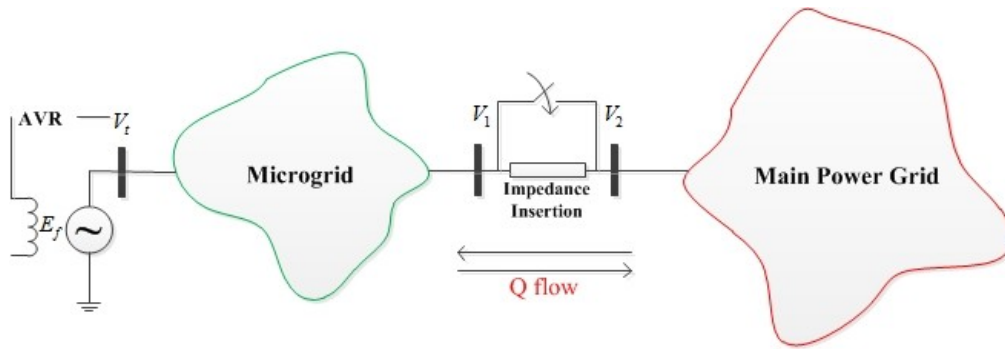


Figure 3.15 Reactive power flows through the impedance insertion

Active power flow through the inserted impedance is also expected. The speed governors of the synchronous generators are operating in droop control mode to assure proper load sharing between the DG units [15]. When the system reaches the steady-state before impedance bypass, the islanded system frequency becomes equal to the main grid frequency. The governor responds to the change in frequency by a percentage change in the mechanical torque or output power as in (3.10). Therefore, a real power exchange between the islanded system and the

main grid exists which can be in either direction depending on the pre-synchronization frequencies of the both sides.

$$\Delta P_m (pu) = \frac{\Delta f (\%)}{R} = \frac{f_{microgrid} - f_{sys}}{f_{nom}} \times \frac{1}{R} \quad (3.10)$$

As a result of the above mentioned inherit machine control settings, the active power injects by the DG unit has to be adjusted and the terminal voltage of the DG remains to be the same as the pre-synchronized condition, before performing a load flow study. Moreover, the terminal voltage of the DG relies heavily on the current loading levels of the islanded system before synchronization. By making the above changes to a load flow case study, the bypass voltage across the inserted impedance can be solved.

3.4.3 Worst Case Based on PQ Limits

The larger the frequency and voltage differences prior to synchronization, the larger the power flowing through the impedance. The worst case caused by the highest voltage difference should be identified to make sure that the worst possible transient is lower than the acceptable limit. Possible worst case bypass voltages can be identified as *case (2, 3), case (4, 1), case (3, 2) and case (1, 4)* to be the same as the resulted in the first switching surge as shown in Figure 3.3. The voltage across the impedance can be found through load flow studies. Then the highest voltage difference is compared to the acceptable voltage limit. If the maximum voltage is lower than the limit, the bypass is realized in one step. Otherwise, more bypass steps are required. The voltage difference limit is 0.1855 p.u. based on the IEEE standard C50.12.

3.5 Summary of Design Process

The design method for the pre-insertion impedance size to enable open-loop synchronization scheme can be summarized as follows:

1. The acceptable transient current and torque limits are determined. This report uses IEEE standard C50.12 synchronizing criteria to establish the acceptable level of transient. However, other standards can be applied based on the types of the energy source within the islanded system.
2. The four possible worst cases are identified based on the pre-established PQ limits of the two parties to be synchronized. The PQ limits are typically established as utility protocols.
3. The worst case from step 2 is then used to determine the minimum impedance size through analytical approach or EMTP simulation.
4. Analytical approach or simulation is then used to find the maximum acceptable impedance to maintain the transient stability of the generators.
5. An acceptable impedance range is now developed according to transient current and transient stability limits. This impedance size should be selected in the lower range to ensure a maximum transient stability margin.
6. Power flow studies are utilized to find the case causing the highest voltage across the inserted impedance among the four cases identified before. The highest voltage ΔV across the impedance is then compared to the maximum acceptable value to ensure the bypass transients are within the acceptable level. Moreover, multi-step impedance bypass can be considered if the voltage is greater than the acceptable level.

Chapter 4

Case Study Simulation and Evaluation Results

It is always important to verify and confirm the analytical derivations and predictions by means of computer simulations. Moreover, simulation results can provide more insights into the system behaviors and practical concerns when actually comes to implementations. Based on the impedance design method developed previously in Chapter 3, in the current chapter, simulation and evaluation results of a case study based on a real islanded system are presented. In addition, this chapter shows the feasibility and performance of the open-loop synchronization proposed scheme.

Section 4.1 first describes the schematic diagram of the islanded system under study. All the power system elements and parameters data are also given in this section. Section 4.2 presents the design results of this case study corresponding to each of the issues mentioned in Chapter 3. A proper impedance size has been determined based on the design results to meet both the first switching surge and transient stability requirements. An evaluation of the proposed method has been presented in section 4.3. Performances of peak stator current, torque, and maximum rotor swing have been evaluated by comparing the two cases: with and without impedance insertion. Summary is included in section 4.4.

4.1 Description of Studied System

To evaluate the effectiveness of the method, it is applied to a system shown in Figure 4.1. This islanded system is based on a real system in Brazil [10], where the hydro plant is located far away from the PCC. The system consists of one 6.6 MVA synchronous generator connected through a 30 mile (25kV) feeder to the main substation. A total load of 6MW is distributed along the feeder as shown in the figure. The impedance pre-inserted at the circuit breaker location is considered to be purely inductive. Resistor insertion investigations are shown in [Appendix D](#).

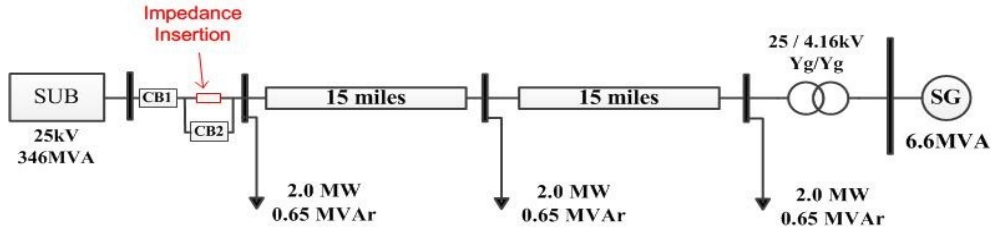


Figure 4.1 Single line diagram of case study

The system is modelled by a Thevenin voltage source behind the short circuit system impedance, system impedance, which the data is shown in Table 4.1. The salient pole rotor based synchronous generator is represented by a sixth-order state-space model with one damper winding modelled on the direct axis and two damper windings modelled on the quadrature axis. The detailed synchronous machine parameters are shown in Table 4.2. The AVR control and governor-turbine system data for the hydro generator are shown in

Table 4.3.

Table 4.1 Thevenin Equivalent (SUB) Data [10]

| | |
|---------------------------|-----|
| Short circuit power (MVA) | 346 |
| Nominal voltage (kV) | 25 |
| X/R Ratio | 7 |

Table 4.2 Synchronous Generator Data [10]

| | |
|------------------------|--------|
| Nominal Power (MVA) | 6.6 |
| Nominal Voltage (kV) | 4.16 |
| Pair of poles | 2 |
| Inertia constant (s) | 2.52 |
| Stator resistance (pu) | 0.00 |
| X_d (pu) | 1.26 |
| X'_d (pu) | 0.26 |
| X''_d (pu) | 0.18 |
| X_q (pu) | 1.24 |
| X''_q (pu) | 0.21 |
| T'_{do} (pu) | 1.4446 |
| T''_{do} (pu) | 0.0218 |
| T''_{qo} (pu) | 0.0690 |

Table 4.3 Excitation Control and Governor-Turbine Data [15]

| | | | |
|-----|---------------|--------------------|------|
| AVR | IEEE (Type 1) | Governor - Turbine | Type |
|-----|---------------|--------------------|------|

| | | System | (Hydro) |
|------------|--------|--------|---------|
| T_r | 5 ms | R_p | 0.05 |
| K_a | 300 | T_g | 0.2 s |
| T_a | 50 ms | T_w | 1.0 s |
| K_E | 1.0 | R_t | 0.38 |
| T_E | 0.65 s | T_r | 5.0 s |
| K_f | 0.048 | | |
| T_f | 0.95 s | | |
| E_{fmin} | -5 | | |
| E_{fmax} | 8 | | |

4.2 Design Results of the Proposed Scheme

As a first step of the impedance design method, acceptable level of current and torque transients must be determined. Based on the acceptable transient region presented earlier in Figure 3.1, there are four corner cases to consider, and the worst case through simulation has been found to be the top right corner, where the synchronizing condition is ($\Delta V=+0.05$ p.u., $\Delta f=+0.067$ Hz). The peak stator current and the torque transients of the synchronous generator under this synchronizing condition can be observed in time domain EMTP simulation, shown in Figure 4.2.

Based on EMTP simulations, maximum acceptable transient current and torque are found to be 1.5 p.u. and 1.7 p.u., respectively. As shown, the transient current occurs within 1~2 cycles of time, then it is followed by an electromechanical oscillation of the rotor, and due to the natural damping, the steady state shall be reached.

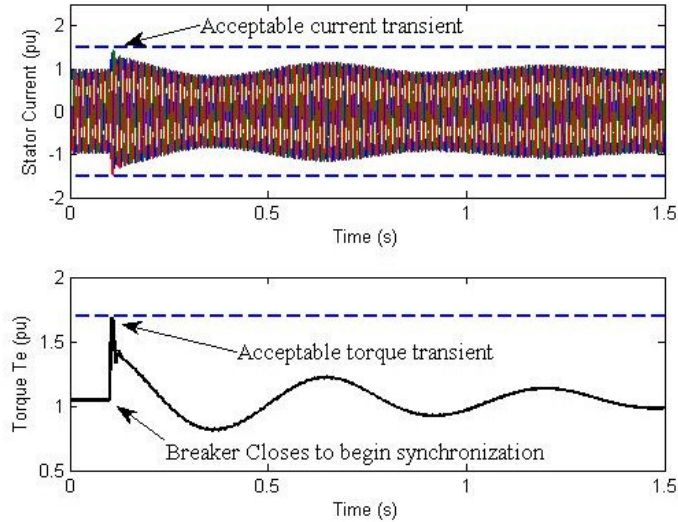


Figure 4.2 Time domain simulation to obtain acceptable transient levels for current and torque

After the acceptable level of transients are established, the worst case transients without the impedance insertion and synchronized under the power quality limits need to be identified. As discussed earlier, there are four worst synchronization scenarios to consider from Figure 3.3: **Case (2, 3)**, **Case (4, 1)**, **Case (3, 2)** and **Case (1, 4)**.

The 4 possible worst cases for the first switching are presented again in Table 4.4. The Peak current and torque for these cases are presented in Figure 4.3. As it can be seen, the worst transients occur in **Case (2, 3)**. The brief reasoning behind why this appears to be the worst case is discussed earlier in subsection 3.2.1.

Now that the worst case is identified, the minimum size of impedance required to limit the transients can be found either by repetitive EMTP simulations or by the analytical expression derived in (3.2).

Table 4.4 Synchronizing Conditions for Worst Case Transients

| Worst Cases | $ V_1 $ (p.u.) | $ V_2 $ (p.u.) | f_1 (Hz) | f_2 (Hz) | $\Delta\theta$ ($^\circ$) |
|-------------|----------------|----------------|------------|------------|-----------------------------|
| Case (2,3) | 1.1 | 0.9 | 60.2 | 59.95 | +20 $^\circ$ |
| Case (4,1) | 1.1 | 0.9 | 59.7 | 60.05 | +20 $^\circ$ |
| Case (3,2) | 0.9 | 1.1 | 59.7 | 60.05 | +20 $^\circ$ |
| Case (1,4) | 0.9 | 1.1 | 60.2 | 59.95 | +20 $^\circ$ |

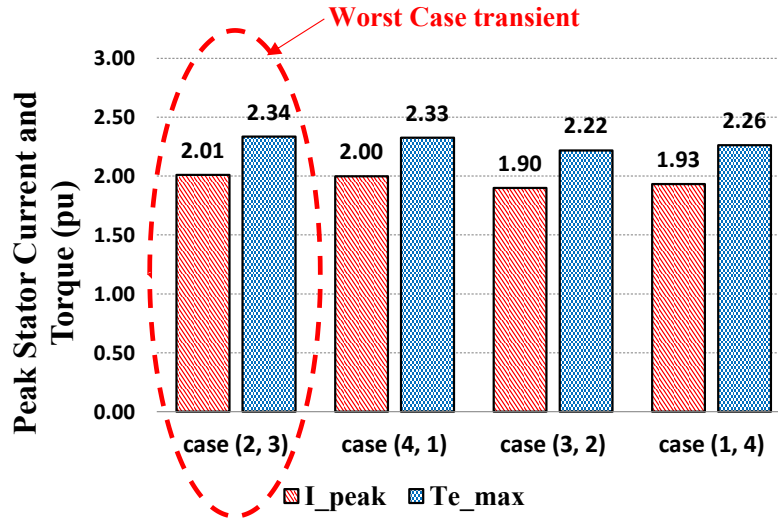


Figure 4.3 Worst case transients based on PQ limits

A comparison of the two approaches is shown in Figure 4.4 below and also in Appendix C. The analytical method provides an upper bound for the peak stator current. For this case study, the impedance value¹ determined analytically is 0.6 p.u. or 56.82 Ω .

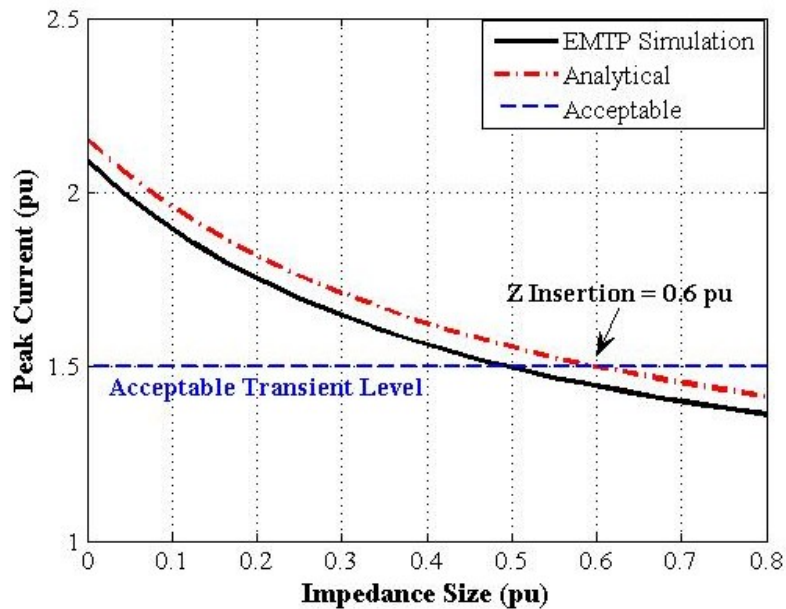


Figure 4.4 Peak current versus size of impedance insertion for the worst case

¹ The estimated cost of the inductor insertion is about \$5100 based on the maximum voltage difference of 5.762kV and maximum current of 306.36A [43].

In this case, the analytical approach predicts a higher stator current because the approach simply adds the transient synchronizing current computed to the load current before the synchronization process in time domain. However, in EMTP simulation, a small amount of synchronizing current actually flows to the constant impedance load rather than all to the machine stator, therefore, the stator current from simulation results is slightly lower than the analytical approach.

For transient stability analysis, the worst case occurs in *Case (1, 3)*. Similar to the previous step, either EMTP simulations or analytical approach could be used to determine the predicted maximum rotor angle. The theoretical prediction of the maximum rotor angle is obtained by simplifying the circuit in Figure 4.1 to Figure 3.10 using Y- Δ transformations. The maximum swing angle can then be calculated by (3.9). The maximum rotor angles found by simulation and analytical approaches for different impedance sizes are compared in Figure 4.5.

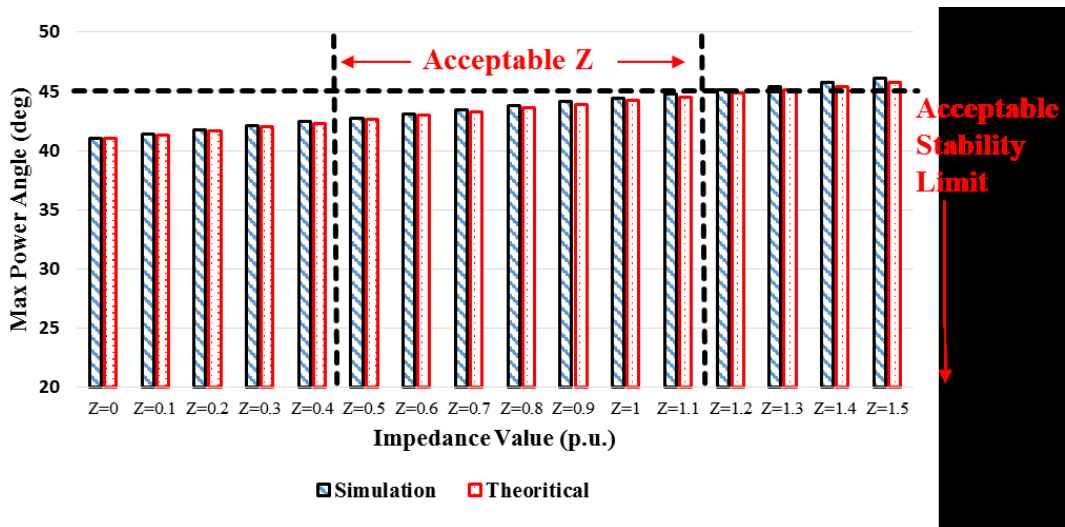


Figure 4.5 Feasible impedance range based on first switching transient and transient stability analysis

It can be seen that the results of the two methods are close to each other. In addition, increasing the inserted impedance size does not have a significant effect on the maximum rotor angle based on the reasoning discussed in subsection 3.3.2. According to the maximum acceptable transient level and stability limit, the

feasible impedance range is within 0.5 p.u. to 1.1 p.u. However, to ensure a high stability margin, 0.6 p.u. is chosen as the required impedance size.

The last design step is to evaluate the severity of bypass transients. As discussed earlier in Section 3.4, before conducting power flow studies, the active power at PV busses or the P_m injects by the synchronous generator is adjusted according to the frequency difference Δf for every cases in Table 4.4. Moreover, due to AVR in terminal voltage regulating mode, the voltage magnitude at the PV busses are kept the same as the value before synchronization. After these minor but necessary adjustments, load flow studies are used to find the worst bypass voltage among the four possible cases mentioned in subsection 3.4.3 and the results are presented in Table 4.5, and illustrated in Figure 4.6.

Table 4.5 Power flow results for the four possible worst cases

| Worst Cases | S (p.u.) | \Delta V (p.u.) |
|-------------|-----------|------------------|
| Case (2,3) | 0.208 | 0.125 |
| Case (4,1) | 0.297 | 0.178 |
| Case (3,2) | 0.241 | 0.156 |
| Case (1,4) | 0.257 | 0.170 |

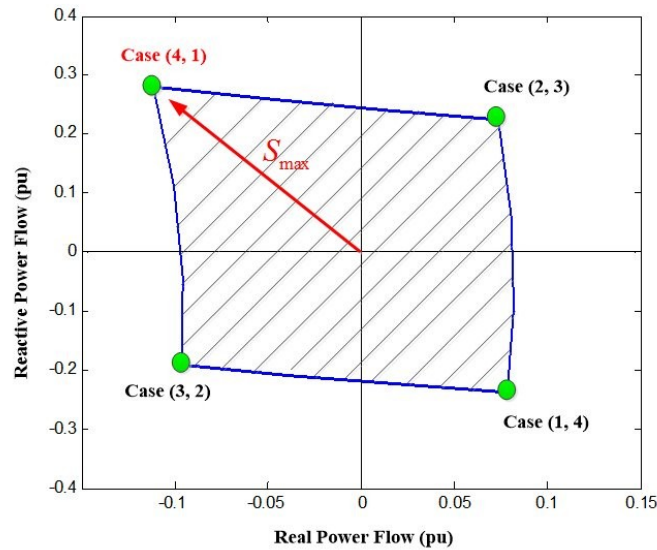


Figure 4.6 Worst power flow through the impedance based on load flow studies

As it can be seen, *Case (4, 1)* has the highest complex power which leads to the highest voltage across the impedance. For the selected impedance size (0.6p.u.), this complex power incurs a voltage difference of 0.178p.u. , which is lower than the acceptable level of 0.1855p.u. Therefore, the impedance can be bypassed in one step while the transient levels are acceptable.

4.3 Evaluation of the Proposed Method based on Case Study

To better show the performance of the proposed method based on the design results shown in Section 5.2, the whole synchronization process using the designed impedance is shown in Figure 4.7 to Figure 4.9. For these simulations, it is assumed that the synchronization is done under *Case (2, 3)*, which has the worst transient at the synchronization instance. The voltage angle difference across the breaker is assumed that the islanded system side voltage leads the main power grid by 20° as mentioned before taken from the industrial survey. For comparison, the synchronization disturbances and performances under the same case are shown in the following figures for both without the inserted impedance and with the impedance pre-insertion.

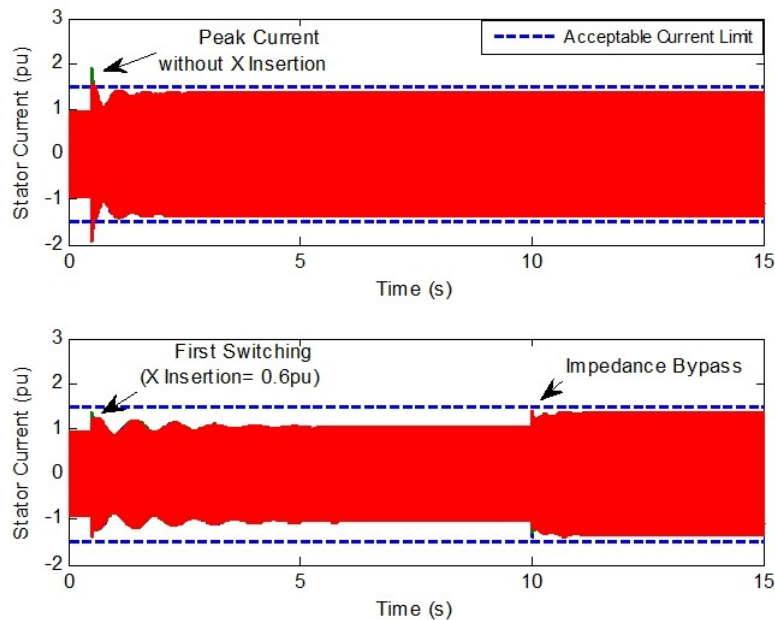


Figure 4.7 Stator current during synchronization with and without impedance insertion

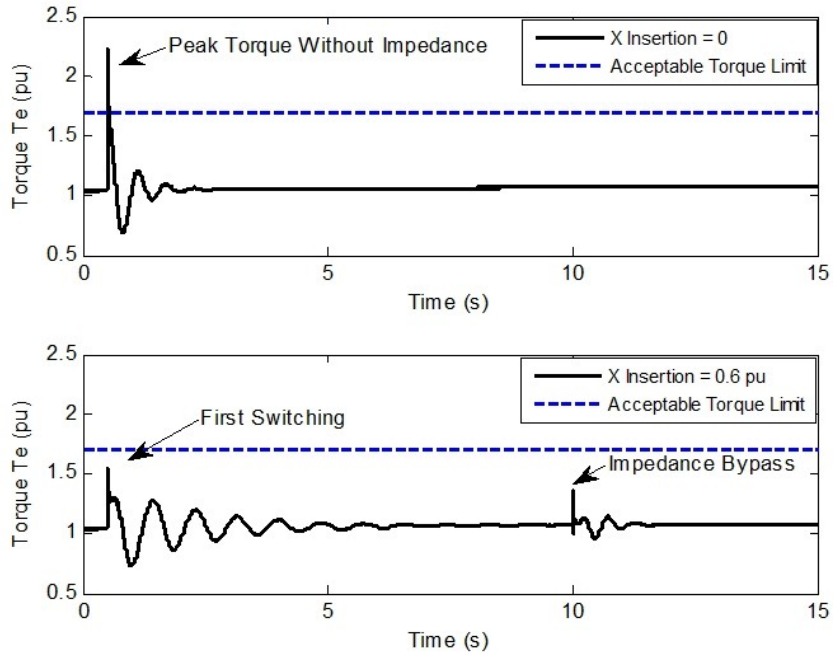


Figure 4.8 Torque transients during synchronization with and without impedance insertion

As it can be seen in Figure 4.7 and Figure 4.8, without the inserted impedance the current and torque could reach as high as 2 p.u. and 2.34 p.u., respectively, which are higher than the acceptable limits from the perspective of the hydro synchronous generator. This can severely damage the generator and transformer windings, and incur excessive stress on the mechanical parts of the rotor. After inserting the impedance, the peak current for the first and second switching are 1.37 p.u. and 1.38 p.u., which are within the acceptable limit. Also the peak torque for the first and second switching are 1.54 p.u. and 1.36 p.u., respectively, which are below the maximum acceptable limit.

By comparing the rotor angles in Figure 4.9, although inserting the impedance increases the oscillations, but the oscillations are damped and will not causing the rotor to pass the maximum stability limit (45°). The generator also remains stable after the entire synchronization process. Without impedance insertion, it can be seen that the rotor reaches steady state much faster than the case with impedance insertion. This is because of the high synchronizing power between the synchronous generator and the main power grid when there is no impedance

insertion to decrease the stability margin. However, when impedance insertion is introduced, there expects to be less synchronizing power to bring the rotor in synchronism with the system. Therefore, it takes some time for the rotor to reach steady state before bypass the impedance, which depends on the machine inertia and other system damping factors. The excessive rotor oscillations due to less synchronizing power are generally not a primary concern as long as the rotor stays stable (i.e. maximum rotor swing does not reach beyond the stability limit).

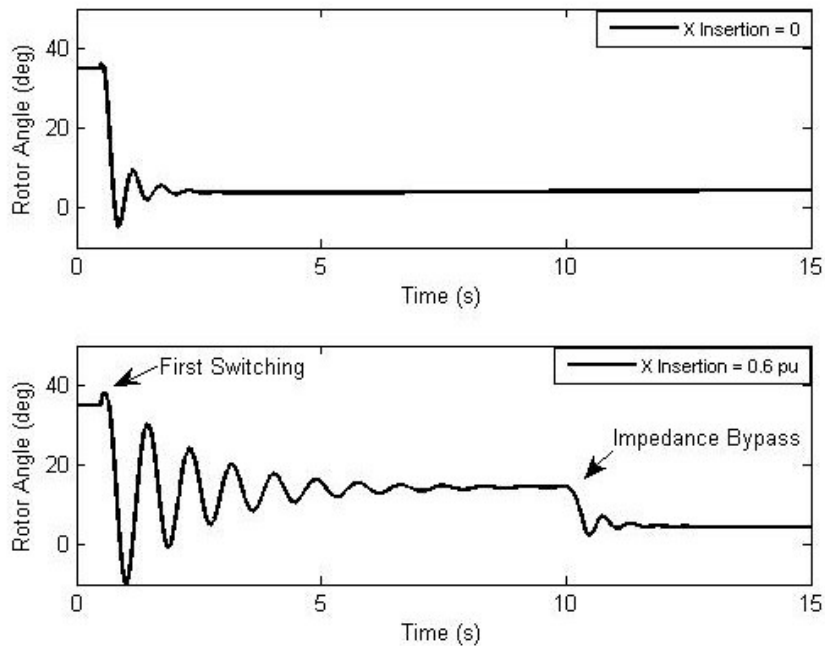


Figure 4.9 Rotor angle behavior with and without impedance insertion

Lastly, it is worth to comment on the similarities between synchronization of a generator and 3-phase fault at terminal of a generator. From a transient stability's point of view, both events are classical power system problems. Both events will cause advancements in the rotor angle within the first swing, which the maximum angle reached can be computed analytically based on $P-\delta$ curve. The increase in angle in the synchronization case is primarily due to the angle and frequency differences across the breaker before synchronization. However, for a 3-phase short circuit, the increase in angle is due to P_{max} of the power transfer capability curve dropped below the P_m level. In addition, in a 3-phase to ground fault case,

the transient disturbance impacts on the rotor angle is far greater than the case of synchronization because the rotor angle may reach beyond 90° after the fault is cleared.

4.4 Conclusions and Summary

This chapter presented a novel and effective strategy to mitigate the concerns and challenges in the islanded system synchronizations. The design issues of the impedance pre-insertion method are fully investigated in chapter 4. The design results based on a real islanded system are presented in this chapter. The main contributions of this work can be summarized as follows.

- The proposed scheme implements the impedance pre-insertion method such that the open-loop synchronization of two systems can be achieved.
- The impedance can be implemented near the breaker location, and no communication links are required between the breaker location to the individual DG units. As a result, this becomes very attractive in terms of costs and infrastructures needed compared to the traditional feedback control scheme.
- A practical design procedure has been developed for impedance pre-insertion. This chapter also presented the evaluation results to show the effectiveness of this method in solving the challenges related to islanded system synchronizations.

The proposed open-loop synchronization scheme and its design method have been demonstrated through the case study by computer simulations. The results have shown that the designed impedance is quite effective to reduce peak inrush current and is also capable to enable open-loop synchronizations of power system islands. A similar case study based on two DG units has been shown in [Appendix A](#) and the effects of different governor/turbine systems on the open-loop synchronization are studied in [Appendix C](#).

Chapter 5

Feasibility Investigations of Soft Starter Based Method

In earlier chapters, the design method and computer based simulation results have been presented for the impedance pre-insertion based method to enable open-loop synchronization. As mentioned in section 2.1.4, there are other methods that exist for mitigating switching transients that is worth to investigate. Therefore, in this chapter, the thyristor based method traditionally used for motor soft starters is investigated to see its feasibility and effectiveness in synchronizing an island to the main power grid. It is quite common for the soft starter method to be extensively implemented in reducing the inrush current from motor starting. However, in the current case, the thyristor based synchronizer shall be applied to the main breaker location for the purpose of synchronizing two systems. The intent is to softly synchronize the two systems by two anti-parallel thyristors (SCRs) instead of applying the traditional method of feedback control through communication links.

In order to investigate whether the soft synchronizer is feasible, steps have been taken to investigate and understand the phenomenon and design considerations of the proposed method. As a first step, the top level view of the synchronizer has been illustrated in section 5.1 and a preliminary procedure is established shortly. The phenomenon is understood by examining the voltage and current waveforms of the synchronizer, which is shown in section 5.2. Practical design considerations for the proposed synchronizer have been discussed in section 5.3, and the simulation/evaluation results of the thyristor based approach of a test system are documented in section 5.4.

5.1 Synchronization of Two Systems by Soft Starter Method

As known previously, the main concern on synchronizing two power systems is the transients produced when the synchronizing circuit breaker is closed. Just to recall, excessive transients can lead to large inrush current and transient torque, damaging generator and other equipment. The current practice of reducing synchronization transients is to limit the voltage, angle, and frequency differences between the two parties through the method of feedback control. Due to the main drawbacks of the traditional synchronization method stated in sub-section 2.1.2, an impedance based method to enable open-loop synchronization has been proposed in Chapter 2.

Soft starter method has been used for motor starting in temporarily reducing the electrical current surge for several decades [39]. This is a concern because large starting current will cause line voltage to sag, impacting other sensitive loads. As well, the current surge should not exceed certain limits. Moreover, high torque produced with the large starting current can cause failures in the mechanical system such as motor shaft, belts, gearbox and etc. [40]. In this section, the proposed synchronization scheme based on the method of soft starter shall be explained in details. The scheme is illustrated in Figure 5.1.

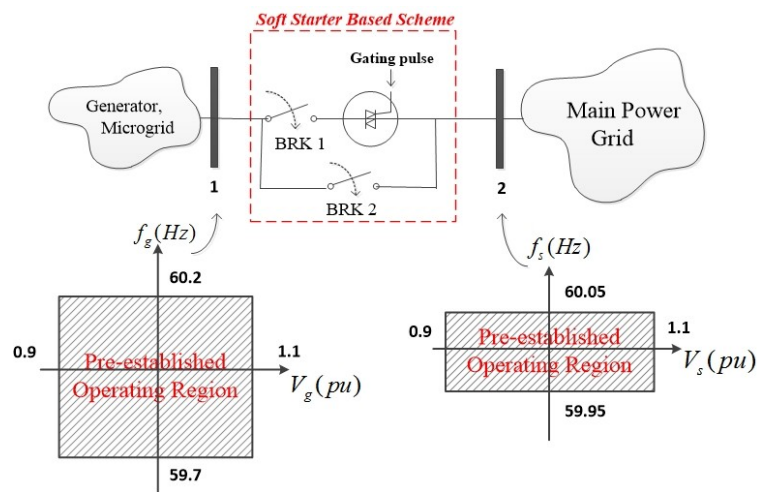


Figure 5.1 Proposed Scheme based on soft starter and power quality limits for both sides

As shown, soft starters consist of two anti-parallel SCR's (TRIAC) for each phase, which the gate pulsing of the thyristor is varied by controlling the firing angle (α) in order to adjust the effective voltage difference across busses 1 and 2 after the first breaker is closed. An overview of the soft starter based synchronization process of an islanded system to the main power grid is shown in Figure 5.2.

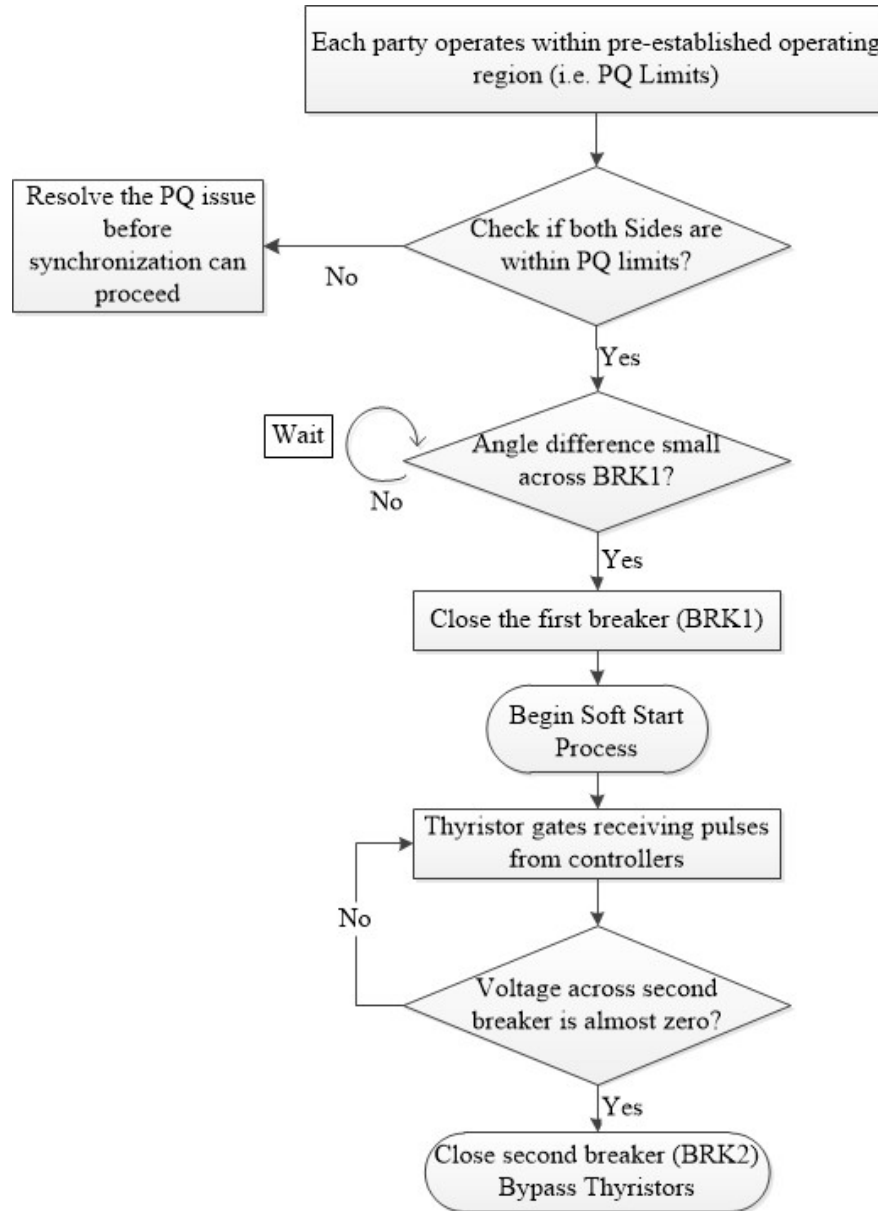


Figure 5.2 Islanded system to the main power grid synchronization procedure with thyristors based synchronizer

The first breaker is in place just to protect the SCR devices in cases of high voltage difference. Once the voltage difference is within an acceptable range from the perspective of SCR ratings, the first breaker can be closed. For the purpose of synchronization, the reference voltage waveform used to initiate the firing time of gating pulses is the voltage across the thyristor, which is different from motor starting applications where the voltage reference waveform is typically just the grid voltage.

Initiate the gating pulses to the SCRs will allow current to gradually conduct through the first breaker. Due to the inertias of the synchronous generators and a low synchronizing power at first, the rotors will slowly adjust its positions to become in synchronism with the grid. Therefore, the voltage difference across the soft starter is actually decreasing in value. When the voltage is near zero, the 2nd breaker is closed to bypass the soft starter.

5.2 Voltage and Current Waveforms during Soft Start Process

Based on the theory of TRIAC tuning for an $R-L$ series impedance load, the effective RMS voltage and current applied to the load depends on 2 parameters, the firing angle (α) and the equivalent impedance angle (φ). If $\alpha > \varphi$, as α firing angle increases, the effective voltage and current applies to the load decreases. If $\alpha < \varphi$, as α firing angle decreases, the effective voltage and current applies to the load will reach its rated value, and current becomes fully conducting. When $\alpha < \varphi$, the DC offset occurs in the current surge.

In synchronizing two electric systems, it can be realized by equivalence both sides as voltage sources before the soft start process through the TRIAC. The voltage across the SCRs becomes the voltage difference between the generator side and the main power grid side as shown in Figure 5.3 b). This voltage is also the reference waveform used for triggering the soft start process based on a zero-crossing of the waveform. As explained earlier, by controlling the firing angle at a

value larger than 90° , the initial voltage across the SCR, thus the resulting current through the SCRs can be reduced.

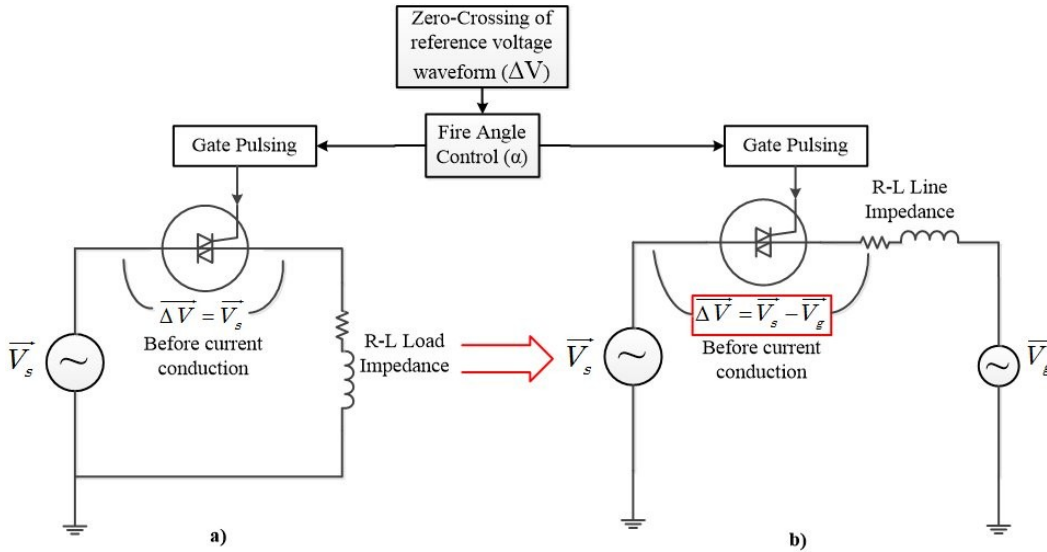


Figure 5.3 Voltage difference across SCRs for a) R-L load impedance applications
b) Synchronizing with two voltage sources representation

An example of the Phase A voltage and current waveforms at firing angle of 130° are shown in Figure 5.4.

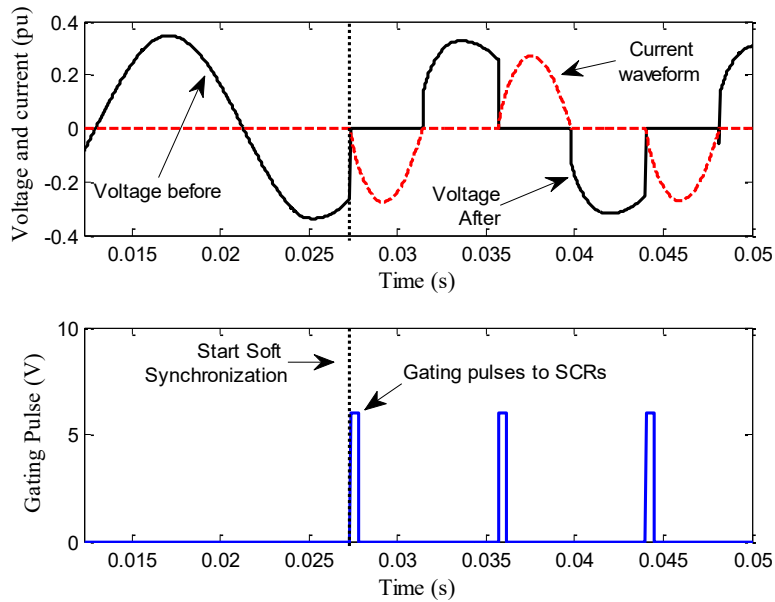


Figure 5.4 Voltage and current waveforms at $\alpha=130^\circ$ of the soft starter device (Top), gating pulses applied to SCRs (Bot.)

Due to the characteristics of the SCR, it can be seen that the SCR can be turned on if the anode is positive respective to the cathode of the device and a pulse signal is applied to the gate. However, SCR turns off only if the current flow through the SCR is zero ideally, or below the holding current level [41].

Once the SCRs are turned on based on the zero-crossing of the reference voltage as shown in Figure 5.4, the pulses are applied to the gates of the TRIAC at regular intervals thereafter until the SCRs are bypassed.

5.3 Design Considerations

In this section, the design aspects are considered to meet the requirements of the acceptable level of transients. Hence, these considerations are divided into different subsections to characterize their impacts on the transient levels. Subsection 5.3.1 investigates into the impacts of the synchronizing parameters on the voltage difference across the thyristors. Constant firing angle and time voltage ramp techniques have been illustrated, and their effects have been explained through the usage of power-angle curves, which is shown in subsection 5.3.2. Finally, SCR bypass and generator grounding issues have been discussed in subsection 5.3.3.

5.3.1 Impacts of synchronizing parameters

The synchronizing parameters voltage, angle and frequency, for both the islanded system and the main power system are needed to be considered for the soft starter based open-loop synchronization.

Voltage difference ΔV can be present at the time of synchronizing an islanded system to the main power system. As known, this can be a result from a mismatch between $|V_1|$ and $|V_2|$, or a mismatch in voltage phase (angle difference). For a fixed firing angle (Alpha), the larger the ΔV , the higher the current surges for both the soft starter and the machine stators. Hence, the higher the transient torque. In addition, if the machine is at terminal voltage regulating mode, a mismatch

between $|V_1|$ and $|V_2|$ can either increase or decrease the field excitation voltage of the AVR. If field voltage is increased during the soft synchronization process, it may help in stabilizing the rotor oscillations by providing more synchronizing power for high firing angles. If field voltage is decreased during the process, the lacking of synchronizing power problem initially from high Alpha may become worse. Therefore, for a worst case angle difference across the SCRs, a lower islanded system voltage than the system should be investigated to see if the DG units can be stabilized without excessive rotor oscillations.

The impact due to an initial frequency difference Δf on the soft synchronizing process is quite similar to the transient stability explanations developed earlier in Section 3.3. For a higher islanded system frequency than the grid, i.e. $f_1 > f_2$, the rotors are initially running faster than the frequency of the system. Consequently, immediately after the soft synchronizing process begins, the extra kinetic energy stored in the rotating masses of the synchronous machine is dissipated as the rotor reduces its speed to match the synchronous speed of the system. As a result, rotor angle respective to the system increases, which in turn increases the voltage difference across the SCRs. This effect is illustrated in Figure 5.5. As shown, for the $\Delta f = 0$ case, the ΔV across the SCRs is decreasing to zero almost linearly within 0.3 seconds. However, for $\Delta f > 0$, the voltage difference initially is increased as expected, then drops down to zero. In this case, $f_1 = 60.2\text{Hz}$ and $f_2 = 59.95\text{Hz}$.

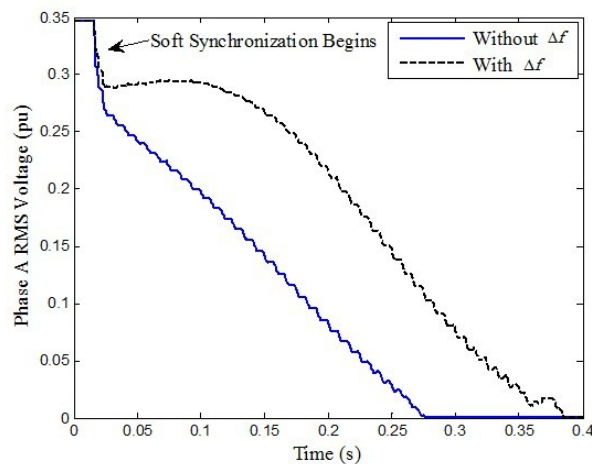


Figure 5.5 RMS voltage across the SCRs with and without Δf for $\alpha = 130^\circ$

5.3.2 Constant α Firing Vs Time Voltage Ramp System

There are two basic types of gate triggering to the SCRs for the soft starter device as shown in Figure 5.6. The first type is a constant firing angle scheme for every cycle of the soft synchronizing process. The second type has a time varying firing angle, which the period of SCR conduction increases per every cycle of time.

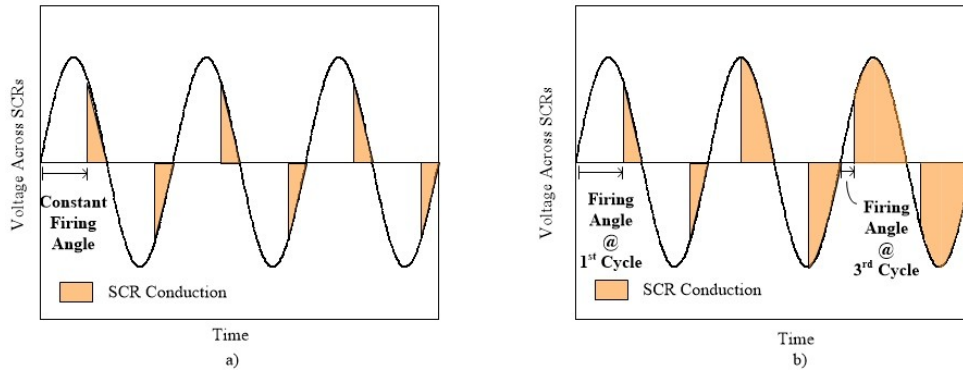


Figure 5.6 Differences in soft synchronizing schemes a) Constant firing angle
b) Time voltage ramp system

Both types of gate triggering scheme can be realized by the power transfer capability curves to understand the behaviors of rotor dynamics as shown in Figure 5.7.

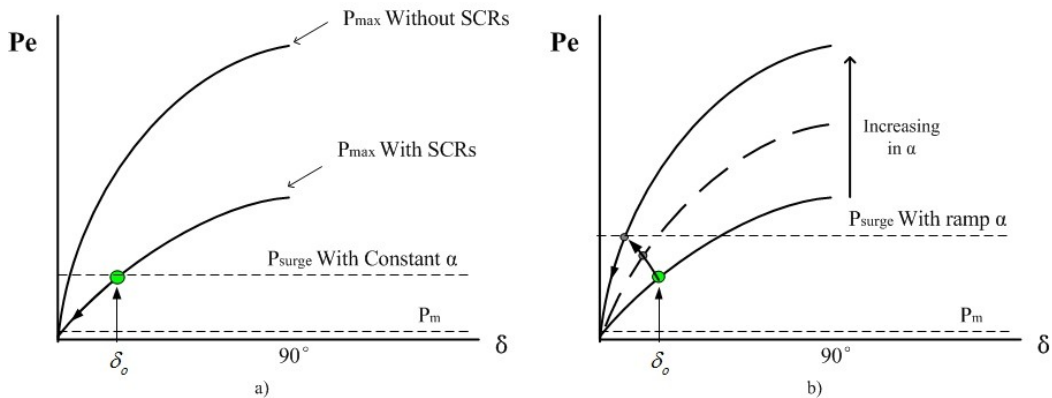


Figure 5.7 P- δ curve representations of a) constant firing angle
b) time voltage ramp system

From the perspective of synchronizing transients, assuming the equivalent line impedance is mostly inductive, a firing angle larger than 90° can significantly reduce the effective inrush current value in the beginning of the synchronization process. However, the synchronizing power and torque are also reduced. The negative side to a low synchronizing power is the potential possibility that the machine might lose synchronism with the main power grid. Therefore, time voltage ramp system may provide a promising solution for the low synchronizing power problem if encountered.

5.3.3 Other Technical Issues to Consider

Once the first zero voltage difference is reached across the SCRs, the device should be bypassed in order to restore normal system operations to prevent excessive rotor oscillations from lacking of synchronizing torque and power. In addition, as discussed earlier in the impedance bypass, the severity of the transients associated with the bypass switching is heavily dependent on the voltage difference across the bypass breaker at the instant it is closed. Therefore, bypass at the first voltage zero can also limit the peak current. However, for an increase in the firing angle α value, the time to bypass also increases due to a delay in reaching zero voltage difference across the SCRs as shown in Figure 5.8.

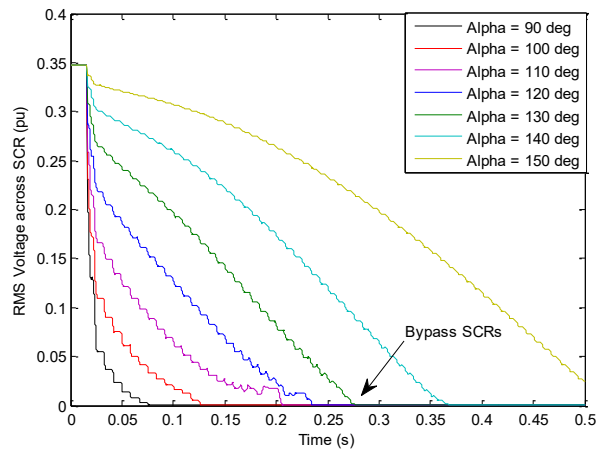


Figure 5.8 Bypass times for different α between 90° ~ 150°

Another important issue to consider is the effect of generator neutral to ground impedance on the synchronizing transients. According to the IEEE recommended practice for grounding of a single unparalleled generator, a reactor is usually connected between the neutral and the grounded conductor to limit the momentary ground fault current to be no more than the three-phase fault current [42]. Accordingly, the value of this neutral reactor X_n , should be calculated as,

$$X_n = 1/3(2X''_d - X_2 - X_0) \quad (5.1)$$

Where X''_d is the direct axis sub-transient reactance, X_2 and X_0 are the negative and zero sequence reactance of the generator, respectively. Based on typical average values of synchronous machine constants [36] and equation (5.1), the typical value of X_n for a turbo-generator with solid rotor is calculated to be 0.02 p.u. However, the neutral reactor value within the typical range from 0.01p.u. to 0.05p.u. does not significantly impact both the transient current and torque using the thyristor based synchronizer.

Resistor groundings were also used in distribution systems. In such cases, the voltage waveforms during the soft synchronizing process are becoming distorted, which means the conductions by the thyristors are more visible in the voltage waveforms. However, the resistor groundings have negligible effects on the peak transients.

5.4 Application Example

The thyristor based synchronizer is applied to a test system for different case studies, which the studied system diagrams and evaluation results have been documented in this section. The system is built in Simulink environment and the different module diagrams are shown in subsection 5.4.1. Simulation results of the proposed method are presented in subsection 5.4.2, where the possibility of the open-loop synchronization under the power quality limits is investigated.

5.4.1 Test System under Study

The entire system overview diagram for the case study is shown in Figure 5.9. There are three main modules as part of the system: DG generation module, thyristor based synchronizer module, and the system module.

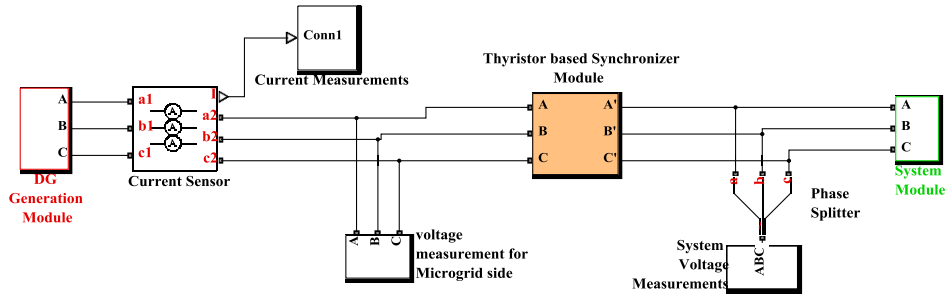


Figure 5.9 System Diagram (Top Level)

The DG generation module is modelled by a salient pole synchronous generator with an impedance load connected to the machine terminals, as shown in Figure 5.10. The data for the synchronous machine parameters are shown earlier in Table 4.2. The excitation system model (AVR) is of type AC1A according to the IEEE recommended practice for excitation system models for power system stability studies (IEEE standard 421.5). The parameters of the AC1A type exciter is extracted out of the sample data section of the IEEE standard 421.5.

The thyristor based synchronizer module schematic and thyristor parameters are shown in Figure 5.11 and Table 5.1, respectively. This module includes two main subsystems: gate pulsing generator and thyristor triggering. Thyristor triggering subsystem triggers the soft synchronizing process based on a zero voltage crossing of the voltage difference across the SCRs. The gate pulsing generator subsystem takes in the triggering signals and decides the proper time to switch on the SCRs based on a user defined firing angle.

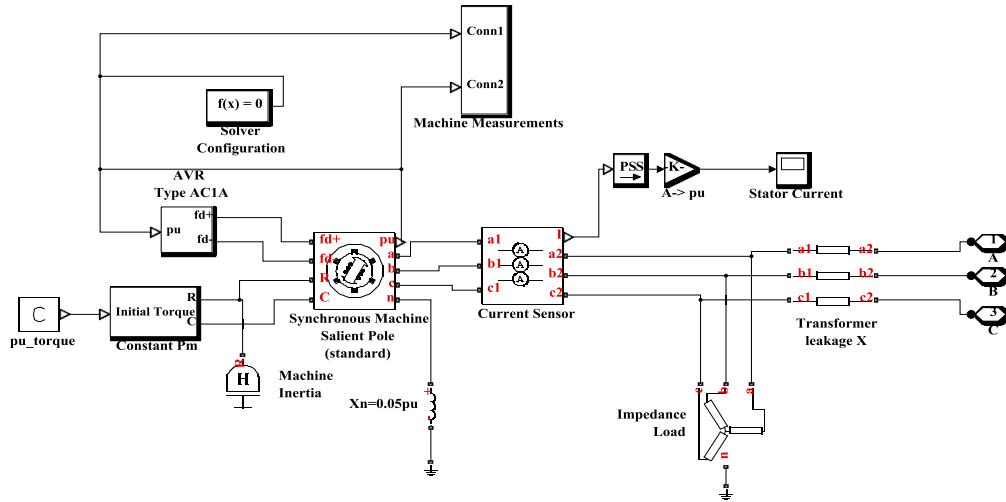


Figure 5.10 DG generation module diagram

Table 5.1 Thyristor Parameters

| | |
|---|-------|
| Forward Voltage (V) | 0.8 |
| On-state resistance (Ω) | 0.001 |
| Off-state conductance (Ω^{-1}) | 1e-6 |
| Gate triggering voltage (V) | 5 |
| Holding current (A) | 1 |

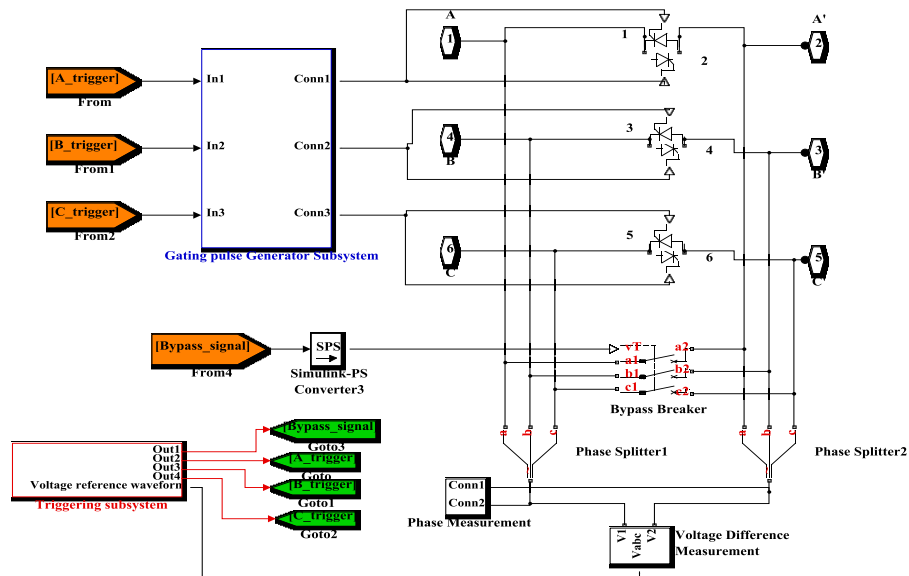


Figure 5.11 Thyristor based Synchronizer Module

5.4.2 Simulation Results

Simulation results of machine torque and frequency at different initial angle differences 5° , 10° , and 20° have been shown in Figure 5.12 based on the test system with constant firing angle at 130° . Acceptable transient levels from the perspective of the SG are obtained similarly to section 4.1, which is based on IEEE standard C50.12. The acceptable current and torque for the current case study for the SG are 1.54 p.u. and 1.6 p.u., respectively.

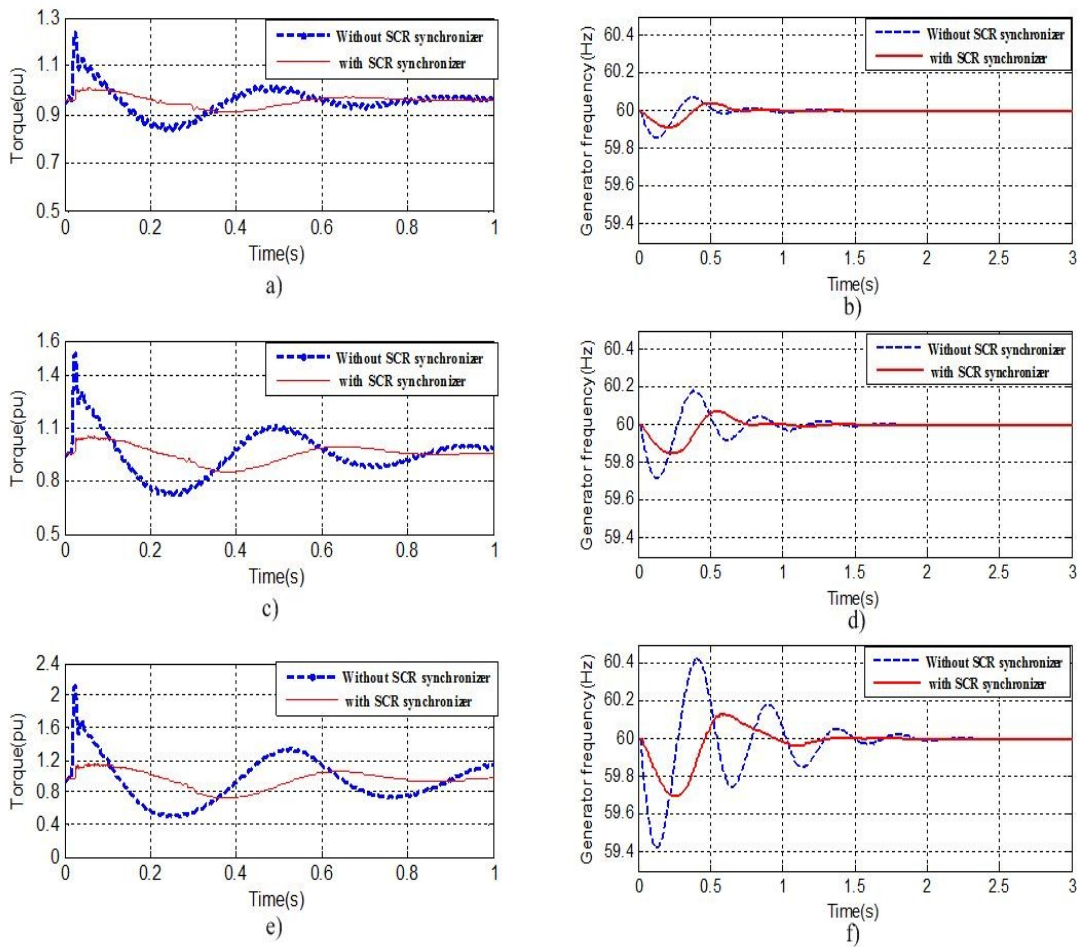


Figure 5.12 Comparisons of Transient machine torque, rotor frequency of SG at angle differences of 5° , 10° , and 20° with and without thyristor based synchronizer ($\alpha=130^\circ$). a) Electric torque of SG, at $\Delta\theta=5^\circ$, b) Frequency of SG, at $\Delta\theta=5^\circ$, c) Electric torque of SG, at $\Delta\theta=10^\circ$, d) Frequency of SG, at $\Delta\theta=10^\circ$, e) Electric torque of SG, at $\Delta\theta=20^\circ$, f) Frequency of SG, at $\Delta\theta=20^\circ$.

As shown in Figure 5.12, the transient torque has been significantly reduced from 2.1 pu (without SCR based synchronizer) to 1.18 pu (with the synchronizer)

even for the worst angle difference of 20° . The reduced peak torque is also lower than the acceptable torque level. Moreover, by reducing the torque, the synchronizing power is also reduced while the rotor is decelerating in the beginning. Therefore, the rotor frequency deviation is decreased for the first swing with the thyristor based synchronizer. In addition, after thyristors are bypassed, synchronizing power is then restored. The rotor oscillations will be damped even more, so the steady state operation can be reached in a shorter time span.

As mentioned earlier, a higher islanded system frequency than the power system may lead to an increase in the voltage difference across SCRs immediately after the SCRs are triggered. As a result, the impacts due to the frequency differences on the peak stator current are shown in Figure 5.13. As shown, firing angle larger than 125° can reduce the maximum transient current to be within the acceptable level. As expected, a positive frequency difference $\Delta f = +0.25\text{Hz}$ will increase the peak current due to an increase in the voltage difference across the thyristors.

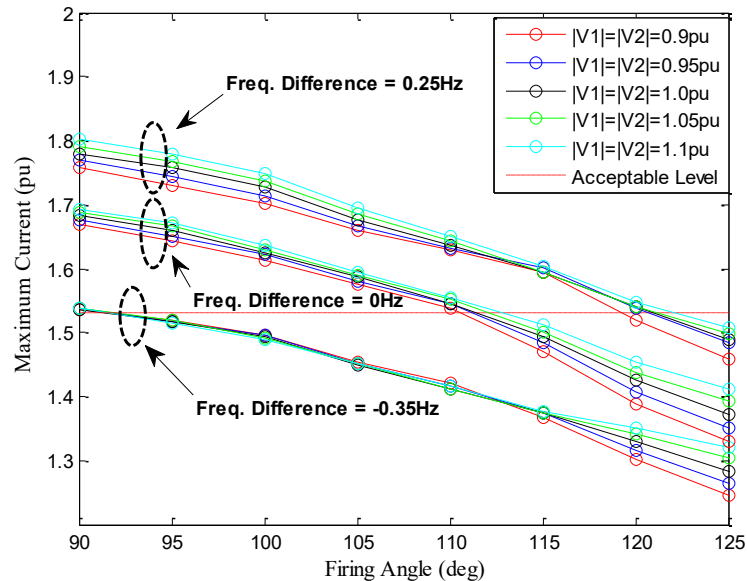


Figure 5.13 Impact of Δf on the peak stator current for different voltage levels from 0.9~1.1pu and $\Delta\theta=20^\circ$

The impacts due to voltage magnitude difference $\Delta V=|V_1|-|V_2|$ on the peak stator current and torque are investigated at $\Delta f=+0.25\text{Hz}$ and $\Delta\theta=20^\circ$. First, several cases are examined for both $|V_1|>|V_2|$ and $|V_1|<|V_2|$, then, the peak stator current and torques under those synchronizing conditions are extracted from repetitive EMTP simulation results based on the test system. The cases to be examined are listed below in Table 5.2, which are the possible synchronizing conditions within the power quality limits.

Table 5.2 Case studies on the effects due to voltage magnitude difference ΔV

| Synchronizing Conditions: $ V_1 > V_2 $, $\Delta\theta=20^\circ$, $\Delta f=+0.25\text{Hz}$ | | Synchronizing Conditions: $ V_1 < V_2 $, $\Delta\theta=20^\circ$, $\Delta f=+0.25\text{Hz}$ | |
|--|--------------------------|--|--------------------------|
| Case 1 | $ V_1 =1.1, V_2 =1.05$ | Case 1 | $ V_1 =0.90, V_2 =0.95$ |
| Case 2 | $ V_1 =1.1, V_2 =1.00$ | Case 2 | $ V_1 =0.90, V_2 =1.00$ |
| Case 3 | $ V_1 =1.1, V_2 =0.95$ | Case 3 | $ V_1 =0.90, V_2 =1.05$ |
| Case 4 | $ V_1 =1.1, V_2 =0.90$ | Case 4 | $ V_1 =0.90, V_2 =1.10$ |
| Case 5 | $ V_1 =1.05, V_2 =1.00$ | Case 5 | $ V_1 =0.95, V_2 =1.00$ |
| Case 6 | $ V_1 =1.05, V_2 =0.95$ | Case 6 | $ V_1 =0.95, V_2 =1.05$ |
| Case 7 | $ V_1 =1.05, V_2 =0.90$ | Case 7 | $ V_1 =0.95, V_2 =1.10$ |
| Case 8 | $ V_1 =1.00, V_2 =0.95$ | Case 8 | $ V_1 =1.00, V_2 =1.05$ |
| Case 9 | $ V_1 =1.00, V_2 =0.90$ | Case 9 | $ V_1 =1.00, V_2 =1.10$ |
| Case 10 | $ V_1 =0.95, V_2 =0.90$ | Case 10 | $ V_1 =1.05, V_2 =1.10$ |

For a higher islanded system voltage level than the system side, after the thyristors are switched on, the internal voltage of the machine due to excitation control tends to increase in magnitude to hold the machine terminal voltage close to the value before synchronization. As a result, a raise in the P_{max} of the $P-\delta$ curve after thyristors are switched on is expected. Moreover, the synchronizing power is increased to stabilize the rotor oscillations afterwards. In other words, constant firing angle scheme still provides sufficient synchronizing power to damp the rotor oscillations. Therefore, a constant firing angle of $\alpha=130^\circ$ is used to

investigate its transient current and torque reduction capabilities, for which the results are shown in Figure 5.14.

As can be observed that for all cases, the peak current levels are quite similar but torque transients tend to decrease primarily due to the decrease of the machine terminal voltage. Based on short circuit theory, the magnitude of current transient is a function of the magnitude of the voltage difference across thyristors. Since all cases have the same voltage magnitude differences (i.e. 0.05p.u.) and angle difference at 20° , then it makes sense that the peak current levels are similar.

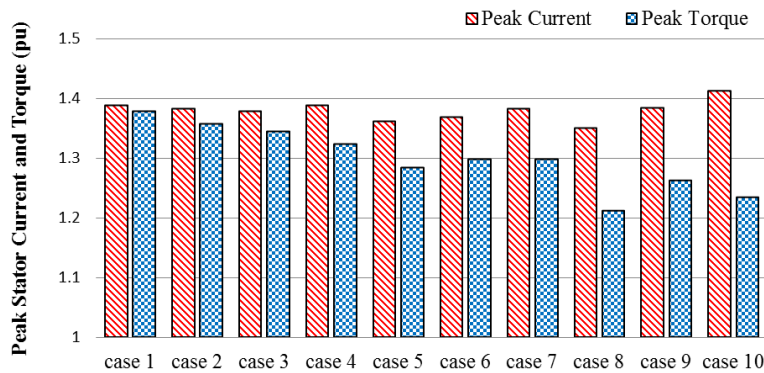


Figure 5.14 Peak current and torque simulation results for cases of $|V_1| > |V_2|$ at $\alpha=130^\circ$

However, machine torque is proportional to the electric power delivered at a given machine frequency. Therefore, the torque transients at the same loading level are heavily dependent on the product of E (internal voltage) and V_t (terminal voltage), this is illustrated by a linear relationship in Figure 5.15.

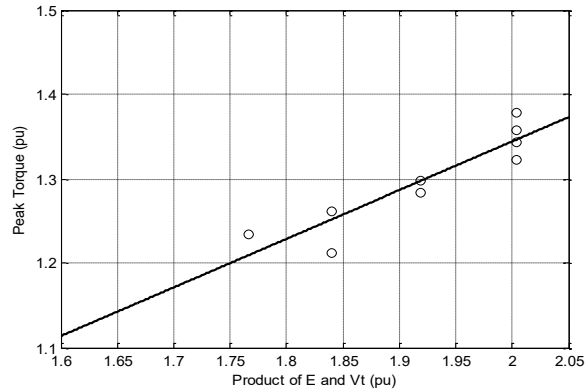


Figure 5.15 Relationship between peak machine torque and product of internal and terminal voltages

For $|V_1| < |V_2|$, time voltage ramp system has been implemented to the thyristor based synchronizer. The reason behind using this technique for synchronization purposes is the insufficient synchronizing power to stabilize the rotor oscillations and difficult to reach steady state operation. This is because of the excitation controls of the machine is in voltage controlled mode, the internal voltage becomes lower due to the direction of the reactive power flow across the breaker. In other words, part of the reactive power consumption of the islanded loads shall be provided by the grid instead of solely dependent on the local SG units.

With time voltage ramp system, the firing angle is decreased every cycle, this decrement is defined by step (in degrees) per cycle. The EMTP simulation results are shown in Figure 5.16 with $\alpha_0 = 130^\circ$ with firing angle decrements of $5^\circ/\text{cycle}$.

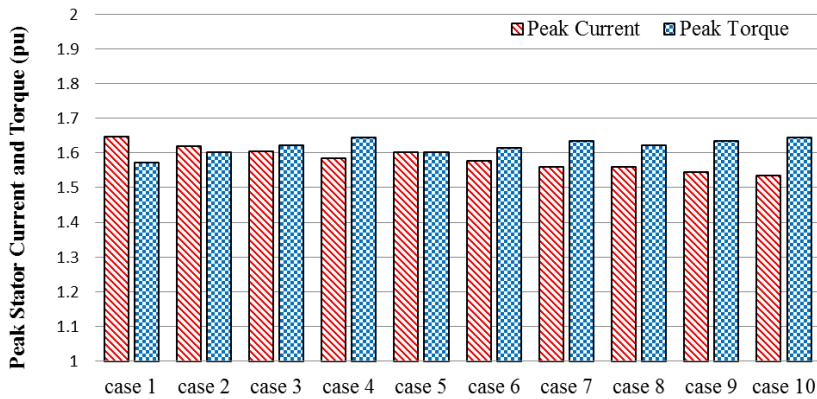


Figure 5.16 Peak current and torque simulation results for cases of $|V_1| < |V_2|$ at $\alpha_0 = 130^\circ$, and ramp decrement of $5^\circ/\text{cycle}$

It can be observed that with the time voltage ramp system, the transient current and torque peak values can be slightly higher than the acceptable limits of a synchronous generator for the cases $|V_1| < |V_2|$. However, significant transient reductions are also achieved when synchronized in an open-loop manner. The detailed time voltage ramp system implementation is demonstrated in [Appendix B](#).

5.5 Summary and Conclusions

This chapter investigates the feasibility of thyristor based synchronizer used in islanded system synchronization applications. The design aspects of the

synchronization strategy have been discussed in section 5.3. The proposed thyristor based synchronizer has been evaluated through simulation studies. The results demonstrate that the transient levels can be significantly reduced and the islanded system can be successfully synchronized with the system. The key results of this work can be summarized as follows:

- The thyristor based synchronizer can be effectively triggered by the voltage zero crossings of the voltage difference waveform across the SCR device.
- The impacts of synchronizing parameters ΔV , $\Delta\theta$, and Δf on the behaviors of voltage and current waveforms have been investigated for the proposed method.
- The effects of constant firing angle and time voltage ramp techniques on the power-angle curves have been illustrated.
- Technical considerations regarding bypassing of the thyristors and generator groundings have been investigated.
- Evaluations of the proposed method through simulation studies have been demonstrated. The possibility the open-loop synchronization application has been investigated by considering different synchronization scenarios.
- The simulation results have shown that for a lower islanded system side voltage than the main grid side, it is recommended to apply the time voltage ramp technique for thyristor firing. However, in this case, the transient levels are slightly higher than the acceptable level.

Chapter 6

Conclusion and Future Work

6.1 Thesis Conclusions and Contributions

This thesis discussed transient reduction methods and developed a scheme to enable synchronization in an open-loop manner for synchronous generator based electrical islands. The existing method of synchronization through feedback control requires communication links between the breaker location to the DG units, which can significantly drive up the infrastructure cost and complexity of islanded system synchronization. Since the primary concern in synchronization is the switching transients, so the impedance pre-insertion and thyristor based synchronizer are proposed in this thesis to enable open-loop synchronization. This scheme presents an attractive solution to synchronizing remote islanded systems. All the discussed synchronization strategies were evaluated by performing simulation studies on different islanded systems. The key conclusions and contributions of the thesis can be summarized as follows.

- Major synchronization issues related to feedback control in modern SG based islanded systems have been clearly identified in the motivations section of Chapter 2. The true concern of synchronization is the switching transients because of their adverse effects on power system equipment, especially of the damages to the machines.
- An open-loop synchronization scheme is proposed. Both the islanded system and main power grid under the normal operating conditions before synchronization are already working in a pre-established utility protocol, which is inside their own power quality limits defined by voltage and frequency bands. As discussed in Chapter 2, if outside these limits, the power systems do not meet the power quality requirements.

- A design method has been developed in accordance to the design issues related to the method of impedance pre-insertion in Chapter 3. A way to establish the acceptable level of transients for the machine is illustrated. The size of the impedance is designed based on the requirements for the transient levels and the stability limits of the generator. The minimum size of the impedance can be determined both analytically and by EMTP simulations. The theoretical predictions of the maximum rotor angle are also derived for a simple islanded system synchronization case. A method to determine the worst case impedance bypass transients is also developed based on the power quality limits. The impedance insertion method has shown promising results in transients reductions based on simulations of a real islanded system case study.
- In chapter 5, thyristor based synchronizer method has found to be feasible in terms of islanded system synchronization applications. An electronic controlled thyristor based synchronizer is built in Simulink environment to test its performances in a sample test system. The results have shown that constant firing angle technique is suitable for island's side voltage higher or equal to the system voltage. However, due to lack of synchronizing power, the time voltage ramp system technique is more suitable for the case where the voltage magnitude is lower than the system.

6.2 Suggestions for Future Work

The author's suggestions for continuing the investigations and studies on open-loop islanded system synchronizations are as follows.

- As mentioned in Chapter 2, one of the main drawbacks of the traditional synchronization method through feedback control is the cost of infrastructure support needed to accomplish islanded system synchronization. Therefore, this thesis proposes an open-loop synchronization scheme based on methods of transients reduction. The

economic costs and benefits associated with both schemes can be compared to more precisely reflect the advantages of open-loop synchronization.

- Among the transient reduction methods, both impedance pre-insertion and soft starter methods have been investigated in the scope of this thesis. Synchronous closing results have not been shown in this thesis, but it is found to be insufficient in reducing the AC component of the transient current due to a large angle difference. However, the feasibility of sequential phase closing as proposed for transformer energization could be investigated.
- The scope of the thesis is based on the studies on synchronous generator based islanded systems. As shown in Chapter 3, the acceptable level of transients (i.e. current and torque) is based on the perspective of the SG unit. However, the concept of open-loop synchronization scheme can be extended for smart grid applications with renewable energy penetrations such as solar and wind power, which the transient and stability aspects are still valuable to investigate.
- Both the impedance insertion method and thyristor based synchronizer methods are evaluated by simulation results in this thesis report. However, experimental synchronization studies can be performed simply on a single islanded SG machine with loads if equipment and measurements at the breaker location are available.

References

- [1] A. Bidram and A. Davoudi, "Hierarchical structure of microgrids control system," *IEEE Trans. Smart Grid*, vol. 3, no. 4, pp. 1963-1976, Dec. 2012.
- [2] F. Katiraei, R. Iravani, N. Hatziargyriou, and A. Dimeas, "Microgrids management: controls and operation aspects of microgrids," *IEEE Power Energy Mag.*, vol. 6, no. 3, pp. 54-65, May/Jun. 2008.
- [3] M. Savaghebi, A. Jalilian, J. C. Vasquez, and J. M. Guerrero, "Secondary control scheme for voltage unbalance compensation in an islanded droop-controlled microgrid," *IEEE Trans. Smart Grid*, vol. 3, no. 2, pp. 797-807, Jun. 2012
- [4] M. S. Golsorkhi Esfahani and D. D. C. Lu, "A decentralized control method for islanded microgrids under unbalanced conditions," *IEEE Trans. Power Del.*, doi: 10.1109/TPWRD.2015.2453251.
- [5] P. Sreekumar and V. Khadkikar, "A new virtual harmonic impedance scheme for harmonic power sharing in an islanded microgrid," *IEEE Trans. Power Del.*, doi: 10.1109/TPWRD.2015.2402434.
- [6] N. W. A. Lidula and A. D. Rajapakse, "Microgrids research: A review of experimental microgrids and test systems," *Renewable Sustainable Energy Rev.*, vol. 15, no. 1, pp. 186-202, Jan. 2011.
- [7] M. J. Thompson, "Fundamentals and advancements in generator synchronizing systems," *65th Annual Conference for Protective Relay Engineers*, pp. 203-214, Apr. 2012.
- [8] IEEE standard for Salient-Pole 50 Hz and 60 Hz Synchronous Generators and Generator/Motors for Hydraulic Turbine Applications Rated 5 MVA and Above, IEEE Standard C50.12-2005.
- [9] IEEE Standard for Interconnecting Distributed Resources with Electric Power Systems," IEEE Std 1547.2-2008
- [10] T. M. L. Assis, G. N. Taranto, "Automatic reconnection from intentional islanding based on remote sensing of voltage and frequency signals," *IEEE Trans. Smart Grid*, vol. 3, no. 4, pp. 1877-1884, Dec. 2012

- [11] C. Cho, J. Jeon, J. Kim, S. Kwon, K. Park, and S. Kim, “Active synchronizing control of a microgrid,” *IEEE Trans. Power Electron*, vol. 26, no. 12, pp. 3707-3719, Dec. 2011.
- [12] F. Tang, J. M. Guerrero, J. C. Vasquez, D. Wu, and L. Meng, “Distributed active synchronization strategy for micro-grid seamless reconnection to the grid under unbalance and harmonic distortion,” *IEEE Trans. Smart Grid*, pp. 2757-2769, Mar. 2015
- [13] “Synchronism Check Relay Instruction Manual GEK-106213C”, GE Multilin 2007 [Online], Available: <file:///C:/Users/powerlab/Downloads/mljman-c.pdf>
- [14] P. Piagi and R. H. Lasseter, “ Autonomous control of microgrids,” in *Proceedings of IEEE PES General Meeting*, 2006
- [15] P. Kundur, “Power system stability and control”, in McGraw-Hill, 1994, pp.45, 581-600.
- [16] G. W. Massey, “Essentials of distributed generation systems”, Jones and Bartlett Publishers, 2010, pp. 62.
- [17] F. A. Viawan and D. Karlsson, “Voltage and reactive power control in systems with synchronous machine-based distributed generation,” *IEEE Trans. Power Delivery*, vol.23, no.2, pp. 1079-1087, Apr. 2008
- [18] N. Jenkins, R. Allan, P. Crossley, D. Kirschen, and G. Strbac, “Embedded Generation”., London, U.K.: Inst. Elect. Eng., 2000.
- [19] *Atlas of Electricity in Brazil* (in Portuguese), 3rd ed. Brasilia, Brazil: ANEEL—Brazilian Electricity Regulatory Agency, 2008 [Online]. Available: <http://www.aneel.gov.br>
- [20] H. Laaksonen, D. Ishchenko, and A. Oudalov, “Adaptive protection and micro-grid control design for hailuoto island,” *IEEE Trans. Smart Grid*, vol. 5, no. 3, pp. 1486- 1493, May. 2014
- [21] K. Malmedal, P. K. Sen, and J. P. Nelson, “Application of out-of-step relaying for small generators in distributed generation,” *IEEE Trans. Ind. Appl.*, vol. 41, no. 6, pp. 1506-1514, Nov./Dec. 2005

- [22] IEEE Working Group Report, “IEEE screening guide for planned steady-state switching operations to minimize harmful effects on steam turbine-generators,” *IEEE Trans. Power App. Syst.*, vol. PAS-99, no. 4, pp. 1519–1521, Jul./Aug. 1980
- [23] J. S. Joyce, T. Kluig, and D. Lambrecht, “Torsional fatigue of turbine-generator shafts caused by different electrical system faults and switching operations,” *IEEE Trans. In Power Apparatus and Systems*, Vol. PAS-97, pp. 1965-1973 , Sept/Oct 1978.
- [24] R. C. Dugan, M. F. McGranaghan, H. W. Beaty, “Electrical Power Systems Quality”, in McGraw-Hill, 1996, pp. 100-103.
- [25] *Solid-State Soft Start Motor Controller and Starter*, Eaton Corporation, USA, 2011 [Online], Available: <http://www.eaton.com/ecm>
- [26] Y. Cui, S. G. Abdulsalam, S. Chen, and W. Xu, “A Sequential Phase Energization Technique for Transformer Inrush Current Reduction – Part I: Simulation and Experimental Results,” *IEEE Trans. Power Delivery*, Vol. 20, No. 2, pp. 943-949, Apr. 2005.
- [27] J. Arrillaga, N. R. Watson, and S. Chen, “Power System Quality Assessment”, in John Wiley & Sons Ltd, 2000, pp.30.
- [28] ITI (Information Technology Industry Council), ITI curve Application Note [Online], Available: http://www.itic.org/iss_pol/techdocs/curve.Pdf
- [29] Technical Requirements for Connecting to the Alberta Interconnected Electric System (IES) Transmission System, ESBI, Alberta, 1999
- [30] WECC Off-Nominal Frequency Load Shedding Plan, WECC, 2011 [Online], Available:<https://www.wecc.biz/Reliability/OffNominalFrequencyLoadSheddingPlan.pdf>
- [31] Balancing and Frequency Control, by NERC Resources Subcommittee, 2011 [Online], Available: <http://www.nerc.com/docs/oc/rs/NERC%20Balancing%20and%20Frequency%20Control%20040520111.pdf>
- [32] IEEE standard for Cylindrical-Rotor 50 Hz and 60 Hz Synchronous Generators Rated 10 MVA and Above, IEEE Standard C50.13-2005.

- [33] N. Mohan, "Electric power systems: a first course", in John Wiley & Sons Inc., 2012, pp. 159-160.
- [34] W. M. Strang, C. J. Mozina, B. Beckwith, T. R. Beckwith, S. Chhak, E. C. Fennell, E. W. Kalkstein, K. C. Kozminski, A. C. Pierce, P. W. Powell, D. W. Smaha, J. T. Uchiyama, S. M. Usman, and W. P. Waudby, "Generator synchronizing industry survey results," *IEEE Trans. Power Del.*, vol. 11, no. 1, pp. 174-183, Jan. 1996.
- [35] L. C. Gross, L. S. Anderson, and R. C. Young, "Avoid generator and system damage due to a slow synchronizing breaker," in *proceedings of the 24th Annual Western protective Relay Conference*, Spokane, WA, Oct. 1997.
- [36] Glover Sarma, "Power system analysis & design", in PWS Publishing Company 2nd Edition, 1994, pp. 305-306, 569.
- [37] R.W. Alexander, "Synchronous closing control for shunt capacitors", *IEEE Trans. On Power Apparatus and Systems*, vol. PAS-104, no. 9, pp. 2619-2626, Sept. 1985.
- [38] P.M. Anderson and A. A. Fouad, "Power system control and stability", in John Wiley & Sons 2nd Edition, 2003, pp. 26-28.
- [39] C. S. Siskind, "Electrical Control Systems in Industry", in McGraw-Hill, 1963.
- [40] Solid-state Soft Start Motor Controller and Starter, EATON, Feb. 2011
[Online], Available:
<http://www.eaton.de/ecm/groups/public/@pub/@electrical/documents/content/ap03902001e.pdf>
- [41] A. E. Fitzgerald, C. Kinsley and S. D. Umans, "Electric Machinery", in McGraw-Hill, 2003, pp. 496-497.
- [42] IEEE Recommended Practice for Grounding of Industrial and Commercial Power Systems, IEEE Standard 142-1991, pp. 45.
- [43] T. Ding and W. Xu, "A Filtering Scheme to Reduce the Penetration of Harmonics into Transmission Systems," *IEEE Trans. Power Del.*, vol. 31, no.1, pp.59-66, Feb. 2016.

- [44] R. Torquato, Q. Shi, W. Xu, and W. Freitas, "A Monte Carlo simulation platform for studying low voltage residential networks," *IEEE Trans. Smart Grid*, vol.5, no.6, pp.2766-2776, Nov. 2014.

Appendix

Appendix A: Simulation Study on Two DG Isolated System

This section presents simulation results for the design method for the impedance pre-insertion on an isolated system that contains two DG units. The procedure is similar to section 3.5. A.1 gives the data and diagram for the isolated system under study. A.2 determines the acceptable level of transients for both machines using the IEEE standard C50.12. The worst case transients based on the power quality limits have determined in A.3. Transient stability results are shown in A.4. Bypass voltages based on load flow studies are conducted in A.5.

A.1 System Description

The Micro-grid under study consists of two DGs, which are 6.6MVA and 10MVA, respectively. The 6.6 MVA synchronous machine is located 30 miles away from the main substation. A second 10 MVA SG is added shown in Figure A.1. A peak loading of 15MVA at an inductive power factor of 0.95 is assumed. The load is evenly distributed along the feeder. The three-phase short circuit level at the point of interconnection is 346 MVA. The system and synchronous generator data are shown in Table A.1. The impedance pre-inserted at the circuit breaker location is purely an inductor.

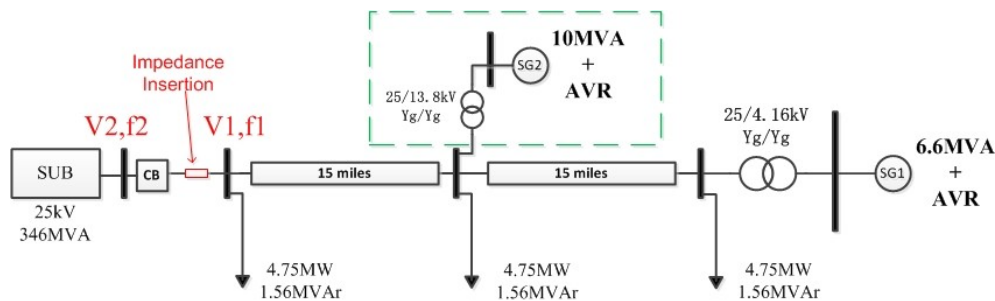


Figure A.1 Case study of two DG units performing open-loop synchronization with impedance pre-insertion method

Table A.1 Synchronous Generator Data

| | SG1 | SG2 |
|------------------------|--------|-------|
| Nominal Power (MVA) | 6.6 | 10 |
| Nominal Voltage (kV) | 4.16 | 13.8 |
| Pair of poles | 2 | 2 |
| Inertia constant (s) | 2.52 | 2 |
| Stator resistance (pu) | 0.00 | 0.004 |
| X_d (pu) | 1.26 | 2.066 |
| X'_d (pu) | 0.26 | 0.259 |
| X''_d (pu) | 0.18 | 0.213 |
| X_q (pu) | 1.24 | 1.044 |
| X''_q (pu) | 0.21 | 0.207 |
| T'_{do} (pu) | 1.4446 | 4.485 |
| T''_{do} (pu) | 0.0218 | 0.068 |
| T''_{qo} (pu) | 0.0690 | 0.1 |

A.2 Acceptable Level of transients

Determination of the acceptable transient level is illustrated through the case study presented in this section. Based on the EMTP simulations in MATLAB/Simulink, the machine's current and torque peaks under the operating point specified in Figure 3.1 are obtained. Their time-domain simulation results are shown in Figure A.2. The acceptable synchronizing current at the breaker location is obtained to be 0.791 p.u.

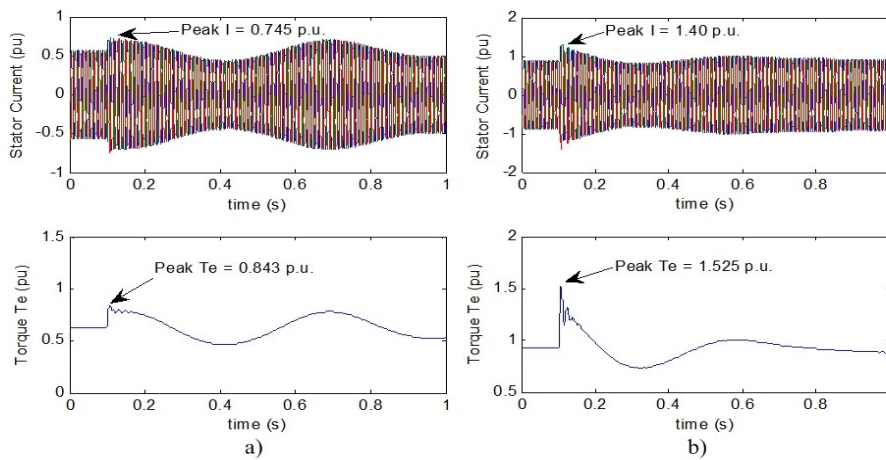


Figure A.2 Acceptable current and torque transient peaks for a) SG1 and b) SG2

A.3 Worst Case transients

Possible worst case synchronizing transients based on power quality limits will take place in the following 4 cases shown in Figure 3.3, where the operating point of both parties deviate the most. The worst transient of all occurs in case (2, 3). This is because prior to synchronization, the Micro-grid side voltage is maintained at 1.1 p.u. and the Micro-grid frequency is +0.25Hz higher than the system frequency.

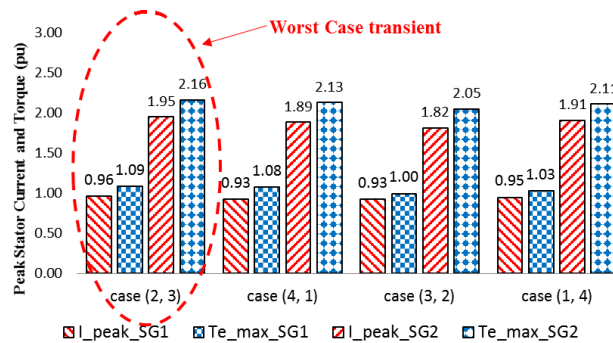
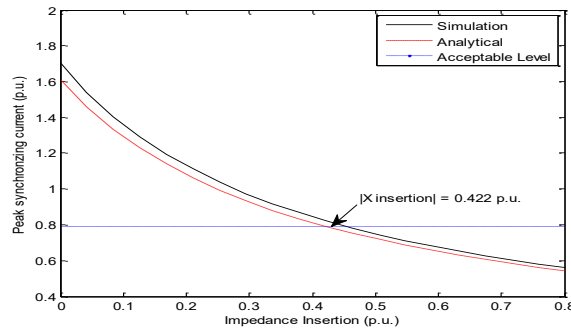


Figure A.3 Worst case transients based on power quality limits for the two machines

Since the worst transients are identified in case (2, 3), then the size of impedance can be determined by EMTP simulations or analytical expressions developed. A comparison of the two approaches is shown in Figure A.4 (a). For this case study, the impedance value determined analytically is 0.422 p.u. or 26.38Ω. As shown in Figure A.4 (b), with the designed impedance value, the stator transient of every synchronous machine has been reduced to be within their acceptable current level.



a)

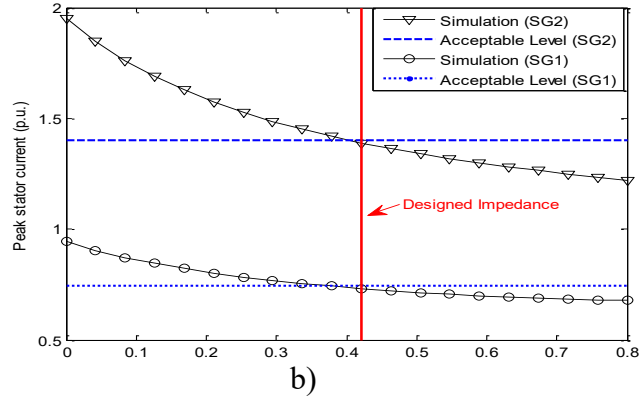


Figure A.4 a) Impedance selection based on breaker current. b) Peak stator current based on the designed impedance value.

A.4 Transient Stability of the Two Machines

For transient stability analysis, the worst case occurs in case (1, 3). From Figure A.5, it can be seen that increasing the inserted impedance does not have a significant effect on the maximum rotor angle. Based on the acceptable stability limit and the designed impedance value, a feasible impedance range is from 0.422p.u. to 0.9p.u. The 6.6MVA synchronous generator (SG1) has reached its stability limit first during the first swing because it is located farther away from the main substation than the 10MVA generator. This is reasonable because SG1 has a lower stability margin than SG2 due to higher line impedance from the machine to system.

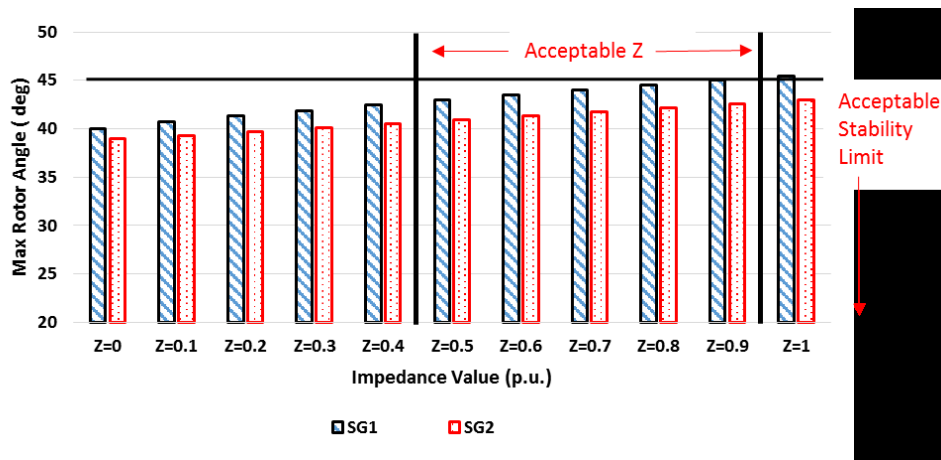


Figure A.5 Feasible impedance range based on short circuit and stability analysis

A.5 Bypass Evaluations

In order to evaluate the severity of bypass transients, load flow study is used to find the worst bypass voltage among the four possible cases. Case (4, 1) is the worst case as shown in Figure A.6 because it results in the largest complex power $|S|$. This $|S|$ through the designed impedance (0.422p.u.) incurs a voltage difference of 0.1793p.u. across the bypass breaker, which is lower than the acceptable level of 0.1855p.u. Therefore, the bypass transient is acceptable.

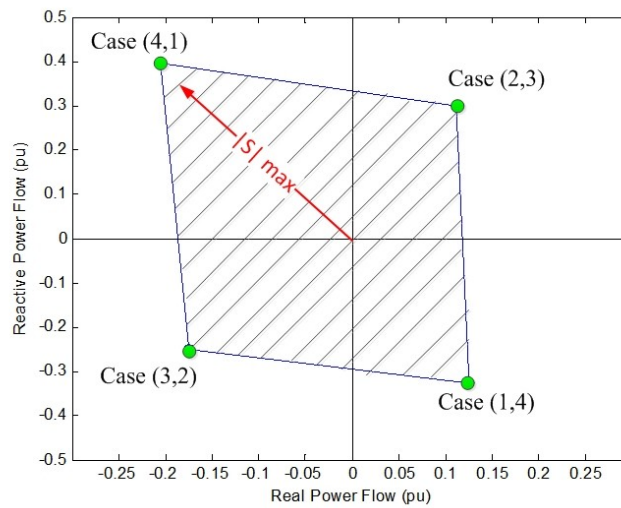


Figure A.6 Worst possible power flows through the impedance computed by load flow studies

Appendix B: Electronic Control Blocks For Thyristor Based Synchronizer

This section of the Appendix discusses about the different components implemented to generate the gating pulses for the thyristors based synchronizer method. First, the key components of the electronic control aspect are illustrated in B.1. Then, sample output waveforms are shown in B.2 to better understand the purposes of each component.

B.1 Components for Thyristor Gate Controls

In order to generate the gating pulses at a chosen firing angle for the TRIAC thyristors in each phase, first, a sawtooth generator function block is needed to generate sawtooth signals ranging from 0 to 360 degrees with time period of $1/(f_g+f_s)$ seconds. Afterwards, the output of the sawtooth generator feeds into the constant/ramp firing schemes in order to generate the correct firing angle for every cycle. Finally, the outputs of both blocks are compared inside the Gating pulse generator to eventually give the correct pulses to turn on the thyristors. The blocks are built in Simulink Environment as shown in Figure B.1.

As discussed earlier, for the synchronizer, both constant and time voltage ramp alpha schemes are to be used depending on the synchronizing conditions. The implementation of this is shown in Figure B.2.

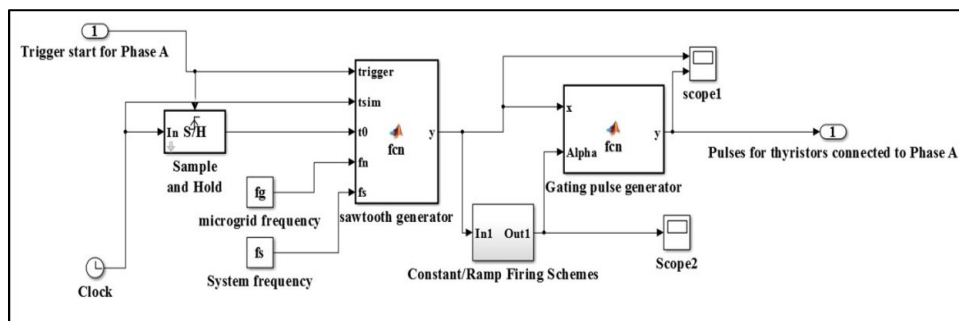


Figure B.1 Key components for generating the gating pulses to thyristors

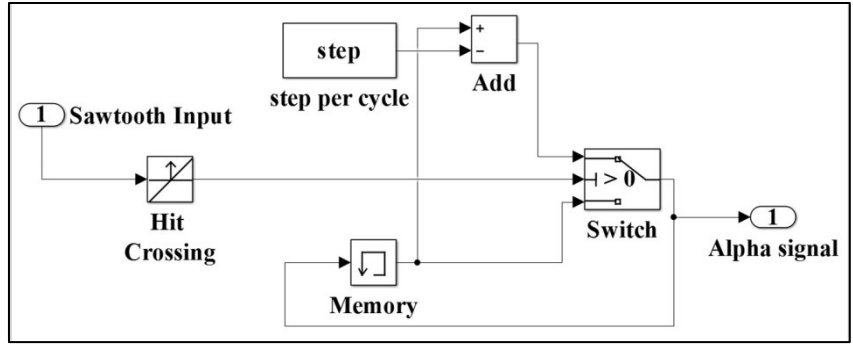


Figure B.2 Constant/Ramp Firing Scheme building blocks

For constant firing angle, step is set to zero. However, for time voltage ramp system, the alpha is expected to change every cycle, so the step is set to a non-zero value, and the firing angle is decreasing every cycle until the thyristors are bypassed.

B.2 Output Signals of Control Blocks

The sample signal output waveforms are shown in Figure B.3 for the sawtooth generator and the pulse generator blocks. This way, the thyristors are turned on at 130 degrees for both the positive and negative half cycles.

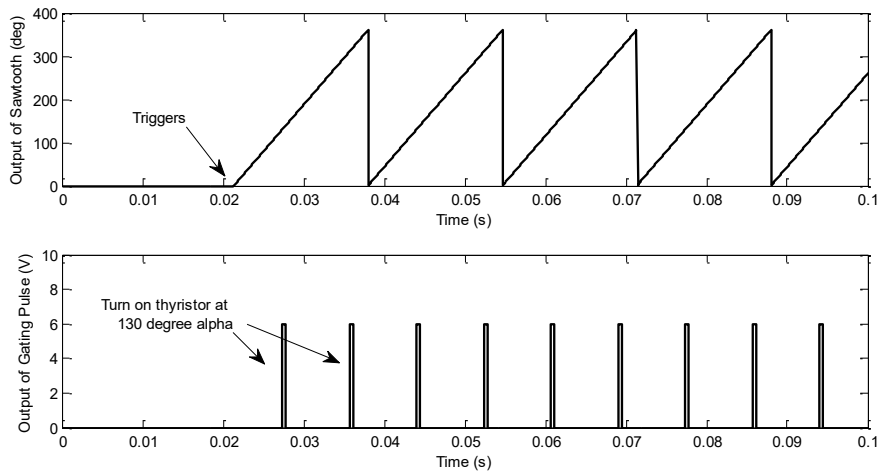


Figure B.3 Sawtooth outputs (top) and gating pulses (bottom) based on comparisons to the sawtooth outputs at $\alpha=130^\circ$

Appendix C: Validation of the Short Circuit Calculation and Effect of Governor Controls on Islanded System Synchronization

This section of Appendix will first validate the short circuit method of calculating synchronizing current in C.1, which is correspondence to subsection 3.2.2. Then, the effects of different turbine systems on the synchronization process are shown and explained by time domain simulations in C.2.

C.1 Validation of the Analytical Approach Against EMTP Simulations

As discussed earlier in Section 3.2, the transient current resulted from the first impedance switching can be obtained and analyzed by the method of short circuit calculations. Therefore, an analytical equation was previously developed in (3.2). The phase synchronizing currents I_{syncA} , I_{syncB} , and I_{syncC} can be expanded into similar forms.

$$\begin{aligned}
 I_{syncA}(t) &= \frac{\overline{\Delta v_A}}{|Z|} \left[\sin(\omega t + \alpha_A - \varphi) - \sin(\alpha_A - \varphi) e^{-Rt/L} \right] \\
 I_{syncB}(t) &= \frac{\overline{\Delta v_B}}{|Z|} \left[\sin(\omega t + \alpha_B - \varphi) - \sin(\alpha_B - \varphi) e^{-Rt/L} \right] \\
 I_{syncC}(t) &= \frac{\overline{\Delta v_C}}{|Z_{eq}|} \left[\sin(\omega t + \alpha_C - \varphi) - \sin(\alpha_C - \varphi) e^{-Rt/L} \right]
 \end{aligned} \tag{C.1}$$

Where α_B and α_C are -120° and $+120^\circ$ shifted from α_A , respectively. α_A is the angle of the voltage difference across the breaker in phase A. The total stator current I_{stator} is obtained by simply adding the load current to the transients.

$$\begin{aligned}
 I_{statorA}(t) &= I_{loadA}(t) + I_{syncA}(t) \\
 I_{statorB}(t) &= I_{loadB}(t) + I_{syncB}(t) \\
 I_{statorC}(t) &= I_{loadC}(t) + I_{syncC}(t)
 \end{aligned} \tag{C.2}$$

The load current depends on the loading level of the islanded system, and in per unit, the value typically varies from 0 to near 1 p.u. In order to validate the results of the analytical method, the calculated stator currents are plotted against that from EMTP simulations for synchronization case (2, 3).

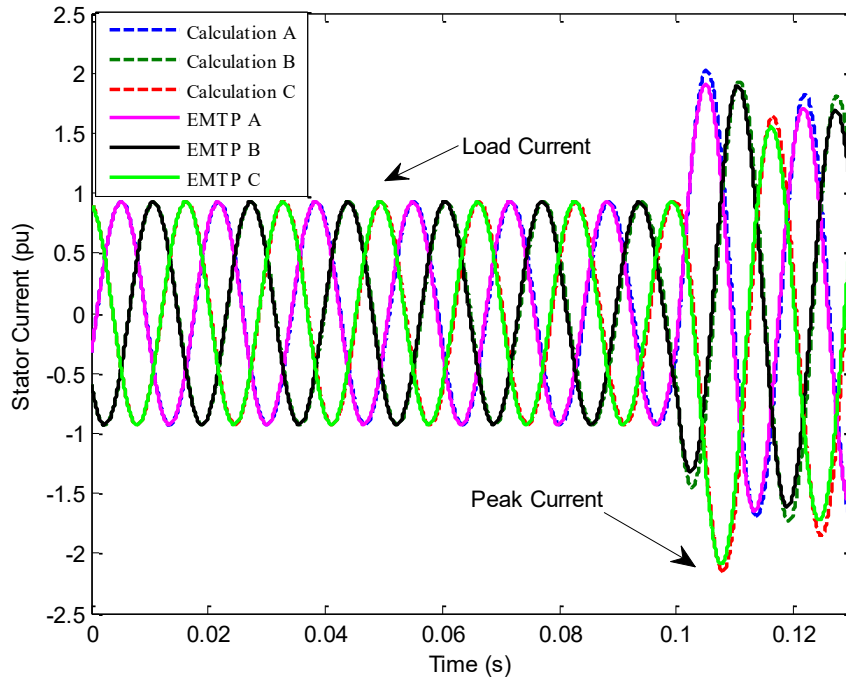


Figure C.1 Comparison of short circuit calculation and EMTP simulation at case (2, 3) without impedance insertion

Based on Figure C.1, it is observed that although the short circuit calculation only takes into account of the sub-transient machine reactance, but it is sufficient to capture the effects of transients in the stator current, which occurs within 1 to 2 cycles after the switching.

C.2 Effects of Different Governor/Turbine Systems on Microgrid Synchronization

This part of Appendix C investigates the impacts on the different turbine systems for open-loop islanded system synchronization based on impedance insertion method. In order to model the governor and turbine systems for both hydraulic and steam applications, the control system parameters of the governors are adopted from the power system and control book in [15]. The key performance outputs of different governor/turbine systems observed are the gate/valve position, mechanical power, and frequency. The responses are plotted from Figure C.2 to Figure C.4 for the process of impedance insertion based synchronization.

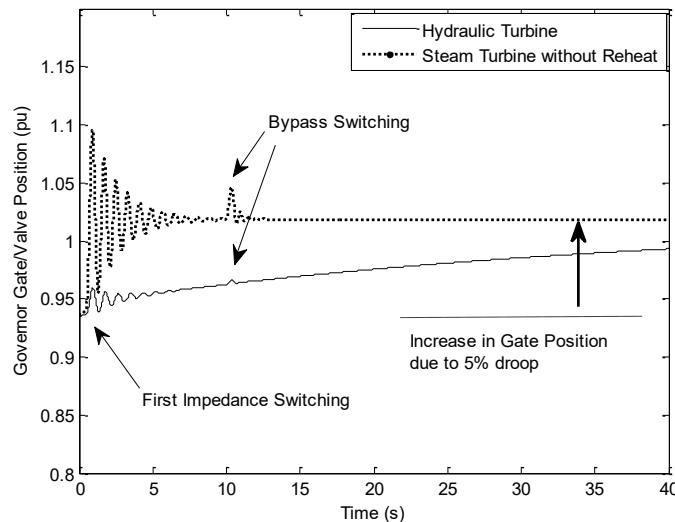


Figure C.2 Gate/valve positions response during islanded system synchronization based on impedance insertion method

Although both hydraulic and steam turbine systems will reach the same steady state values according to Figure C.2 and Figure C.3. However, they have much different transient responses. The reason for a slow response in the hydraulic turbine is because of the large transient droop compensation. As a consequence, a frequency change as shown in Figure C.4 will incur a slow change in the gate

position, and hence, a slow response in the mechanical power output. In addition, it can be seen from Figure C.4 that a faster turbine system response such as in the steam turbine without reheat, can help the rotor to stabilize faster.

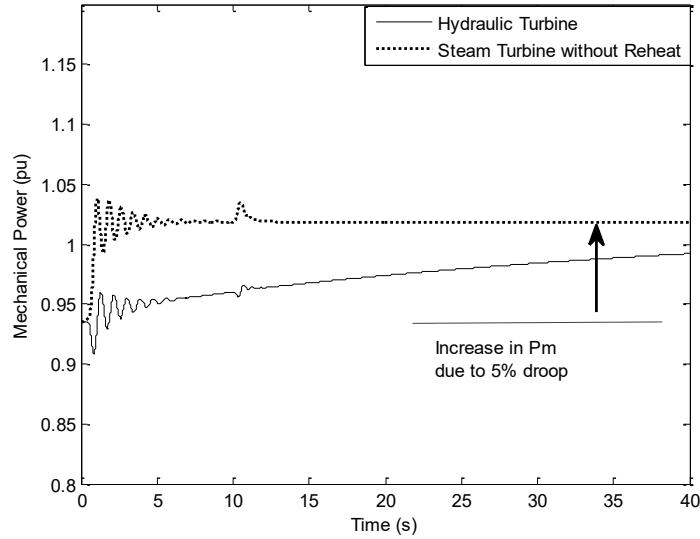


Figure C.3 Mechanical power response during islanded system synchronization based on impedance insertion method

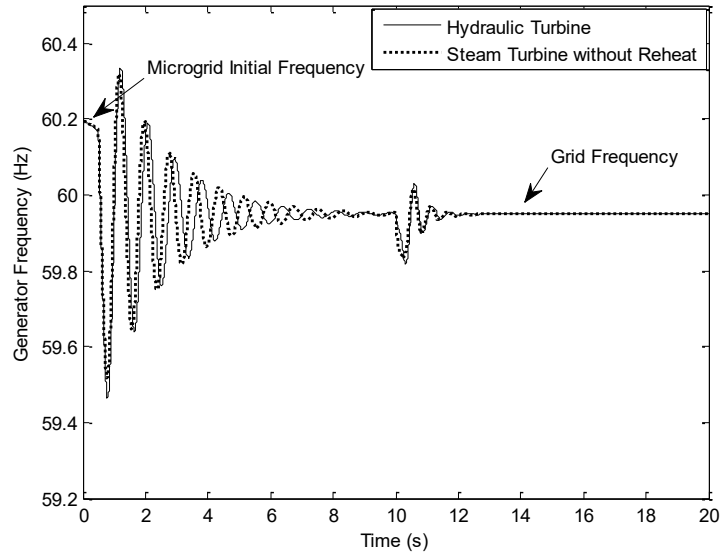


Figure C.4 Machine frequencies during islanded system synchronization based on impedance insertion method

Appendix D: Resistor Vs Inductor Insertion for Synchronizing an Islanded System to Grid

This section investigates the possibility of using resistor insertion towards synchronization of an islanded system to grid. Therefore, representative case studies are presented in D.1. Comparison results between inductor and resistor insertions are shown in D.2. Finally, recommendations have drawn in D.3 when implementing resistor insertion.

D.1 Synchronization Case Studies

Different synchronization studies are performed in Table D.1 on an islanded system based on the sample distribution feeder in Figure 3.5. The cases vary from the simplest of zero voltage and frequency differences towards a more sophisticated case involving differences in all parameters.

Table D.1: Case Investigations into Inductor vs. Resistor Insertion

| Case Studies for Inductor/Resistor Insertion | Synchronization Condition: | | |
|--|----------------------------|----------------|------------|
| | ΔV | $\Delta\theta$ | Δf |
| Case 1 | 0% | 20° | 0Hz |
| Case 2 | 0% | 20° | 0.25Hz |
| Case 3 | 5% | 20° | 0.25Hz |
| Case 4 | 10% | 20° | 0.25Hz |
| Case 5 | 20% | 20° | 0.25Hz |

D.2 Comparison Results for R, X, and Zero Impedance

Based on the sample case study, results are documented in this section to reflect the possibilities in utilizing a resistor insertion for synchronization purposes. In order to arrive the recommendations, the rotor angle, excitation voltage (AVR controls), and generator terminal voltage deviations are simulated to investigate the behaviors of the islanded system based on the case studies mentioned above.

Based on the design process, the size of the impedance insertion (either an inductor or resistor) must be determined first based on the acceptable level of transients from the perspective of the synchronous generator. This process is demonstrated in Figure D.1.

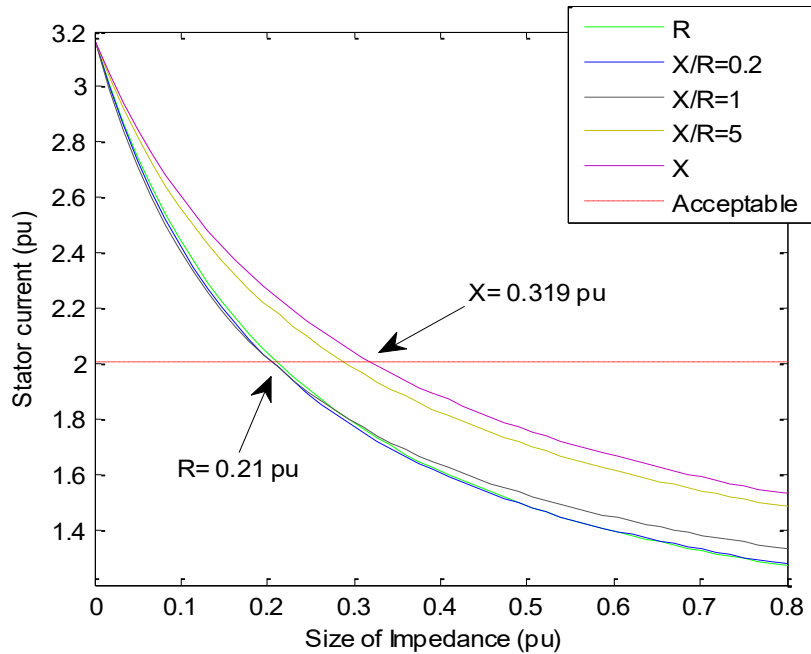


Figure D.1 Size of R or X required to limit the first transient

Based on the values of R and X, one can see that the size is different among the two. The reason is that there exists a X/R ratio of the equivalent line impedance seen across the breaker. The behaviors of the islanded system are simulated as below.

Rotor Angle Stability:

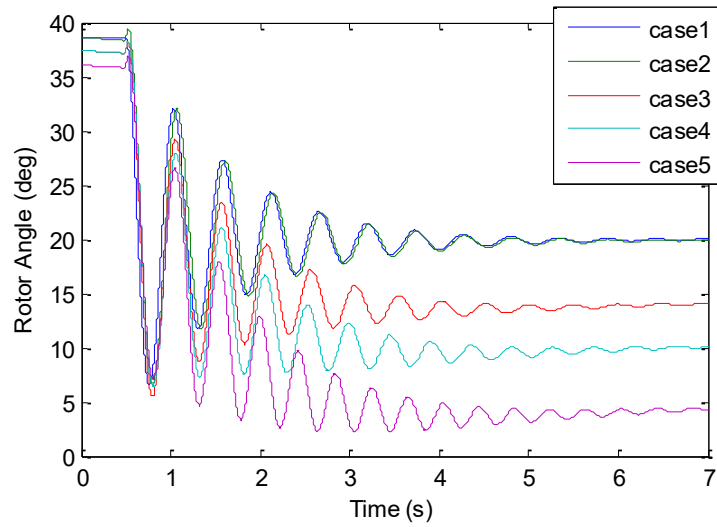


Figure D.2 Rotor angle results for different cases without impedance insertion

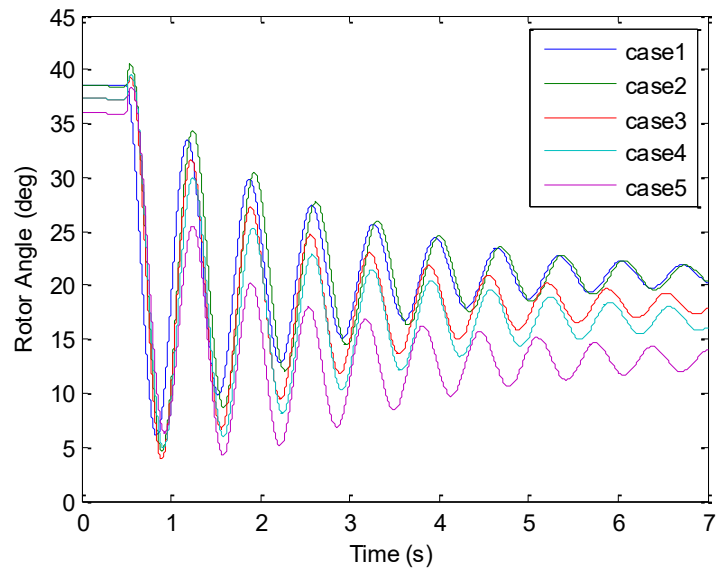


Figure D.3 Rotor angle results for the inductor insertion

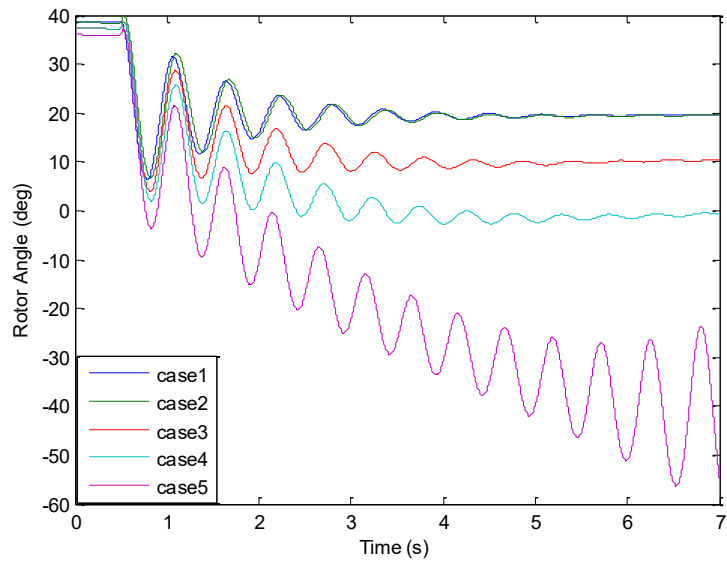


Figure D.4 Rotor angle results for the resistor insertion

As shown in above figures, for both zero impedance insertion and inductor insertion, the generator remains rotor angle stable for the established synchronizing conditions within the pre-defined power quality limits. The resistor insertion can provide more damping in the rotor angles for the stable cases. However, in the resistor insertion case shown in Figure D.4, at 20% voltage magnitude difference, the rotor angle no longer remains stable but increases oscillations, which is one of the main disadvantages using resistor insertion for synchronization purposes. One of the primary reasons is because of the large reactive power flow across the resistor after breaker is closed. Unlike the inductor insertion, resistor has no way of absorbing reactive power when the voltage difference reaches as high as 20%. A closer examination of the excitation voltage and terminal voltage will explain the instability further.

Excitation Voltage:

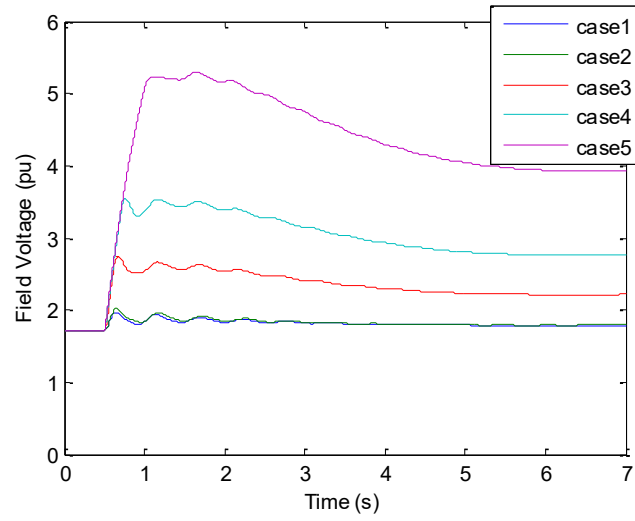


Figure D.5 Field voltage results for zero impedance insertion

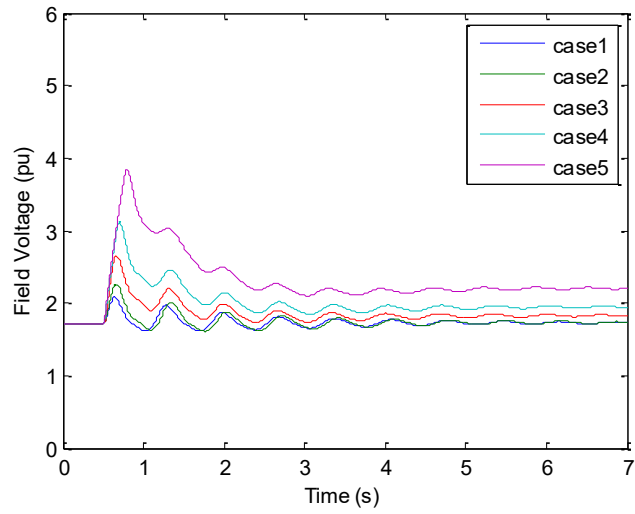


Figure D.6 Field voltage results for inductor insertion

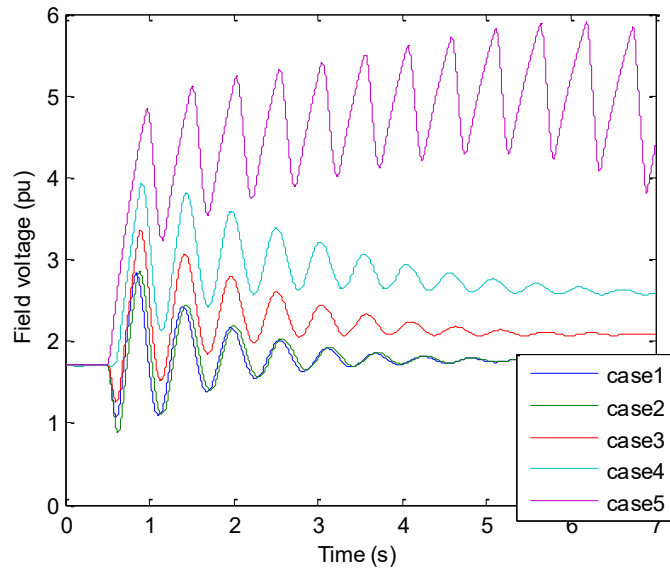


Figure D.7 Field voltage results for resistor insertion

As clearly shown in the plots of the field voltage of the machine, an inductor insertion has the benefit of dissipating reactive power when exists large voltage magnitude difference prior to the closing of the breaker. Therefore, resulting in not as much reactive power as required from the synchronous generator, which can be seen from the field voltage for the inductor insertion. However, in the case of a resistor insertion, the field voltage goes into a hunting mode in case 5, mainly because too much reactive power is required from the generator, and the generator will reach its upper reactive power limit at huge voltage magnitude differences.

Terminal Voltage:

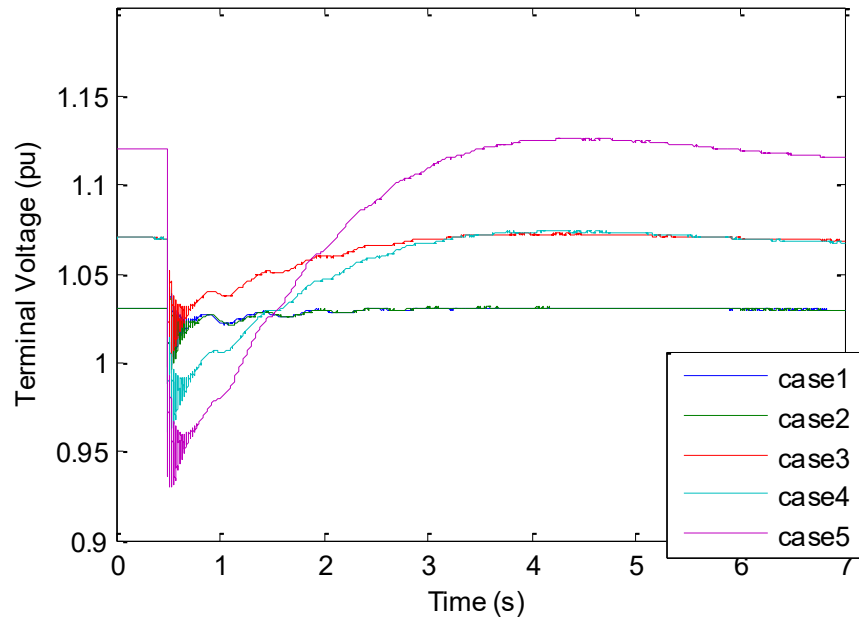


Figure D.8 Terminal voltage deviations for zero impedance insertion

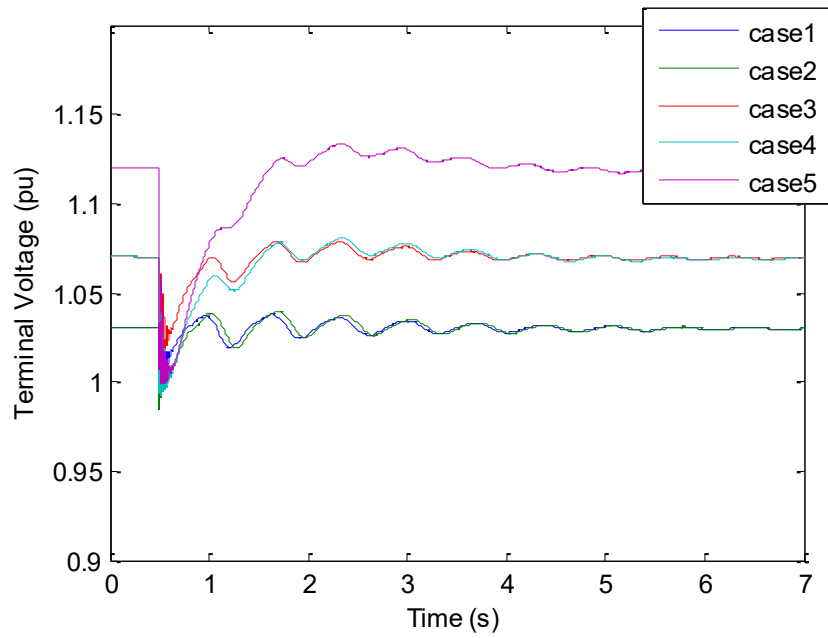


Figure D.9 Terminal voltage deviation for inductor insertion

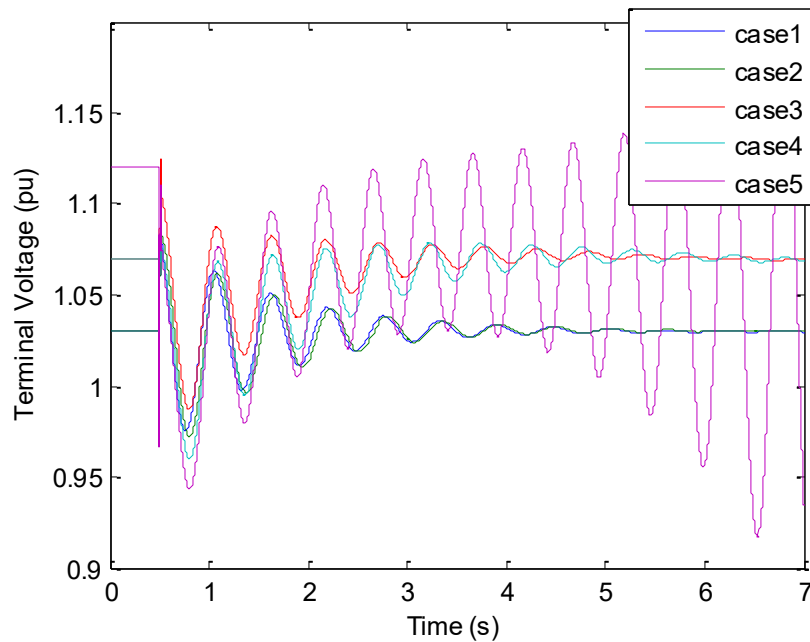


Figure D.10 Terminal voltage deviation for resistor insertion

Voltage deviations behave normal for both no impedance and inductor insertion cases. However, with resistor insertion at case 5, as related to rotor angle oscillations, the terminal voltage also increases its oscillation and becomes unstable.

D.3 Recommendations for Resistor Insertion

- Resistor insertion can be used for transient reduction in synchronizing an islanded system to grid only for negligible or small voltage magnitude differences (i.e $<10\%$ for this case study).
- Another option to use resistor insertion is to have AVR control in manual mode (i.e constant field) or voltage following mode during the process of synchronization, this way, voltage of the islanded system will follow the system voltage, which reduces the amount of reactive power flow generated/absorbed from the local DG units.